Energy, Mines and Resources Canada

Énergie, Mines et Ressources Canada

CANMET

Canada Centre for Mineral and Energy Technology

Centre canadien de la technologie des minéraux et de l'énergie

Mining Research Laboratories

Laboratoires de recherche minière

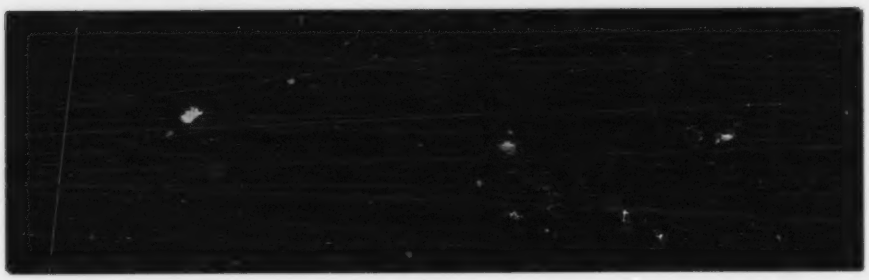

Canada

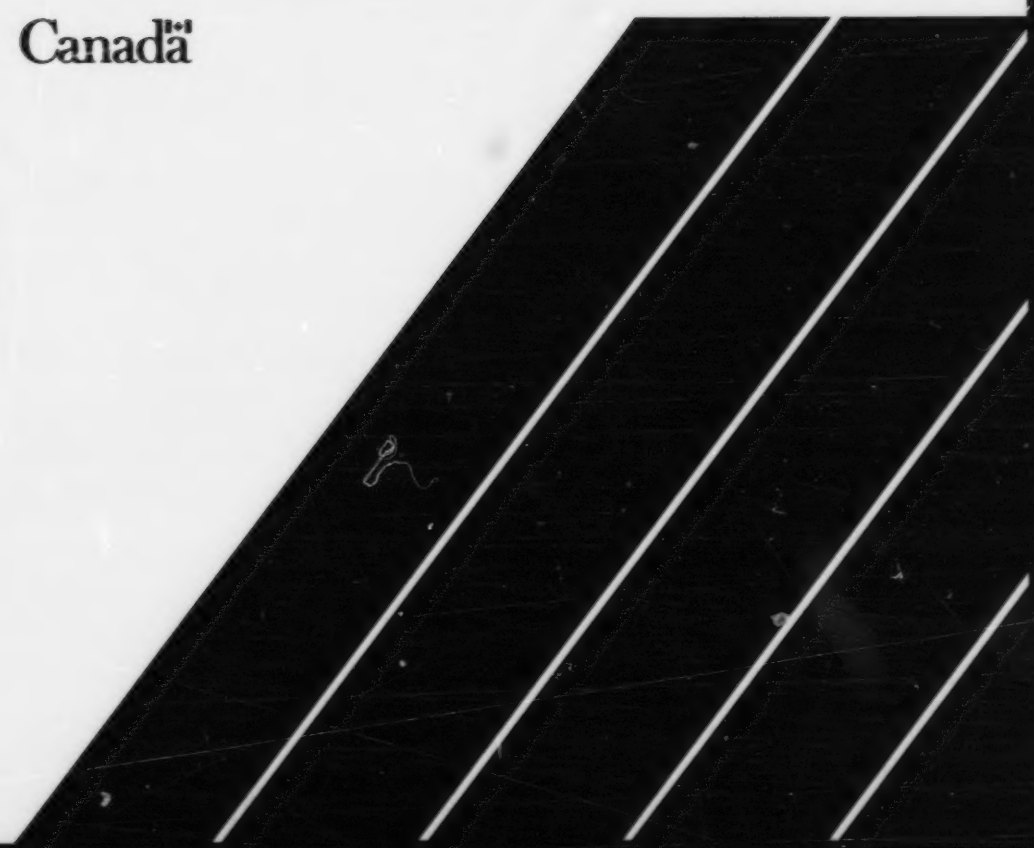

91-06273/

THE EFFECT OF LOADING RATE ON THE UNIAXIAL MECHANICAL PROPERTIES OF LAC DU BONNET GRANITE

R. JACKSON

Division Report MRL 91-058 (TR) May 1991

This document is an unedited internal report prepared primarily for circulation and internal reference purposes. It does not represent a final expression of the opinion of the Canada Centre for Mineral and Energy Technology (CANMET)

Ce document est un rapport provisoire non-révisé et rédigé principalement pour fin de diffusion et de documentation interne. Il ne représente nullement l'expression définitive de l'opinion du Centre canadien de la technologie des minéraux et de l'énergie (CANMET)

74 pp

MICROMEDIA

THE EFFECT OF LOADING RATE ON THE UNIAXIAL MECHANICAL PROPERTIES OF LAC DU BONNET GRANITE

by

Rand Jackson*

ABSTRACT

Uniaxial compression testing was conducted on samples of Lac du Bonnet grey granite at loading rates ranging from 0.75 to 0.00075 MPa/s. As the loading rate decreased: crack closure appeared to occur at lower stress levels than were indicated by standard test procedures; the mean uniaxial compressive strength decreased; and the Poisson's ratio increased. The instantaneous Poisson's ratio and volumetric strain methods of estimating long-term strength both yielded values in the range of 100 to 110 MPa for the Lac du Bonnet grey granite.

---

*Research Officer, Canadian Mine Technology Laboratory, Mining Research Laboratories, CANMET, Energy,Mines and Resources Canada, Ottawa, Ontario.

Keywords:
Loading Rate, Rock Properties, Mechanical, Young's Modulus, Poisson's Ratio, Uniaxial Compressive Strength, Compressive Wave Velocity, Shear Wave Velocity, Lac du Bonnet

EFFET DU TAUX DE CHARGE SUR LES PROPRIÉTÉS MÉCANIQUES UNIAXIALES DU GRANITE DE LAC DU BONNET

par

Rand Jackson*

RÉSUMÉ

Des essais de compression uniaxiale ont été réalisés sur des échantillons de granite gris de lac du Bonnet, avec des taux de charge variant de 0,75 à 0,00075 MPa/s. À mesure que le taux de charge diminuait, la fermeture des fissures semblait se produire à des niveaux de contrainte inférieurs à ceux indiqués par les essais ordinaires, la résistance à la compression uniaxiale moyenne diminuait et le rapport de Poisson augmentait. Les résultats obtenus par les méthodes d'estimation de la résistance à long terme basées sur le rapport de Poisson instantané et sur la déformation volumétrique se situaient dans la fourchette 100-110 MPa pour le granite gris de Lac du Bonnet.

*Agent de recherche, Laboratoire canadien de technologie minière, Laboratoires de recherche minière, CANMET, Énergie, Mines et Ressources Canada, Ottawa (Ontario)

Mots clés :

Taux de charge, propriétés des roches, mécanique, module de Young, rapport de Poisson, résistance à la compression uniaxiale, vitesse de l'onde de compression, vitesse de l'onde de cisaillement, Lac du Bonnet

CONTENTS

Page

ABSTRACT i
RESUME ii
INTRODUCTION 1
IDENTIFICATION OF SPECIMENS AND TESTS 1
DESCRIPTION OF TEST MEASUREMENTS 3
DATA TREATMENT 4
DATA SUMMARY 6
OBSERVATIONS AND DISCUSSION 11
Tangent Modulus of Elasticity 11
Uniaxial Compressive Strength 11
Poisson's Ratio 15
CONCLUSIONS AND RECOMMENDATIONS 15
ACKNOWLEDGEMENTS 18
REFERENCES 18
APPENDIX A 20
APPENDIX B 46

TABLES

No.

1. Summary of specimen dimensions and densities 2
2. Summary of ultrasonic velocities and dynamic properties for URL loading rate specimens 7
3. Uniaxial mechanical properties for 0.75 MPa/s URL loading rate specimens 8
4. Uniaxial mechanical properties for 0.075 MPa/s URL loading rate specimens 8
5. Uniaxial mechanical properties for 0.0075 MPa/s URL loading rate specimens 9
6. Uniaxial mechanical properties for 0.00075 MPa/s URL loading rate specimens 9
7. Summary of mean uniaxial mechanical properties for URL loading rate specimens 10

TABLES: cont'd

No. Page

8. Mean Uniaxial and predicted long-term strengths of the Pinawa grey granite 14

FIGURES

1. Idealized stress/strain curves for URL loading rate specimens 12
2. Uniaxial compressive strength and predicted long-term strength vs. loading rate for URL grey granite specimens 13
3. Poisson's ratio vs. loading rate for URL grey granite specimens 16

INTRODUCTION

As part of the Canadian Nuclear Fuel Waste Management Project, Atomic Energy of Canada Limited is characterizing various rock formations to determine their suitability for the permanent disposal of high level wastes. It has been shown by several investigators that the strengths of some rock types decrease with decreases in loading rate. It becomes imperative, therefore, to determine or estimate the long-term strength of a repository's host rock especially in light of a design lifetime which is to span many thousands of years.

A program has been conducted at the Canada Centre for Mineral and Energy Technology's Mining Research Laboratories to determine the effects of loading rates in the range of 0.75 to 0.00075 MPa/s on the mechanical properties of Lac du Bonnet grey granite. This report summarizes the results of that program and compares alternate methods of estimating the long term strength of the granite.

IDENTIFICATION OF SPECIMENS AND TESTS

The rock can be described as a massive, grey, medium to coarse grained granite, composed of quartz, k-feldspar (oligoclase), plagioclase feldspar and biotite. Twenty-four samples were prepared from core obtained from borehole 209-018-EXT7. Seven each were tested in uniaxial compression at loading rates of 0.75, 0.075 and 0.0075 MPa/s. For practical reasons, it was only possible to test three samples at the slowest loading rate of 0.00075 MPa/s.

Table 1 provides a summary of the specimen identification number and its depth, dimensions and density. The following properties were determined for the samples listed;

1) compressive wave velocity, V_p
2) shear wave velocity, V_s
3) dynamic shear modulus, G_d
4) dynamic Young's modulus, E_d
5) dynamic Poisson's ratio, ν_d
6) uniaxial compressive strength
7) Poisson's ratio, ν
8) 50% secant modulus of elasticity, $E_{s50\%}$
9) 50% tangent modulus of elasticity, $E_{t50\%}$
10) 75% secant modulus of elasticity, $E_{s75\%}$
11) 10 MPa secant modulus of elasticity, E_{s10MPa}
12) 20 MPa secant modulus of elasticity, E_{s20MPa}
13) 30 MPa secant modulus of elasticity, E_{s30MPa}
14) 40 MPa secant modulus of elasticity, E_{s40MPa}
15) 50 MPa secant modulus of elasticity, E_{s50MPa}
16) 60 MPa secant modulus of elasticity, E_{s60MPa}

Table 1: Summary of Specimen Dimensions and Densities

Specimen Identification	Length (mm)	Diameter (mm)	Density (Mg/m^3)
209-018-EXT7 8.27	101.85	44.74	2.63
8.37	103.78	44.80	2.63
8.47	105.08	44.71	2.63
9.04	104.94	44.70	2.63
9.17	103.00	44.78	2.63
9.37	102.90	44.79	2.62
9.48	102.49	44.75	2.63
10.72	100.68	44.82	2.63
10.83	104.24	44.85	2.62
11.29	101.09	44.79	2.63
11.40	100.67	44.80	2.63
11.50	102.91	44.84	2.63
11.61	101.65	44.81	2.63

Table 1: cont'd

Specimen Identification	Length (mm)	Diameter (mm)	Density (Mg/m^3)
208-018-EXT7 11.72	101.71	44.83	2.63
11.97	102.73	44.80	2.64
12.06	102.10	44.82	2.63
12.16	101.91	44.82	2.63
12.27	100.89	44.84	2.63
12.37	104.08	44.86	2.63
12.50	103.23	44.80	2.63
12.61	103.06	44.80	2.63
12.73	112.19	44.47	2.64
12.84	112.00	44.50	2.64
12.96	112.25	44.62	2.65

DESCRIPTION OF TEST MEASUREMENTS

Compressive and shear wave velocity measurements were carried out on samples prior to being gauged for elastic deformation measurement. The testing equipment consisted of: transmitting and receiving platens utilizing piezoelectric transducers, a high voltage pulse generator, a signal amplifier and a Tektronix 2230 100 MHz digital storage oscilloscope equipped with delay sweep and a time base resolution of 0.01 micro-seconds.

With the exception of loading rate, the testing procedures used during this program complied with those described in Technical Data 303410-M01/78 (2). The two Phillips PR 9302 strain bridges and the Mosely Autograph 2FRA X-Y recorder referred to in that document were replaced, in the present study, by two Bruel and Kjaer Type 1526 strain indicators and an HP 7046B X-Y recorder. These equipment were used to continuously monitor and record the axial and transverse strains as a function of axial load. Analog signals from these equipment were also digitally recorded on a PDP11/73 micro-computer at discrete intervals during testing.

DATA TREATMENT

The compressive and shear wave velocities were determined by dividing the specimen length by the wave travel time through the specimen. The dynamic properties were, then, calculated using the following equations (3);

Dynamic Young's Modulus

$$E_d = \frac{\rho V^2 (3V_p^2 - 4V_s^2)}{(V_p^2 - V_s^2)} \qquad (1)$$

where; E_d = dynamic Young's modulus
V_s = shear wave velocity
V_p = compressive wave velocity
ρ = density

Dynamic Shear Modulus

$$G_d = \rho V_s^2 \qquad (2)$$

where; G_d = dynamic shear modulus

Dynamic Poisson's Ratio

$$\nu_d = \frac{V_p^2 - 2V_s^2}{2(V_p^2 - V_s^2)} \qquad (3)$$

where; ν_d = dynamic Poisson's ratio

Analog outputs from the strain monitors and press load cell were used to generate the stress/strain curves contained in Appendices A and B. The tangent moduli of elasticity were calculated for each sample by determining the slope of the tangent to the axial strain curve at the stress levels enumerated earlier. The 50% secant modulus of elasticity ($E_{s50\%}$) was calculated by determining the slopes of the lines joining the origin to a point

on the axial strain curve corresponding to a stress level equal to 50% of the failure load. The ultimate compressive strength of each sample was calculated by dividing sample failure load by the sample's cross-sectional area. The ratio of the tangent to the axial strain curve to the tangent to the transverse strain curve at 50% failure load was used to determine the sample's Poisson's ratio (v).

Practically speaking, there are obvious difficulties in determining directly the long-term strength of any rock type. There is, however, a proliferation of methods which utilize short-term results to obtain an estimate of long-term support capabilities. Most use the onset of unstable fracture propagation as an indication of the limiting strength of the rock type in question. Among these, two have been chosen to analyze the results of loading rate testing on the Lac du Bonnet grey granite.

One widely recognized technique contends that unstable fracturing is marked by a point on the stress versus volumetric strain curve where volumetric strain begins to increase as opposed to decreasing according to elastic theory (Singh, 1977). Volumetric strain in this case is defined by;

$$\varepsilon_{vol} = \varepsilon_{axial} + 2\varepsilon_{circ.}$$

where; ε_{vol} = volumetric strain
ε_{axial} = axial strain
$\varepsilon_{circ.}$ = circumferential strain

The stress level corresponding to a reversal in the stress/volumetric strain curve was picked by inspection from data recorded during testing.

Sangha and Dhir (1977) suggested that, although unstable fracture propagation should coincide with an instantaneous

Poisson's ratio of 0.5 for a linear elastic material, this is often not the case for rock. They determined that some dilation may be accomodated by changes in a rock's microstructure which allow it to continue to maintain load as long as the instantaneous Poisson's ratio does not exceed 0.5. It should, therefore, be the point where the instantaneous Poisson's ratio exceeds 0.5 and not the onset of dilation which indicates the long-term strength of the rock. In this case, third degree equations were fitted in the region of interest (i.e. where $\nu \approx 0.5$) to the axial and circumferential stress/strain data recorded at discrete intervals during testing. An iterative approach was then used to determine when the ratio of the axial tangent modulus to the circumferential tangent modulus equaled 0.5.

DATA SUMMARY

Table 2 contains the results of the ultrasonic velocity measurements for each sample including the calculated values of the dynamic shear modulus, dynamic Young's modulus as well as Poisson's ratio estimated on the basis of velocity measurements. Axial and circumferential stress/strain curves for each sample are contained in Figures A1 through A24 in Appendix A. Volumetric stress/strain curves are contained in Figures B1 through B24 in Appendix B. Tables 3, 4, 5 and 6 summarize the uniaxial mechanical properties for specimens tested at loading rates of 0.75, 0.075, 0.0075 and 0.00075 MPa/s, respectively while Table 7 contains the mean results and standard deviations (in brackets) for each loading rate sample suite. Table 8 summarizes the uniaxial compressive strength and the long-term strength predicted using the volumetric strain and instantaneous Poisson's ratio methods for each loading rate.

Table 2: Summary of Ultrasonic Velocities and Dynamic Properties for URL Loading Rate Specimens

Specimen Identification	P-wave Velocity (km/s)	S-wave Velocity (km/s)	Dynamic Young's Modulus (GPa)	Dynamic Shear Modulus (GPa)	Dynamic Poisson's Ratio
209-018-EXT7 8.27	4.41	3.00	50.62	23.59	0.07
8.37	4.37	2.80	47.41	20.50	0.15
8.47	4.35	2.90	48.69	22.00	0.10
9.04	4.38	2.92	49.42	22.48	0.10
9.17	4.39	2.84	48.41	21.27	0.14
9.37	4.33	2.92	48.42	22.42	0.08
9.48	4.33	2.92	48.58	22.38	0.08
10.72	4.85	3.29	61.21	28.46	0.08
10.83	4.66	3.09	55.53	25.08	0.11
11.29	4.42	2.81	48.21	20.80	0.16
11.40	4.46	2.76	47.70	20.05	0.19
11.50	4.58	2.78	49.12	20.33	0.21
11.61	4.46	3.13	52.30	25.76	0.02
11.72	4.68	3.19	57.18	26.80	0.07
11.97	4.31	3.24	47.31	27.71	-0.15
12.06	4.47	3.08	52.31	24.98	0.05
12.16	4.51	3.02	52.46	23.91	0.10
12.27	4.60	3.05	54.20	24.46	0.11
12.37	4.51	3.03	52.59	24.13	0.10
12.50	4.63	3.17	55.89	26.48	0.06
12.61	4.54	3.04	53.16	24.31	0.09
12.73	5.39	2.72	51.74	19.48	0.33
12.84	5.04	2.73	50.74	19.60	0.29
12.96	4.97	2.70	49.99	19.39	0.29
Mean (Std. Dev.)	4.57 (0.26)	2.96 (0.17)	51.38 (3.51)	23.18 (2.71)	0.11 (0.10)

Table 3: Uniaxial Mechanical Properties for 0.75 MPa/s URL Loading Rate Specimens

Specimen Identification	Uniaxial Compressive Strength (MPa)	Tangent Modulus of Elasticity (GPa)								Poisson's Ratio
		10 MPa	20 MPa	30 MPa	40 MPa	50 MPa	60 MPa	50%	75%	
209-018-EXT7 8.27	187	29.31	43.35	52.27	58.03	61.70	63.74	65.94	61.66	0.25
9.04	186	23.08	39.03	48.76	54.97	58.97	61.30	64.39	61.31	0.29
9.48	191	29.04	42.65	51.59	57.31	60.90	62.83	65.80	65.34	0.23
11.29	175	35.10	45.52	53.19	58.26	61.52	63.32	64.78	60.31	0.26
11.61	170	28.95	44.25	54.11	60.03	63.36	64.63	65.76	67.94	0.25
12.06	181	31.52	45.10	54.03	59.73	63.27	65.09	66.76	62.55	0.26
12.37	167	29.99	39.57	46.52	51.39	54.80	57.10	59.46	55.43	0.27

Table 4: Uniaxial Mechanical Properties for 0.075 MPa/s URL Loading Rate Specimens

Specimen Identification	Uniaxial Compressive Strength (MPa)	Tangent Modulus of Elasticity (GPa)								Poisson's Ratio
		10 MPa	20 MPa	30 MPa	40 MPa	50 MPa	60 MPa	50%	75%	
209-018-EXT7 8.37	171	32.54	44.14	53.05	57.95	60.33	61.94	63.81	60.19	0.29
9.17	176	27.09	39.89	50.00	56.47	60.80	63.98	68.49	64.84	0.29
10.72	161	35.42	45.23	52.75	57.08	59.30	60.71	61.68	56.23	0.20
11.40	157	39.08	48.33	55.31	59.21	61.07	62.55	64.85	68.20	0.34
11.72	159	32.60	43.96	52.40	57.12	59.49	61.05	62.34	60.28	0.25
12.16	164	26.54	40.29	49.88	55.09	57.68	59.50	61.84	61.00	0.19
12.50	162	29.04	38.70	47.69	53.37	57.05	59.81	63.53	64.19	0.32

Table 5: Uniaxial Mechanical Properties for 0.0075 MPa/s URL Loading Rate Specimens

Specimen Identification	Uniaxial Compressive Strength (MPa)	Tangent Modulus of Elasticity (GPa)								Poisson's Ratio
		10 MPa	20 MPa	30 MPa	40 MPa	50 MPa	60 MPa	50%	75%	
209-018-EXT7 8.47	174	32.81	44.43	52.97	57.63	59.82	61.38	63.93	63.54	0.24
9.37	153	28.37	40.54	49.36	54.82	58.23	60.72	63.34	63.43	0.27
10.83	150	34.03	46.03	54.61	59.23	61.33	62.76	64.10	63.62	0.29
11.50	147	34.82	46.83	55.57	60.89	64.02	66.00	66.99	63.96	0.27
11.97	147	34.19	45.24	54.47	60.53	64.56	67.28	68.97	67.02	0.30
12.27	156	34.10	45.50	55.61	61.17	63.86	65.48	66.55	62.05	0.32
12.61	140	27.12	39.89	49.28	55.12	58.75	61.08	62.38	59.51	0.28

Table 6: Uniaxial Mechanical Properties for 0.00075 MPa/s URL Loading Rate Specimens

Specimen Identification	Uniaxial Compressive Strength (MPa)	Tangent Modulus of Elasticity (GPa)								Poisson's Ratio
		10 MPa	20 MPa	30 MPa	40 MPa	50 MPa	60 MPa	50%	75%	
209-018-EXT7 12.73	162	47.30	54.78	59.87	63.27	65.32	66.19	66.00	62.48	0.43
12.84	165	51.93	58.10	62.33	65.11	66.65	67.07	65.90	60.02	0.35
12.96	157	50.69	56.63	60.83	63.72	65.51	66.33	66.00	58.47	0.36

Table 7: Summary of Mean Uniaxial Mechanical Properties of URL Loading Rate Specimens

Loading Rate (MPa/s)	Uniaxial Compressive Strength	Tangent Modulus of Elasticity (GPa)								Poisson's Ratio
		10 MPa	20 MPa	30 MPa	40 MPa	50 MPa	60 MPa	50%	75%	
0.75	180 (9)	29.57 (3.59)	42.78 (2.57)	51.50 (2.86)	57.10 (3.02)	60.65 (2.98)	62.57 (2.71)	64.78 (2.44)	62.08 (3.94)	0.20 (0.02)
0.075	164 (7)	31.76 (4.56)	42.93 (3.44)	51.58 (2.54)	56.61 (1.91)	59.39 (1.53)	61.36 (1.58)	63.79 (2.37)	62.13 (3.91)	0.27 (0.06)
0.0075	152 (11)	32.21 (3.13)	44.07 (2.74)	53.12 (2.74)	58.48 (2.68)	61.51 (2.66)	63.53 (2.68)	65.18 (2.36)	63.30 (2.25)	0.28 (0.02)
0.00075	161 (4)	49.97 (2.40)	56.50 (1.66)	61.01 (1.24)	64.03 (0.95)	65.83 (0.72)	66.53 (0.47)	65.97 (0.06)	60.32 (2.02)	0.38 (0.04)

OBSERVATIONS AND DISCUSSION

TANGENT MODULUS OF ELASTICITY

When analyzing the stress/strain data, tangent moduli of elasticity were determined at stress levels of 10, 20, 30, 40, 50, and 60 MPa and at 50% and 75% of the failure stress. This data treatment made it possible to construct a form of pseudo-stress/strain curve (Figure 1) to summarize the mean mechanical behaviour of each loading rate sample suite. As Figure 1 indicates, there is little difference between the deformational responses of the sample suites tested at 0.75, 0.075 and 0.0075 MPa/s. However, at the slowest loading rate of 0.00075 MPa/s, the rock tends to behave more linearly with an increase in modulus of only 16.56 GPa between stress levels of 10 and 60 MPa as compared to a mean increase of 31.31 GPa for the other loading rates. This runs contrary to behaviour observed by other investigators who, for most rock types, observed an decrease in modulus with decreasing loading rate (Peng, 1975, Friedman, Perkins and Green, 1969). It would appear that crack closure in the Pinawa grey granite may be time dependent and can occur at much smaller stresses than are indicated by loading rates used for standard uniaxial tests. As the rocks enter their respective linear-elastic zones, however, there appears to be little difference in deformational response between the various loading rates as one might expect in a relatively homogeneous rock like the Lac du Bonnet grey granite.

UNIAXIAL COMPRESSIVE STRENGTH

The loading rates and corresponding mean uniaxial compressive strengths, Q_u, as well as the long-term strengths predicted by the two analytical techniques described earlier are summarized in Table 3 and presently graphically in Figure 2.

As expected, the uniaxial compressive strength exhibited a

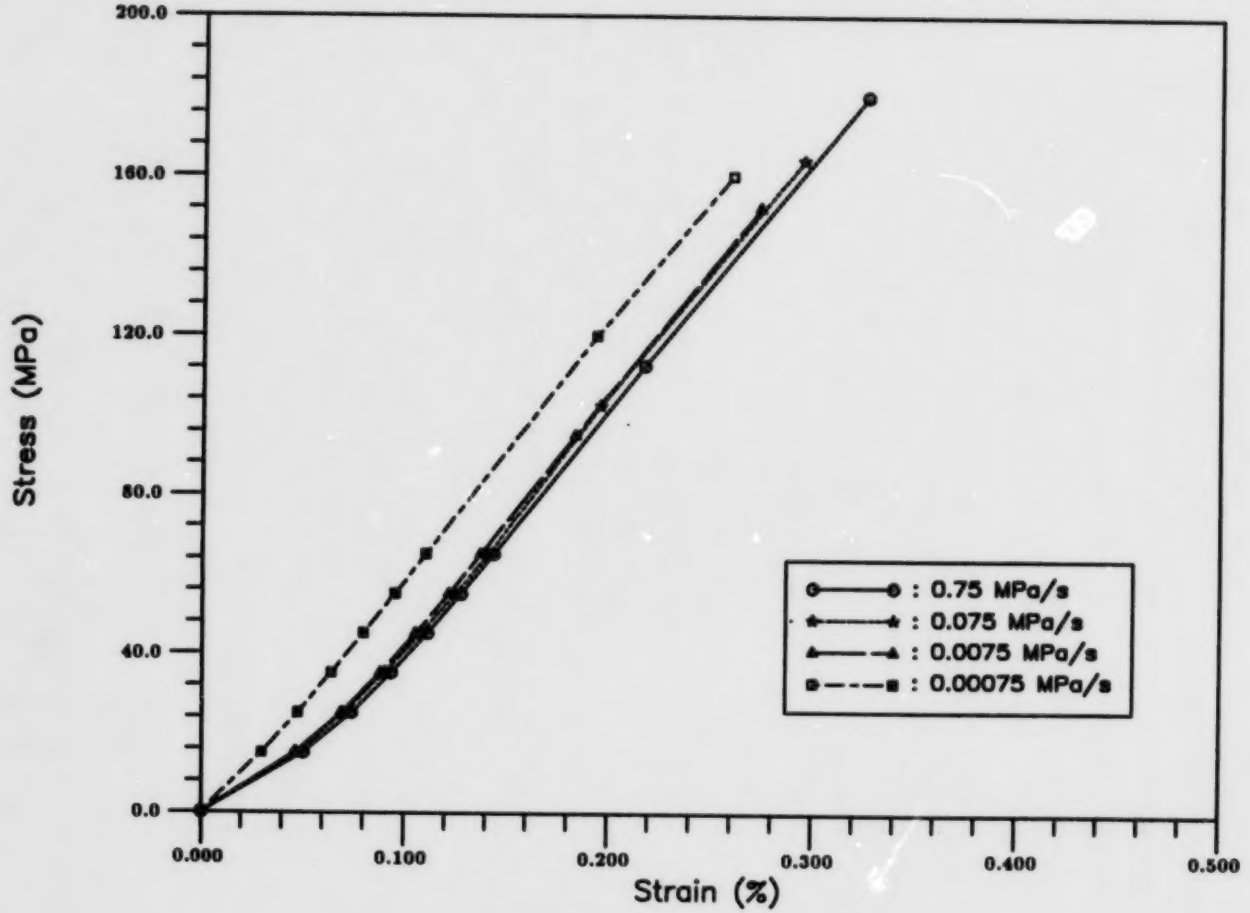

Figure 1 : Idealized stress/strain curves for URL loading rate specimens

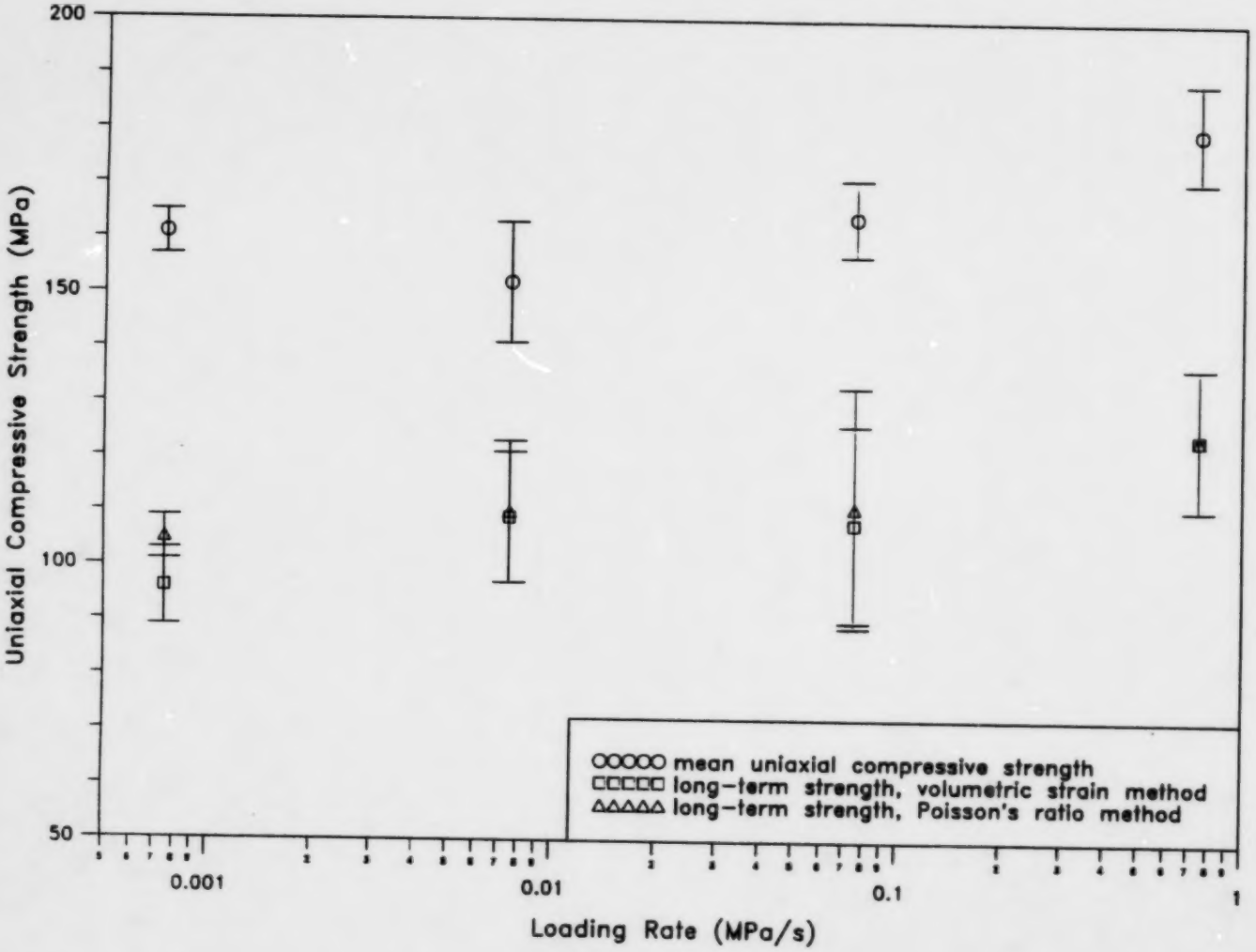

Figure 2: Uniaxial Compressive Strength and Predicted Long-term Strength vs Loading Rate for URL Grey Granite Specimens

considerable decrease as the loading rate decreased from 0.75 to 0.0075 MPa/s (28 MPa). As the loading rate decreased by another factor of ten to 0.00075 MPa/s, however, a slight increase in strength to 161 MPa was observed. It is difficult to determine if this increase is a statistical anomoly due to the small

Table 8: Mean Uniaxial and Predicted Long-term Strengths of the Pinawa Grey Granite

Loading Rate (MPa/s)	Uniaxial Compressive Strength (MPa)	Long-term Strength Volumetric Strain Method (MPa)	Long-term Strength Poisson's Ratio Method (MPa)
0.75	180 (9)	124 (13)	124 (13)
0.075	164 (7)	111 (22)	108 (18)
0.0075	152 (11)	110 (13)	109 (12)
0.00075	161 (4)	105 (4)	96 (7)

sample set (n=3) for this loading rate or an inherent property of the Lac du Bonnet grey granite. Regardless, a power equation fitted to the resultant data yields;

$$Q_u = \dot{\sigma}^{0.018} \times 175$$

where; Q_u = predicted uniaxial strength (MPa)
$\dot{\sigma}$ = loading rate (MPa/s)

As mentioned earlier, the long-term strength of the granite was estimated from the uniaxial compression results using the volumetric strain method. Specimens tested at 0.75 MPa/s indicated a predicted mean long-term strength of 124 MPa compared to values

of 111, 110 and 105 MPa for loading rates of 0.075, 0.0075 and 0.00075 MPa/s, respectively. It seems reasonable to assume that at 0.75 MPa/s, loading is sufficiently fast and fracture propagation sufficiently slow that the sample is able to take on additional loading before fractures can coalesce and result in dilation. By implication, a threshold loading rate between 0.75 and 0.075 MPa/s exists where the onset of dilation becomes unaffected by loading rate and the sample is unable to take on additional loading before failure begins.

As Figure 2 indicates, the results of analysis utilizing the instantaneous Poisson's ratio yielded similar results to those obtained using the volumetric strain method indicating that the onset of dilation is, in fact, the onset of failure for the Lac du Bonnet granite.

POISSON'S RATIO

The effect of loading rate on the Poisson's ratio of the URL grey granite is summarized in Figure 3. The observed increase in Poisson's ratio from 0.20 to 0.28 as the loading rate decreased from 0.75 to 0.0075 MPa/s is, again, the result of the slower rates allowing sufficient time for fractures to coalesce and result in increased transverse deformation. A Poisson's ratio of 0.38 for the 0.00075 MPa/s loading rate appears high and, as mentioned earlier, may be a result of the limited sample population used (n=3).

CONCLUSIONS AND RECOMMENDATIONS

The apparent tightening of the Lac du Bonnet grey granite at lower stress levels (as evidenced by Figure 1) when loaded at 0.00075 MPa/s indicates that crack closure may occur earlier than was observed using standard uniaxial test procedures. This may

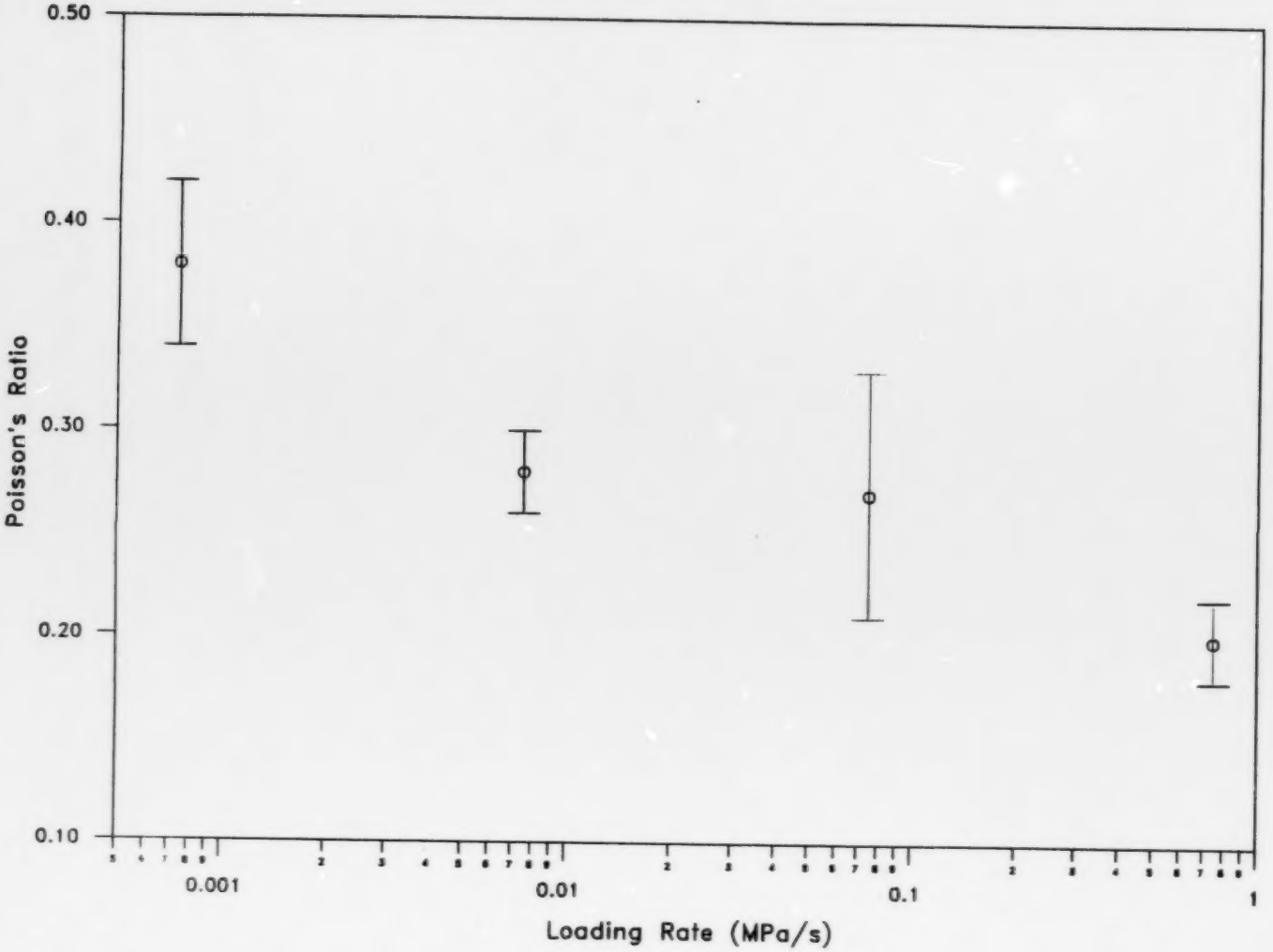

Figure 3: Poisson's Ratio vs. Loading Rate for URL Grey Granite Specimens

result in a lowering of the predicted hydraulic conductivity of the rock, especially in the near field around a possible emplacement vault.

In estimating the long-term strength of the Lac du Bonnet grey granite, both the volumetric strain and instantaneous Poisson's ratio methods show some loading rate dependence with a threshold rate occurring somewhere between 0.75 and 0.075 MPa/s. It appears that the grey granite's long-term strength is between 100 and 110 MPa although 0.00075 MPa/s results do indicate it may be as low as 96 MPa. Additional testing at 0.00075 MPa/s will be conducted in order to give results at that loading rate the same statistical significance as the other sample suites.

While the results of this program give a good indication of the long-term strength of the Lac du Bonnet grey granite, the actual mechanisms associated with underground excavation will more closely resemble instantaneous loading and a resulting stress redistribution around the openings as opposed to a gradual loading to failure. In this respect, it may be more valid, in a subsequent test program, to study the long-term support capabilities of the rock by loading samples quickly to pre-determined stress levels and observing the time to failure if, indeed, failure occurs.

And, finally, several authors have noted that, in many instances, the amount of moisture contained in a sample can have profound effects on its apparent strength (Obert, Windes and Duvall, 1946, Krokosky and Husak, 1968). While earlier work conducted on shallow WN1 core showed little dependence of the uniaxial mechanical properties on moisture content (Jackson and Annor, 1985), prolonged periods of loading may cause mechanisms such as stress corrosion to have greater impact. It is suggested that any subsequent test programs into long-term strength, therefore, are conducted under saturated conditions.

ACKNOWLEDGEMENTS

The author would like to acknowledge the valuable assistance of Mr. Bernie Gorski, Ms. Catherine Mainguy and Ms. Kimberley Emde during this test program.

REFERENCES

1. A. Annor and L. Geller
Dilatational velocity, Young's modulus, Poisson's ratio, uniaxial compressive strength and Brazilian tensile strength for WN! and WN2 samples, CANMET/MRL Technical Data 303410-M01/78, 1978.

2. M. Friedman, R.D. Perkins and S.J. Green
Observation of brittle-deformation features of the maximum stress of Westerly Granite and Solenhofen Limestone, Int. J. Rock Mech. Min. Sci., Vol. 7, 1970.

3. R. Jackson and A. Annor
The effects of water content on the uniaxial mechanical properties of WN1 core samples, CANMET/MRL Division Report ERP/MRL85-118(TR), 1985.

4. E.M. Krokosky and A. Husak
Strength characterisitics of basalt in ultra-high vacuum, J. Geophys. Res., Vol. 7, 1970.

5. L. Obert, S.L. Windes and W.S. Duvall
Standardized tests for determining the physical propeties of mine rock, USBMRI 3891, 1946.

6. S.S. Peng

A note on the fracture propagation and time dependent behaviour of rocks in uniaxial tension, Int.J. Rock Mech. Min. Sci. & Geomech. Abstr., Vol. 12, 1975.

7. C.M. Sangha and R.K. Dhir

Influence of time on the strength, deformation and fracture properties of a lower Devonian sandstone, Int. J. Rock Mech. Min. Sci., Vol. 9, Pergamon Press, 1972.

8. D.P. Singh

Long-term strength of rock, Colliery Gaurdian, Nov., 1977.

Appendix A

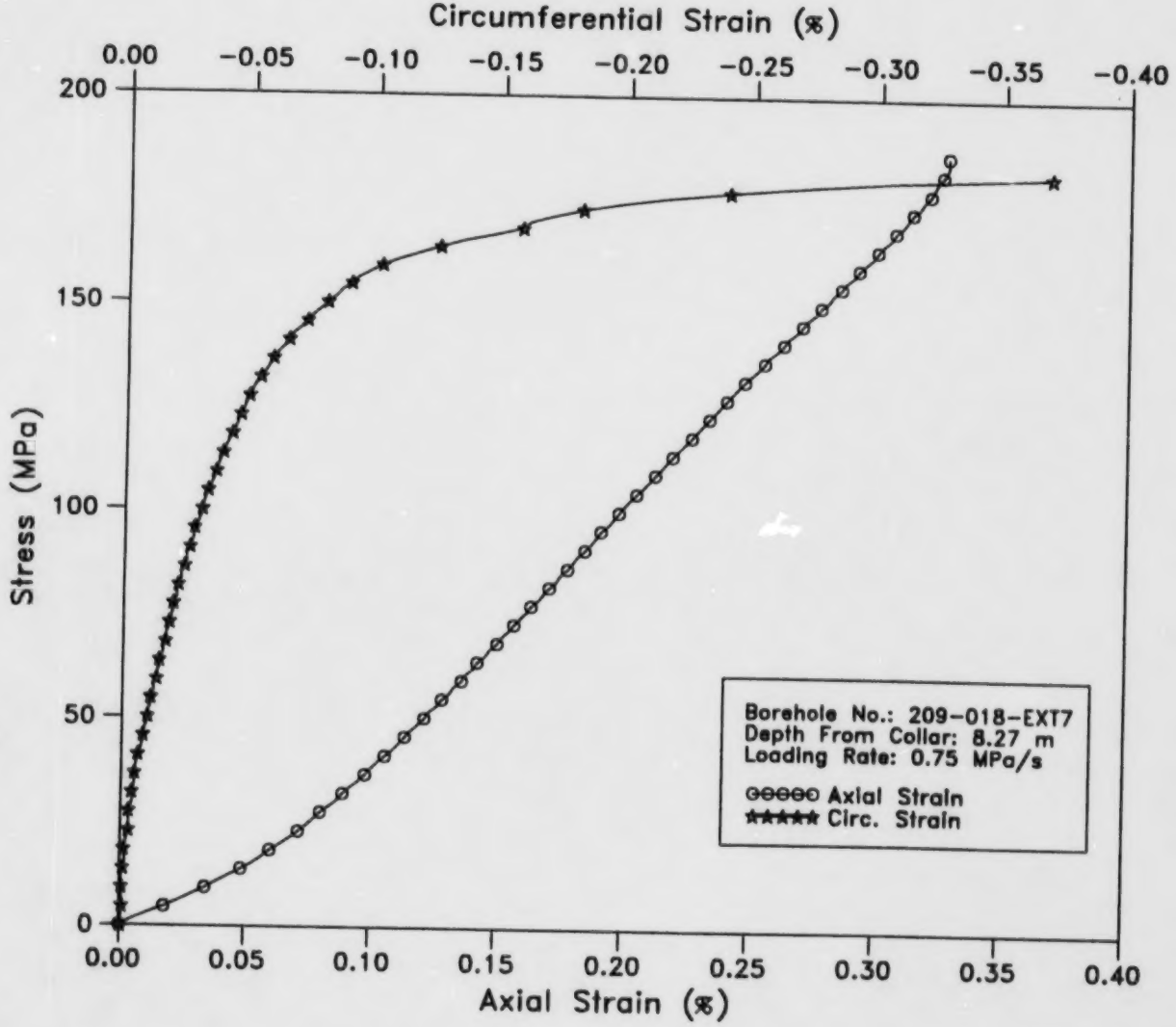

Figure A1: Stress/strain curves for Lac du Bonnet loading rate specimens

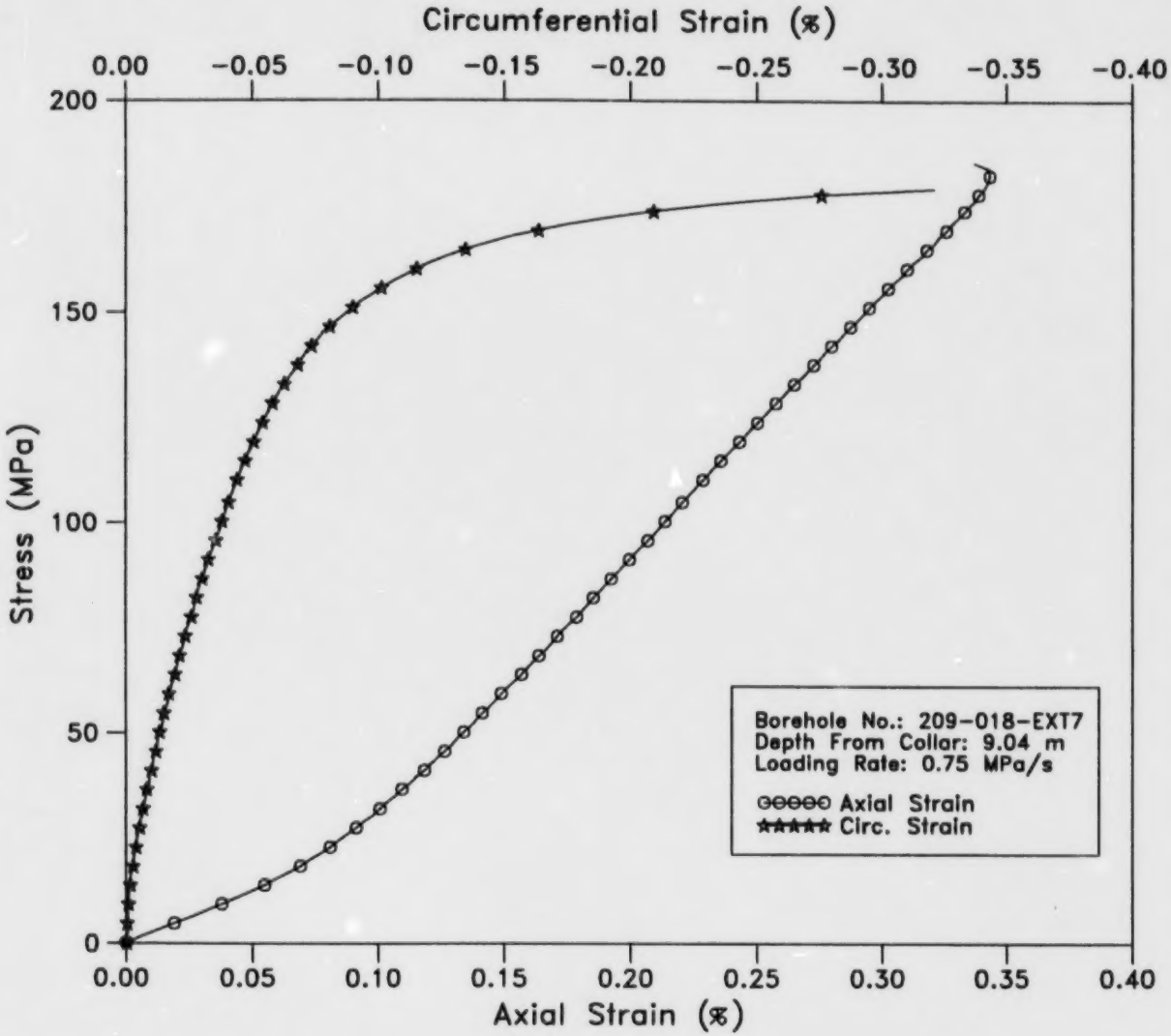

Figure A2: Stress/strain curves for Lac du Bonnet loading rate specimens

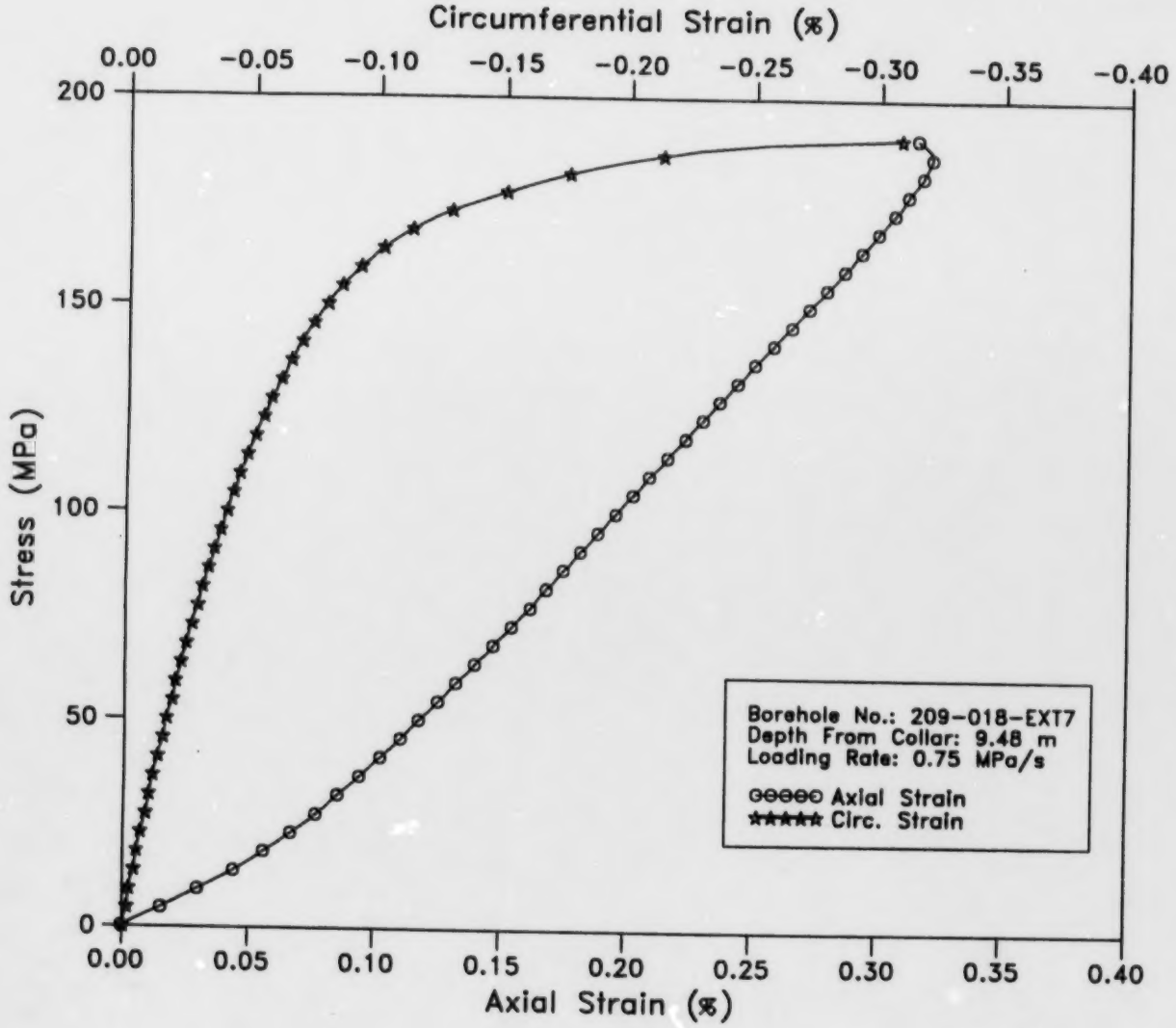

Figure A3: Stress/strain curves for Lac du Bonnet loading rate specimens

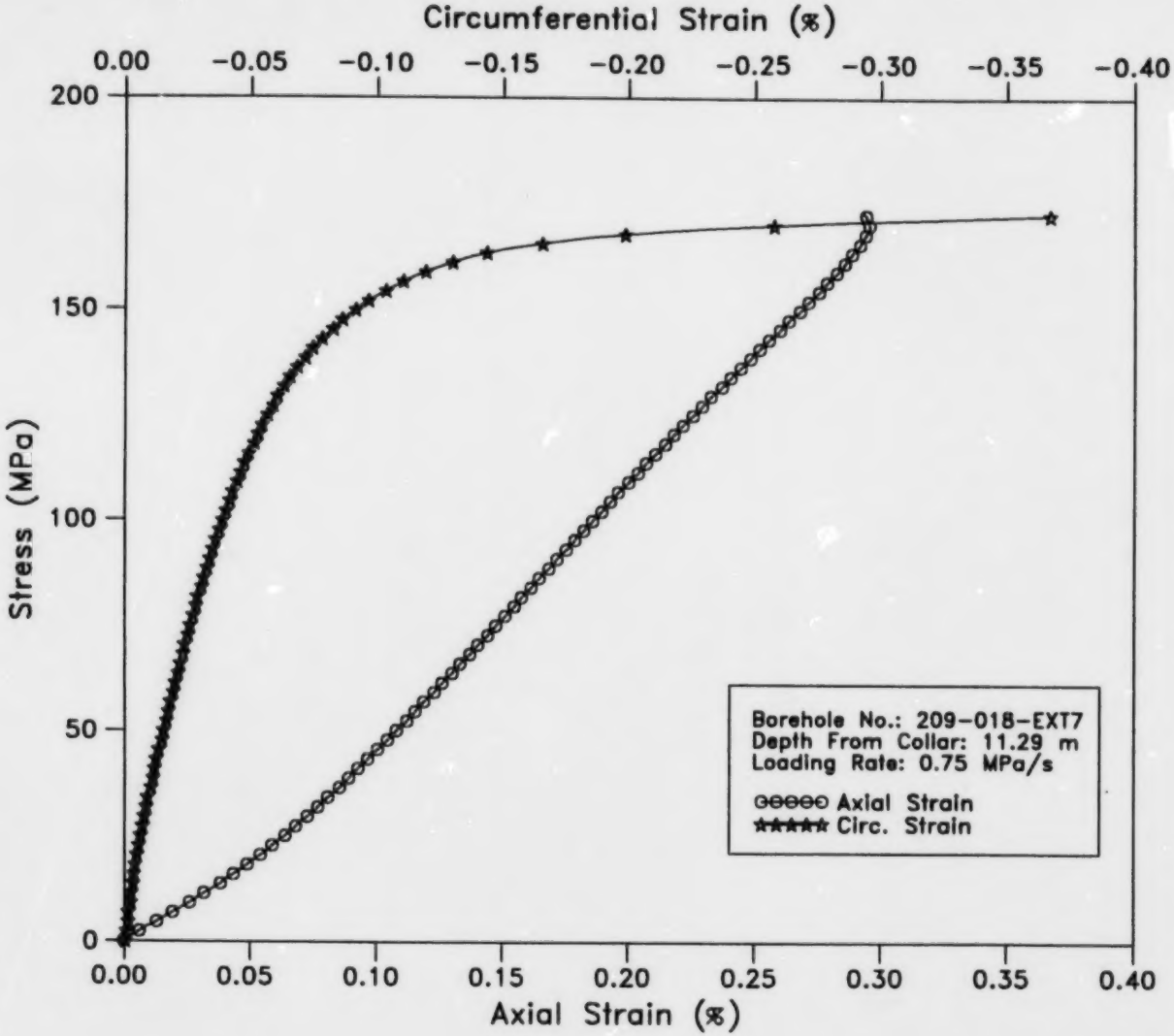

Figure A4: Stress/strain curves for Lac du Bonnet loading rate specimens

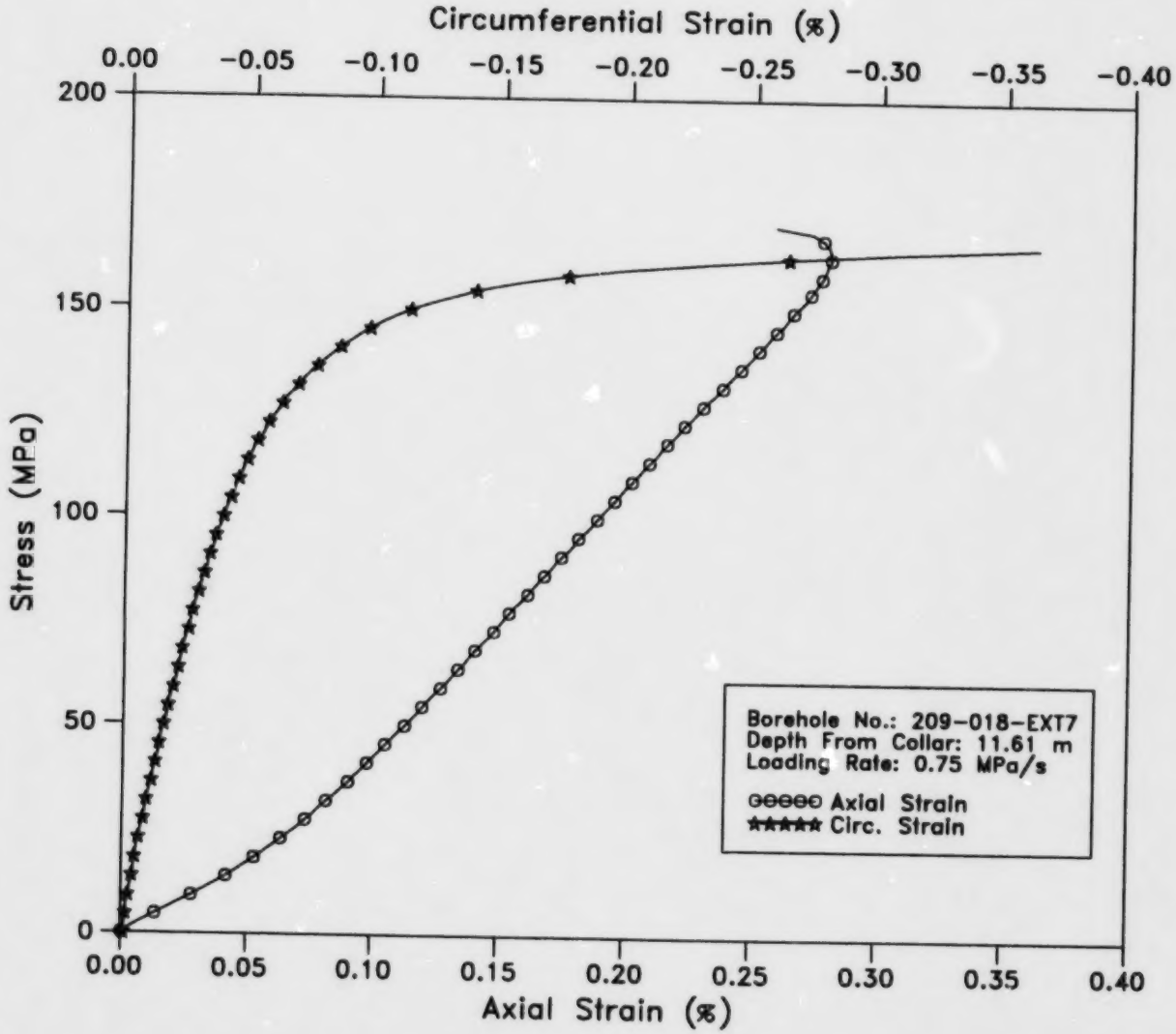

Figure A5: Stress/strain curves for Lac du Bonnet loading rate specimens

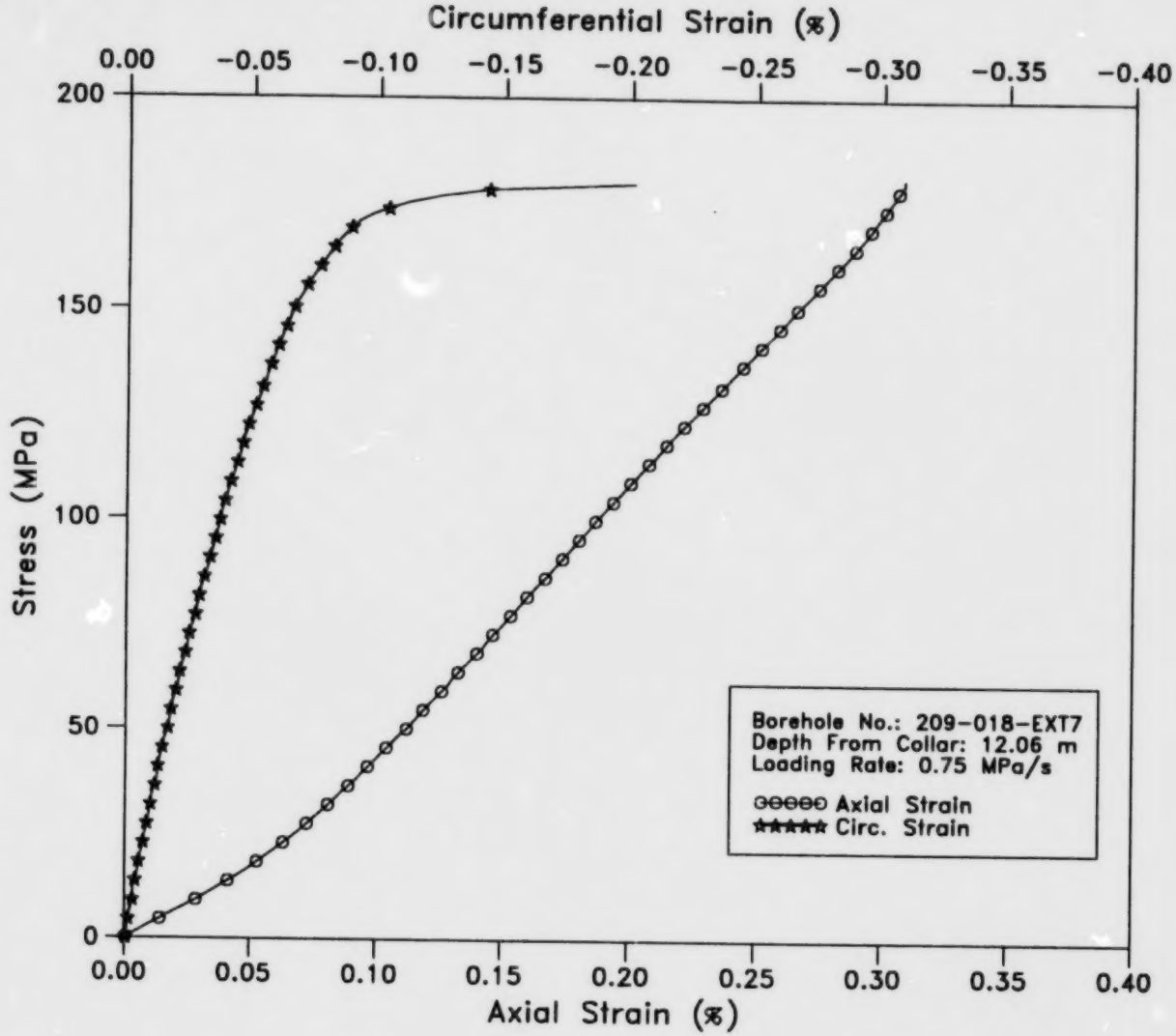

Figure A6: Stress/strain curves for Lac du Bonnet loading rate specimens

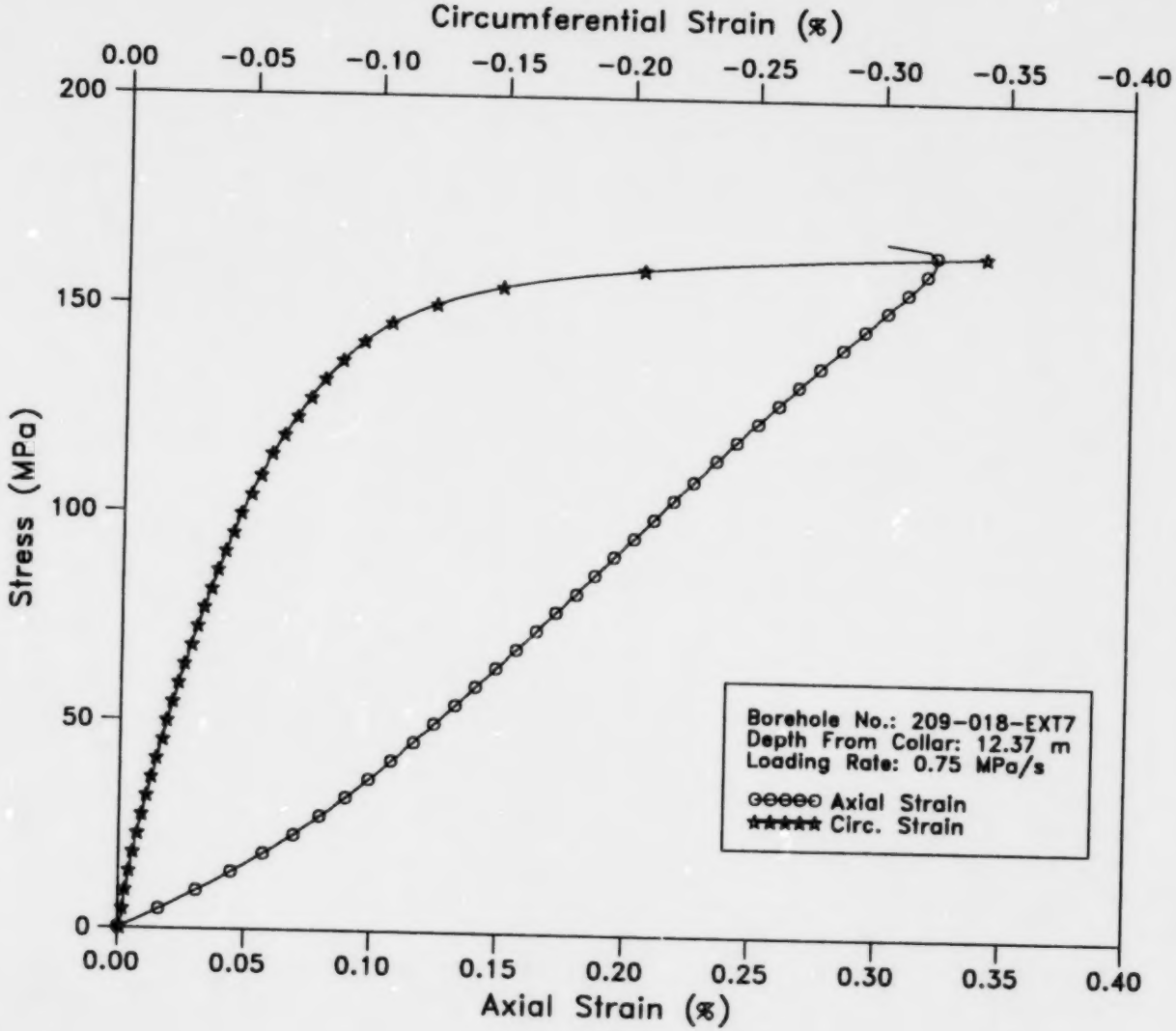

Figure A7: Stress/strain curves for Lac du Bonnet loading rate specimens

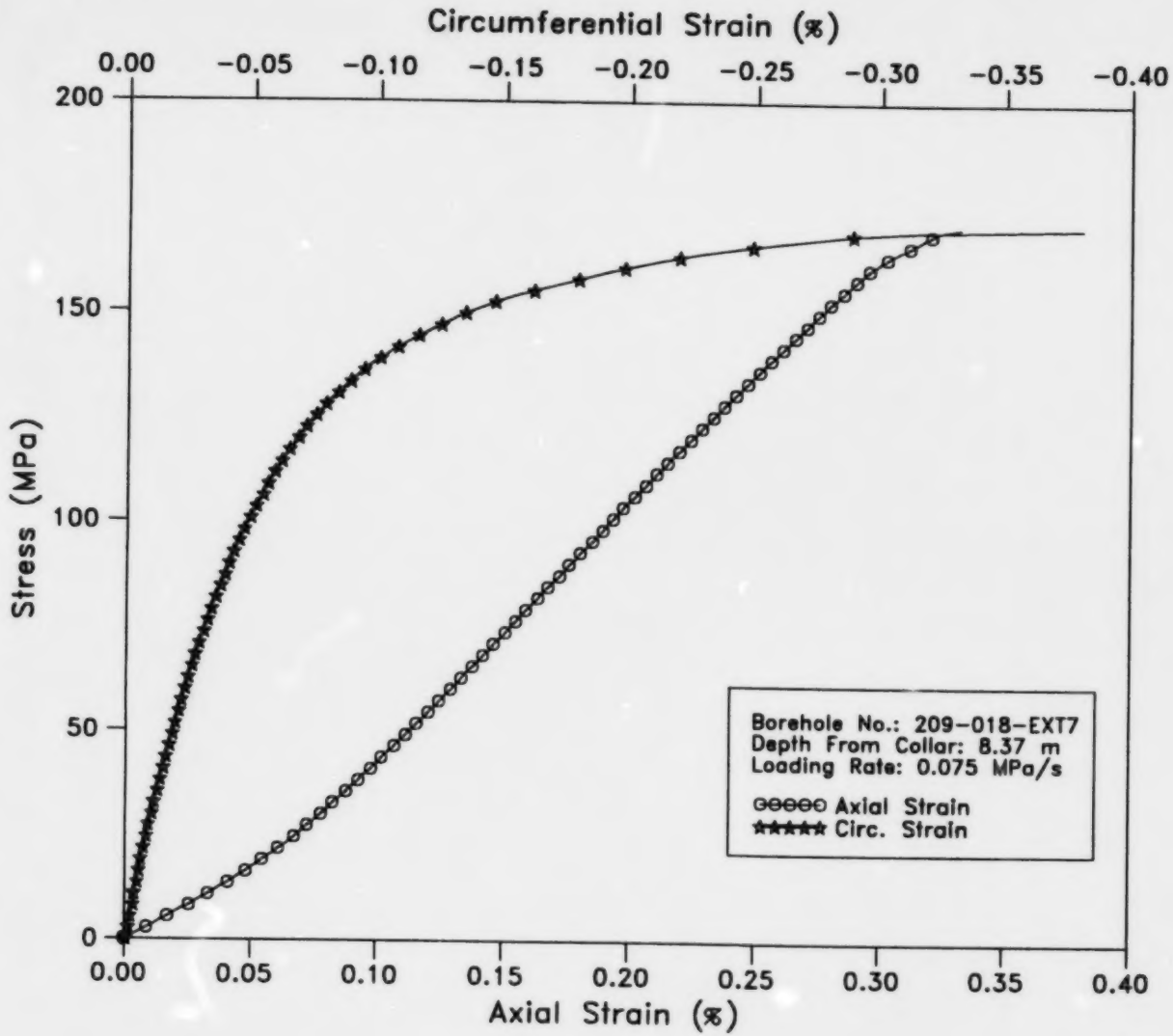

Figure A8: Stress/strain curves for Lac du Bonnet loading rate specimens

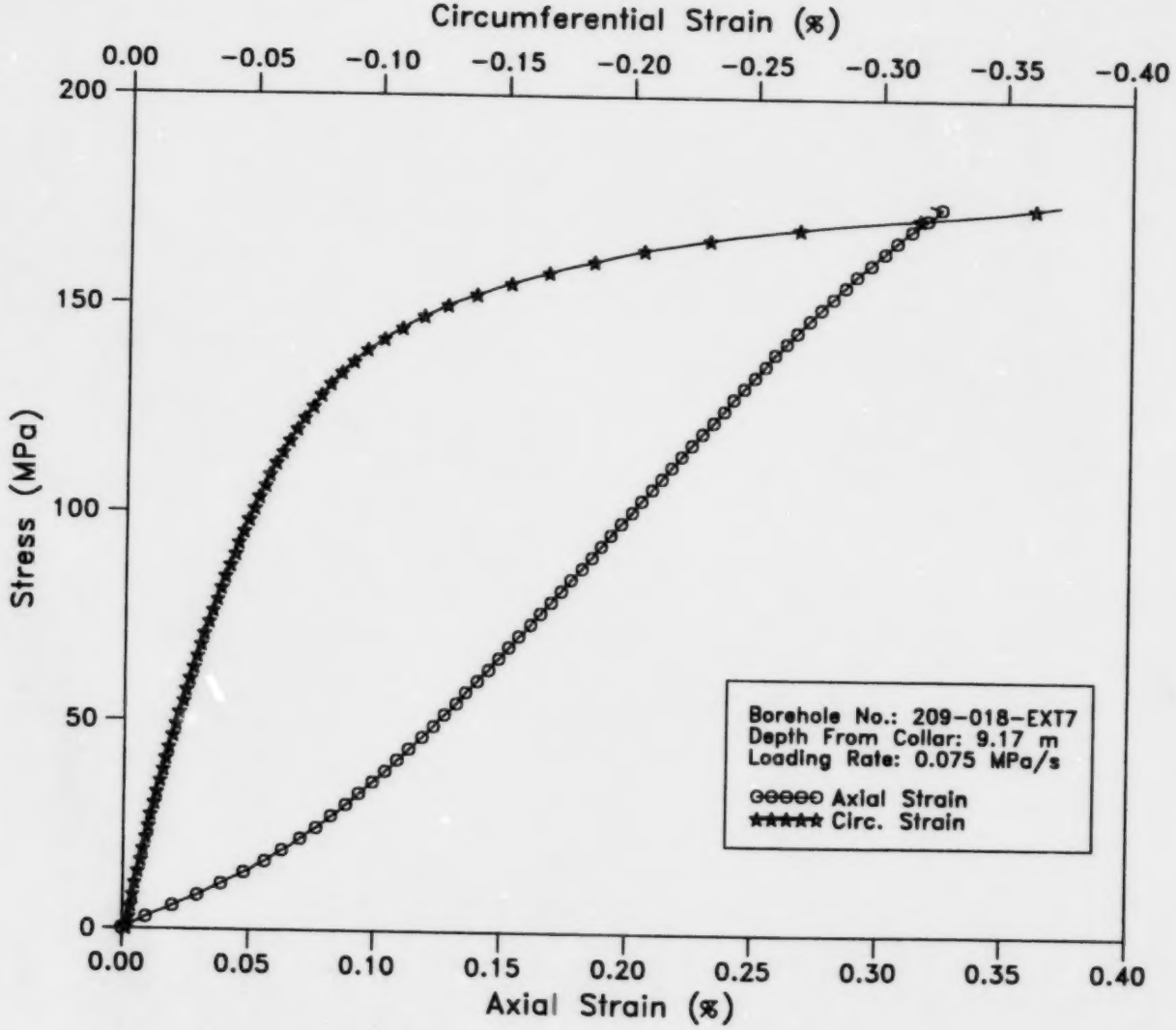

Figure A9: Stress/strain curves for Lac du Bonnet loading rate specimens

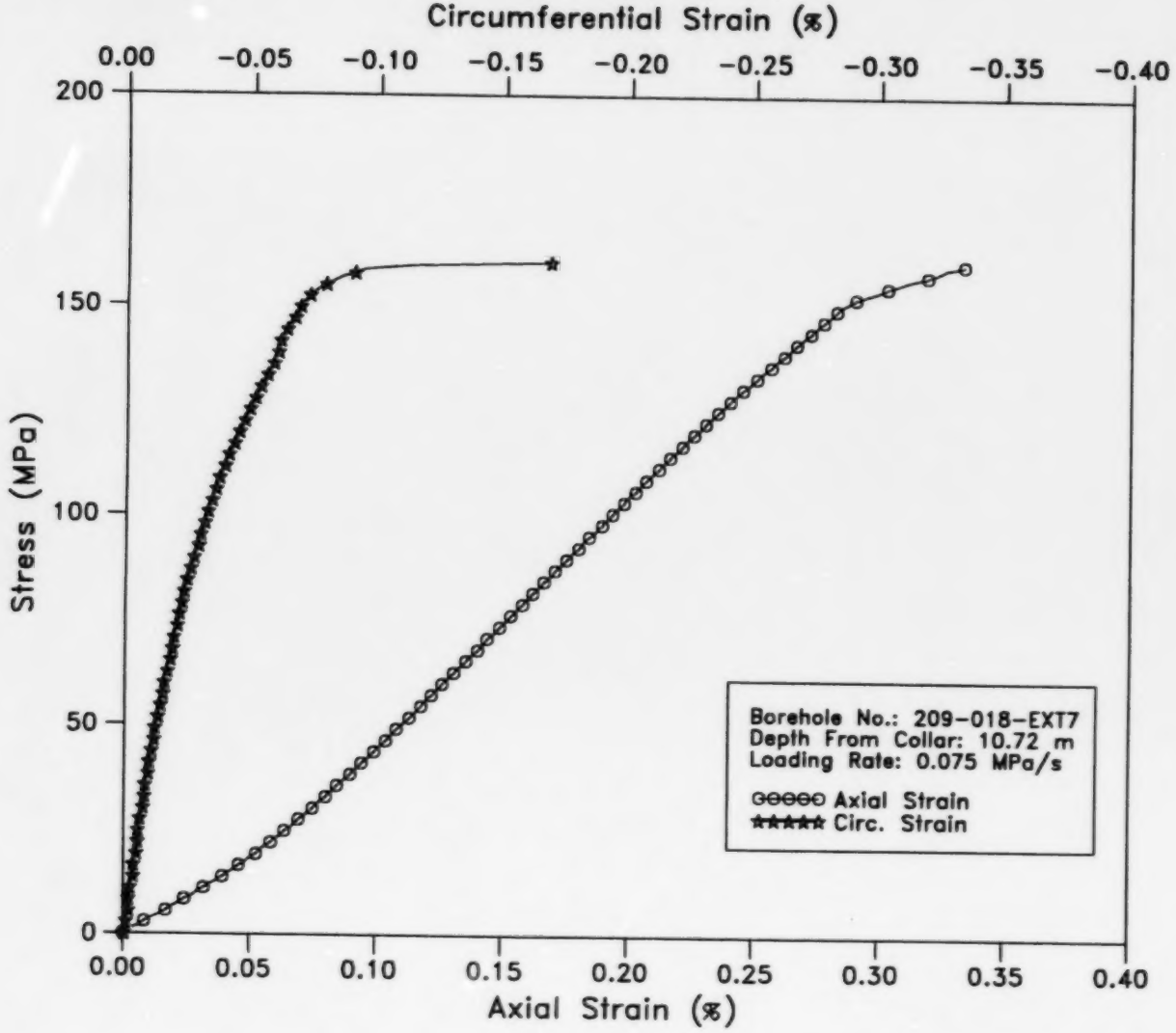

Figure A10: Stress/strain curves for Lac du Bonnet loading rate specimens

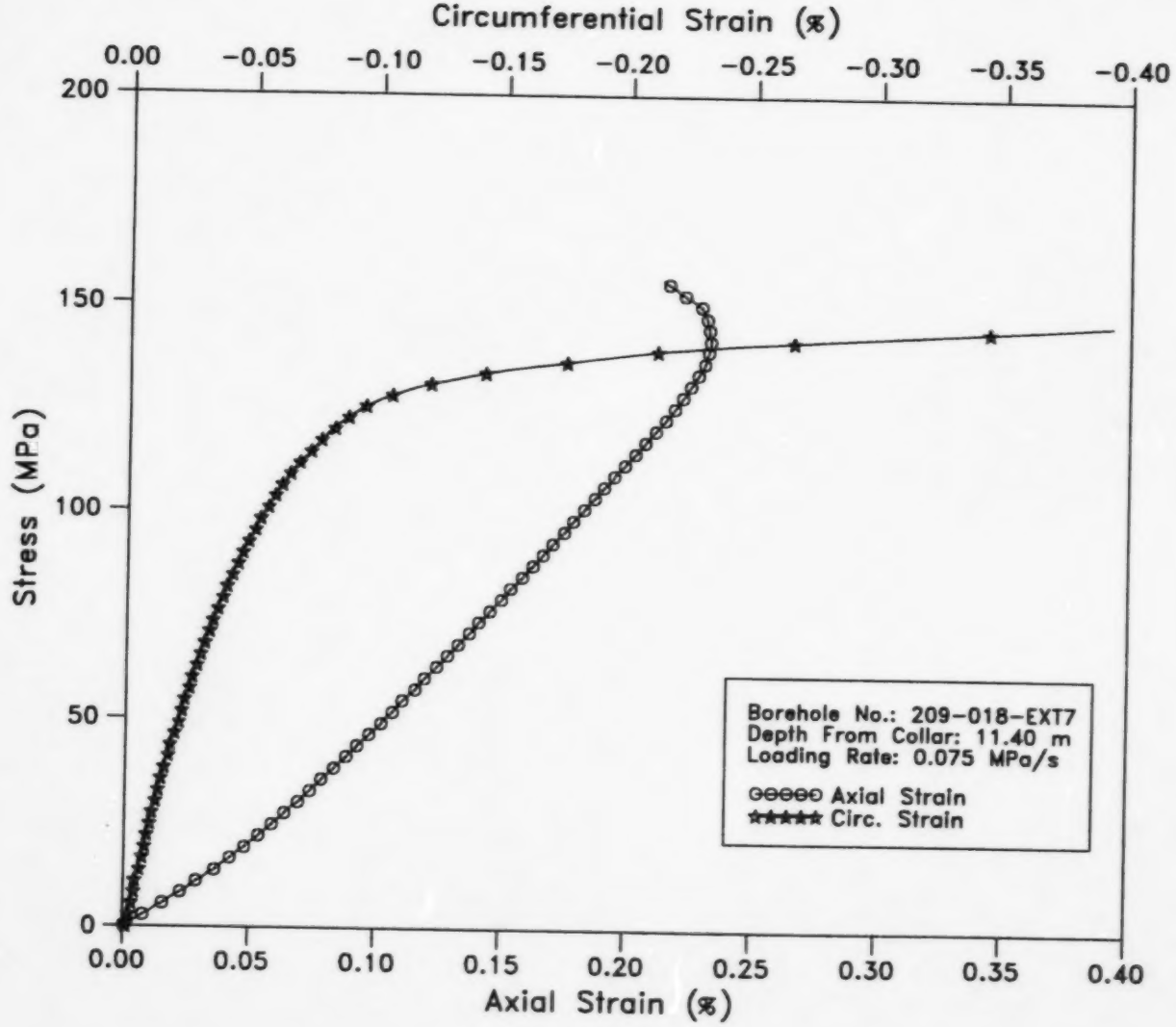

Figure A11: Stress/strain curves for Lac du Bonnet loading rate specimens

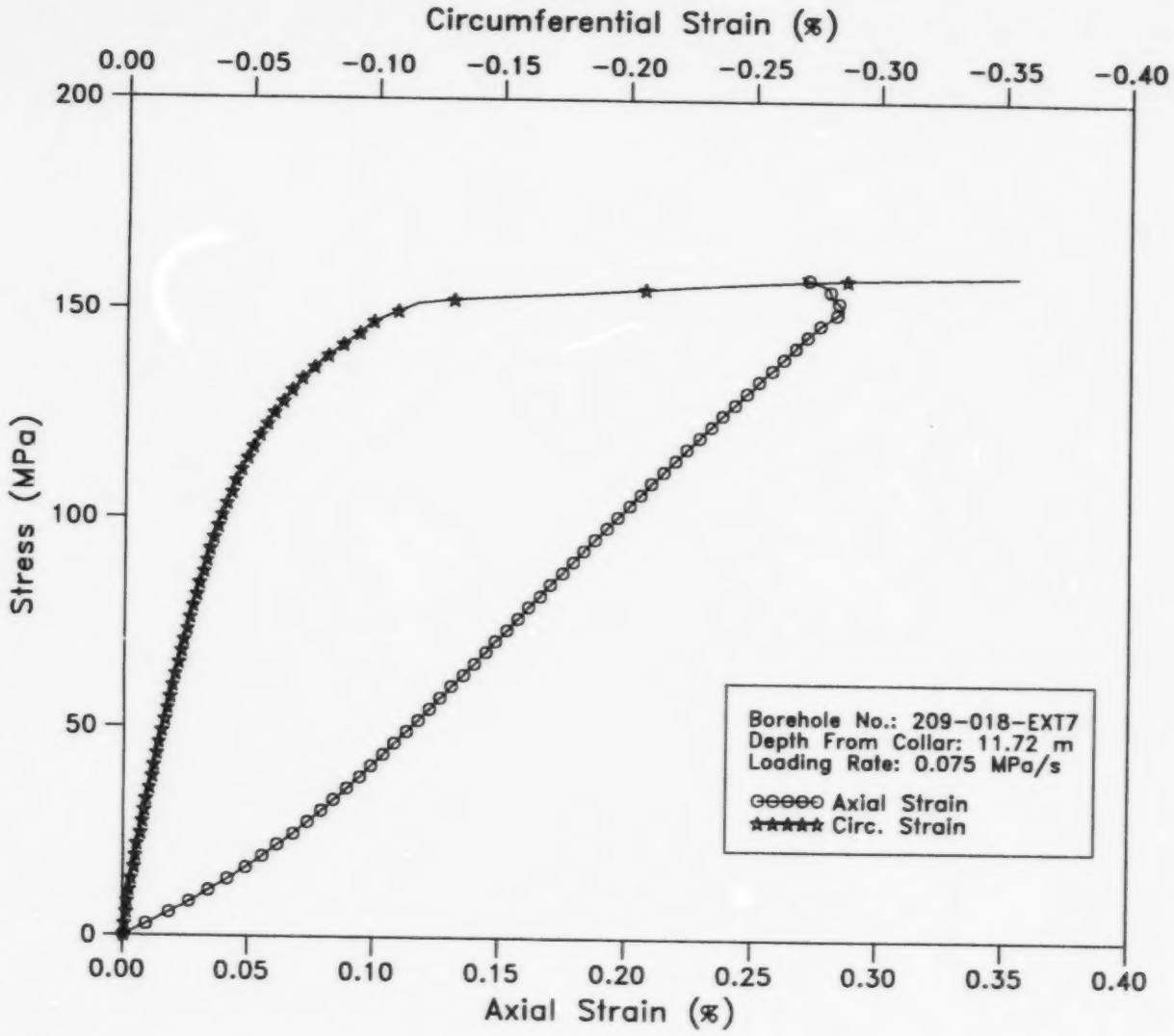

Figure A12: Stress/strain curves for Lac du Bonnet loading rate specimens

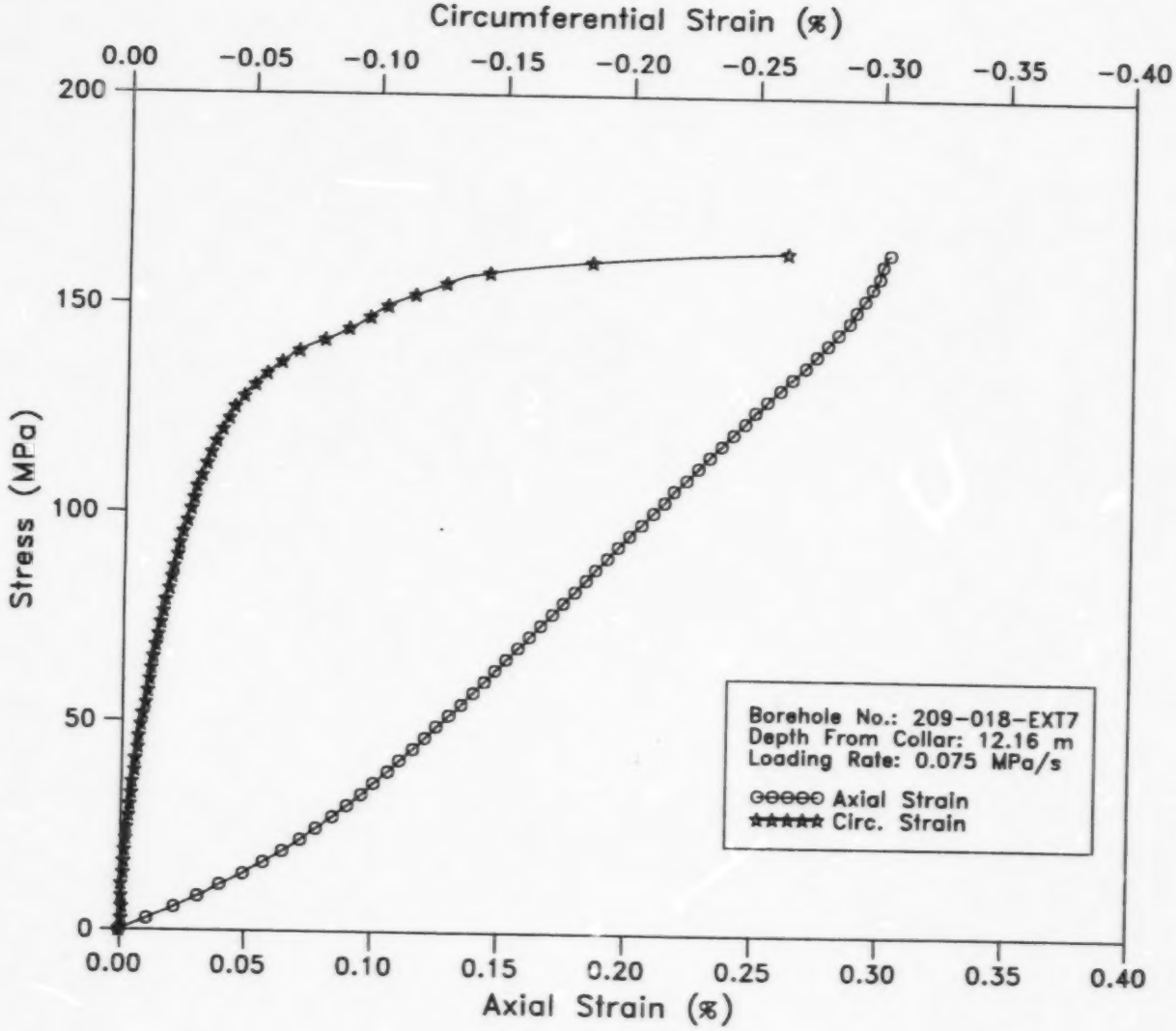

Figure A13: Stress/strain curves for Lac du Bonnet loading rate specimens

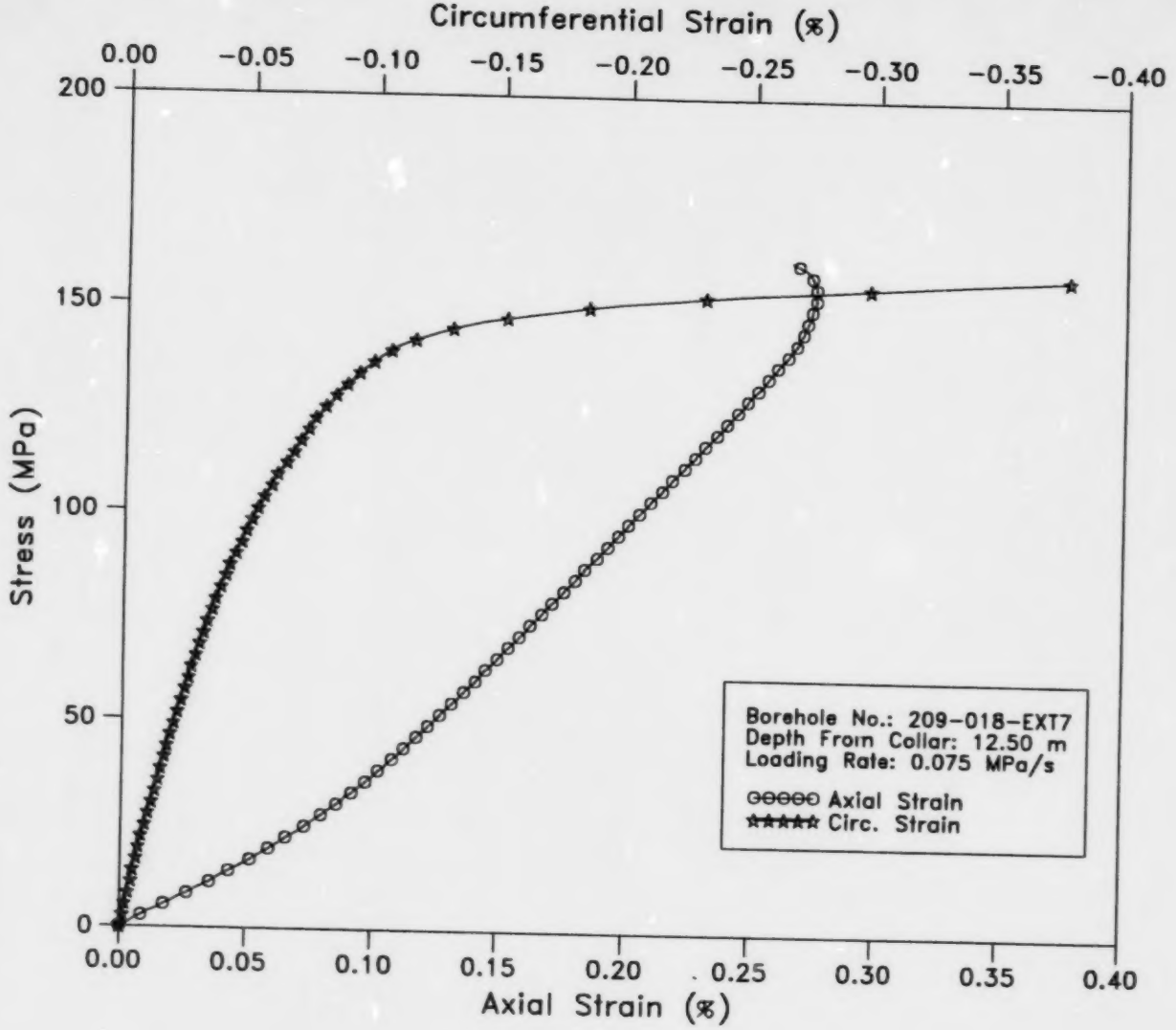

Figure A14: Stress/strain curves for Lac du Bonnet loading rate specimens

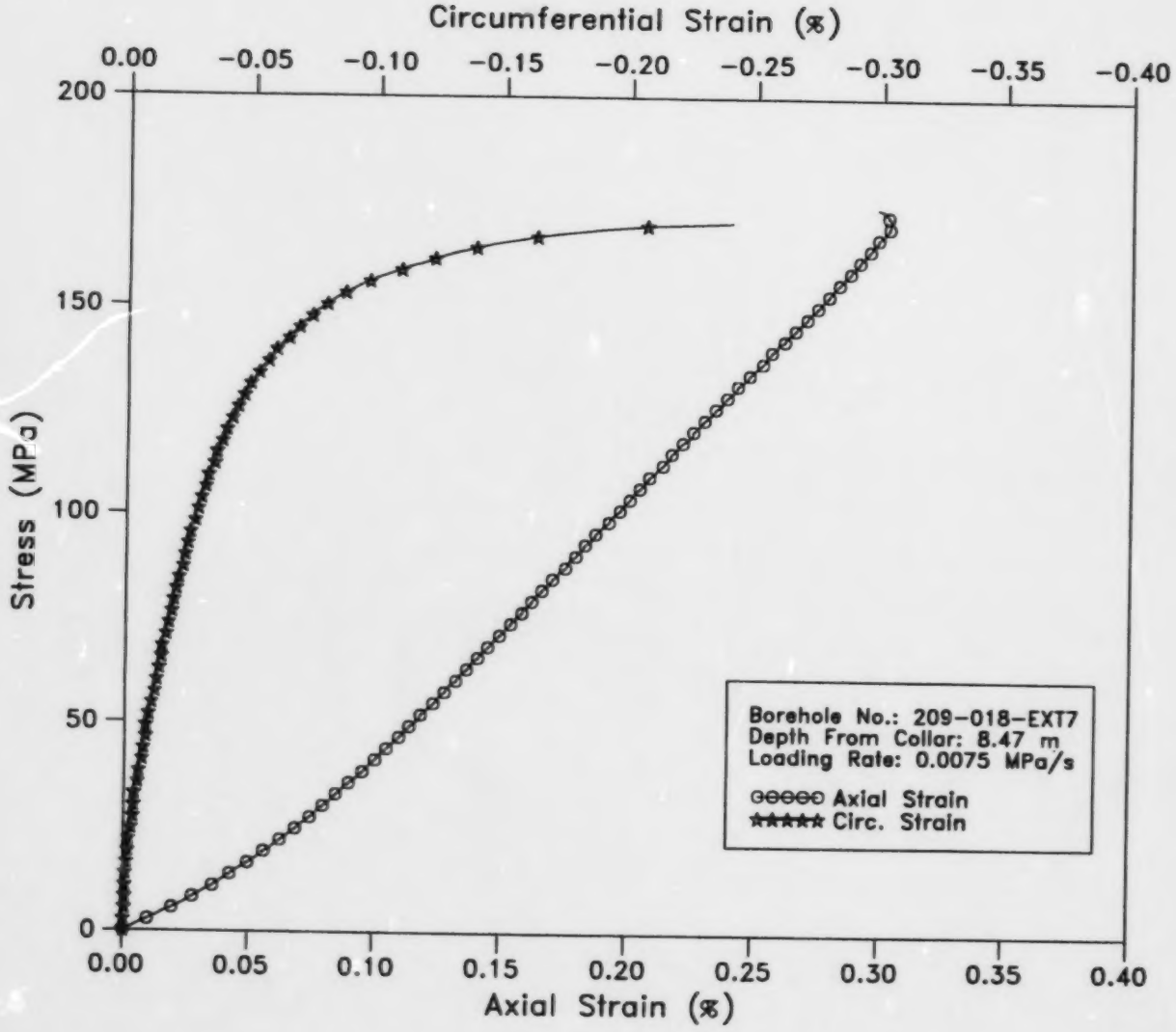

Figure A15: Stress/strain curves for Lac du Bonnet loading rate specimens

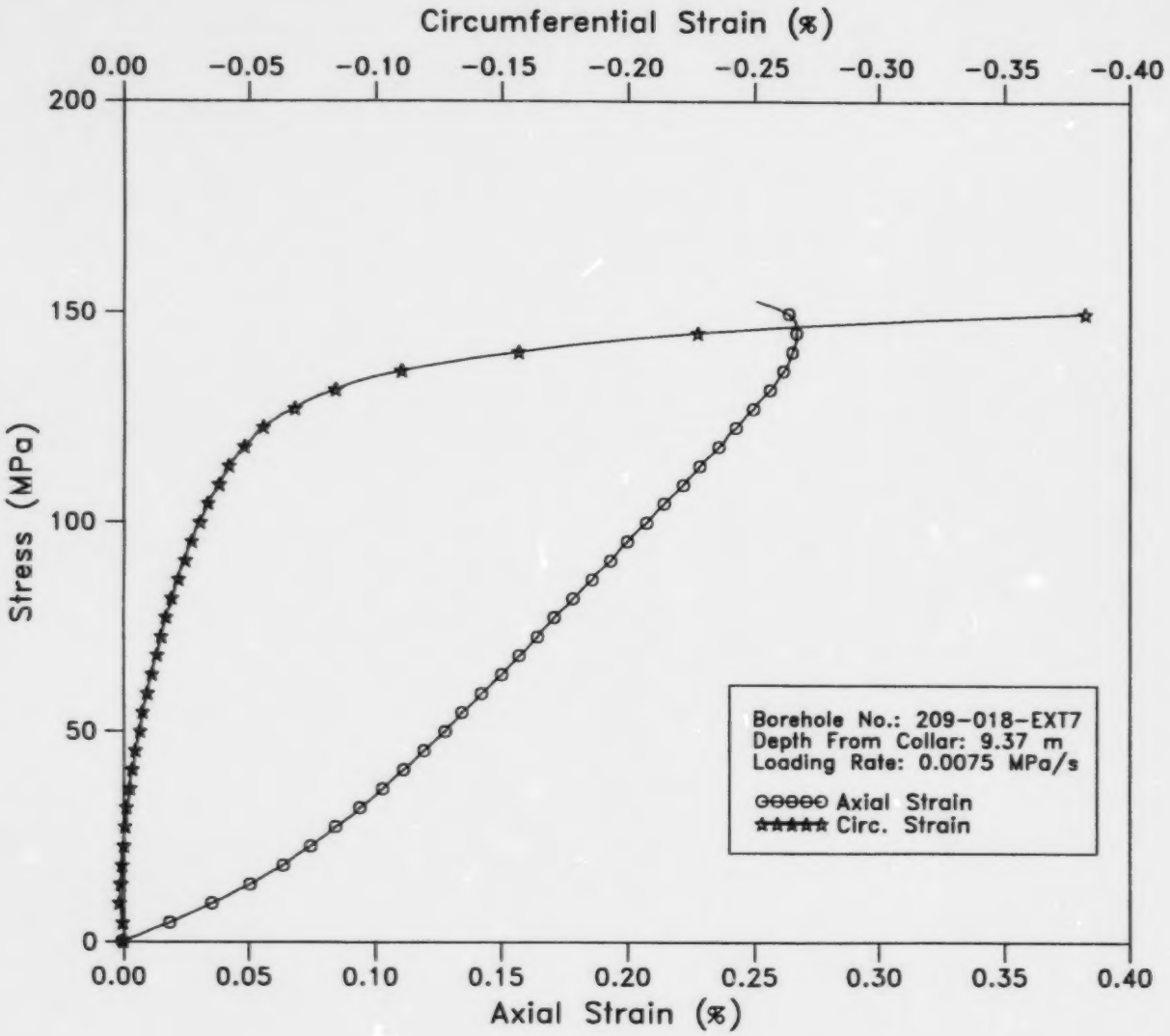

Figure A16: Stress/strain curves for Lac du Bonnet loading rate specimens

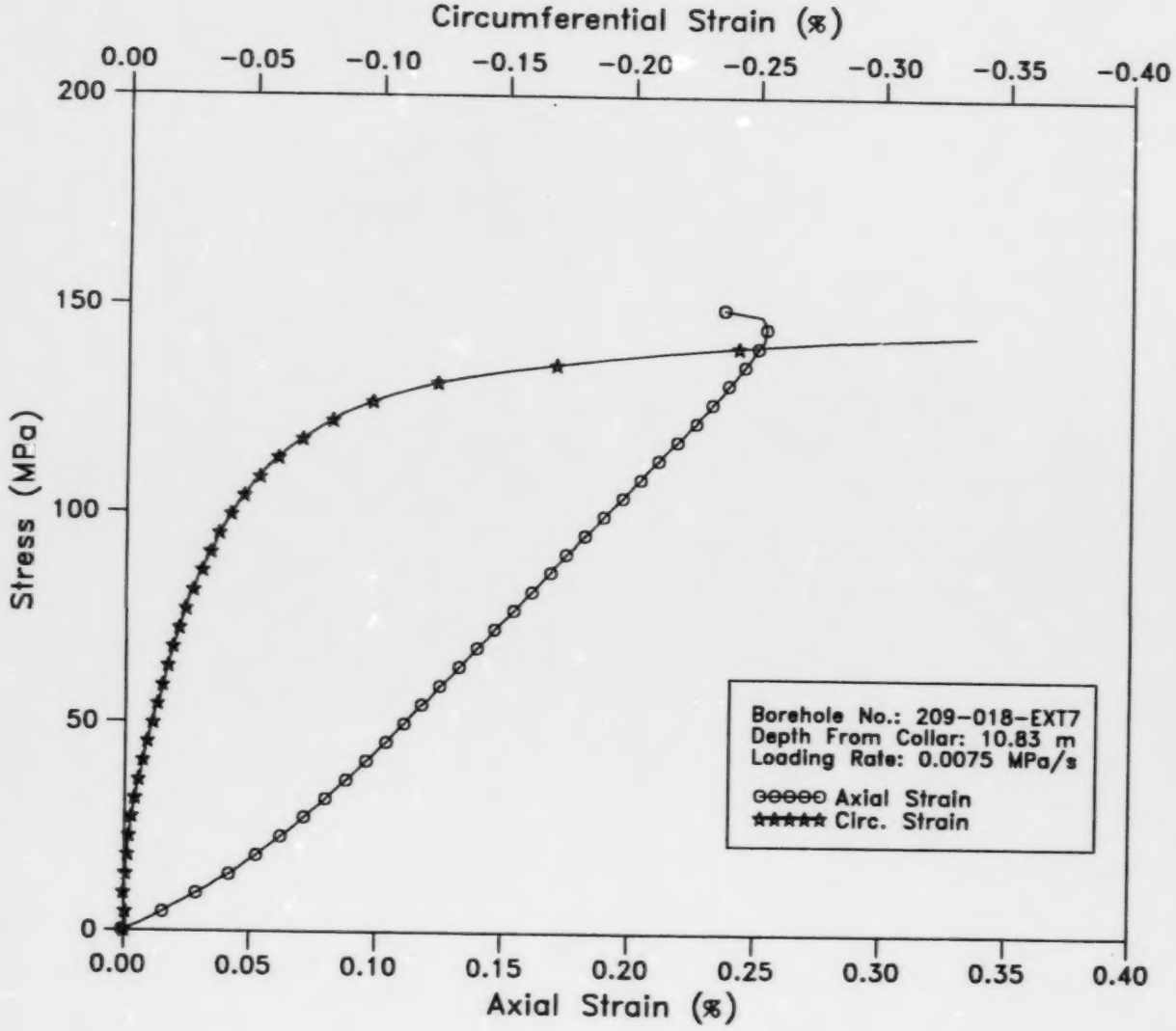

Figure A17: Stress/strain curves for Lac du Bonnet loading rate specimens

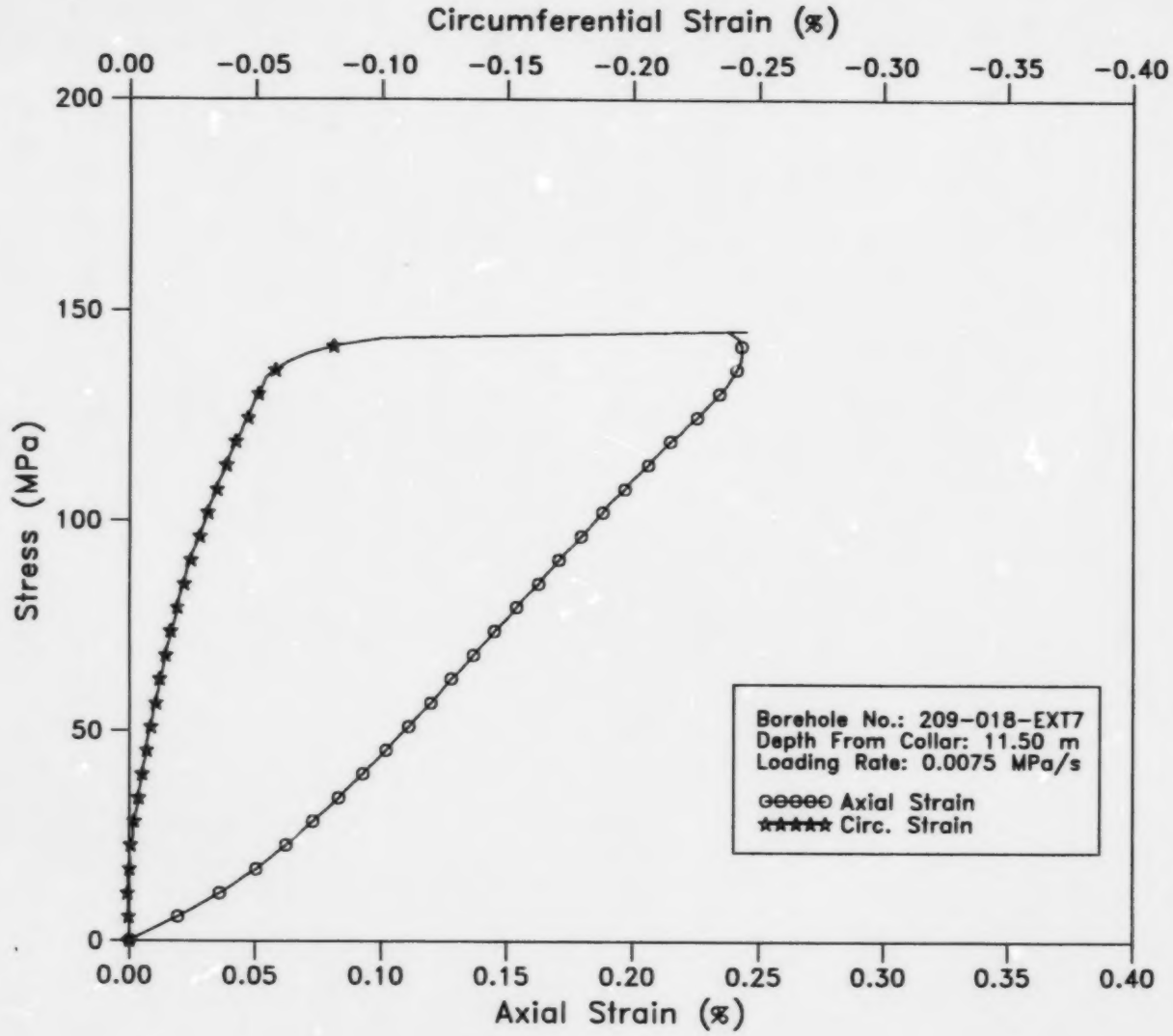

Figure A18: Stress/strain curves for Lac du Bonnet loading rate specimens

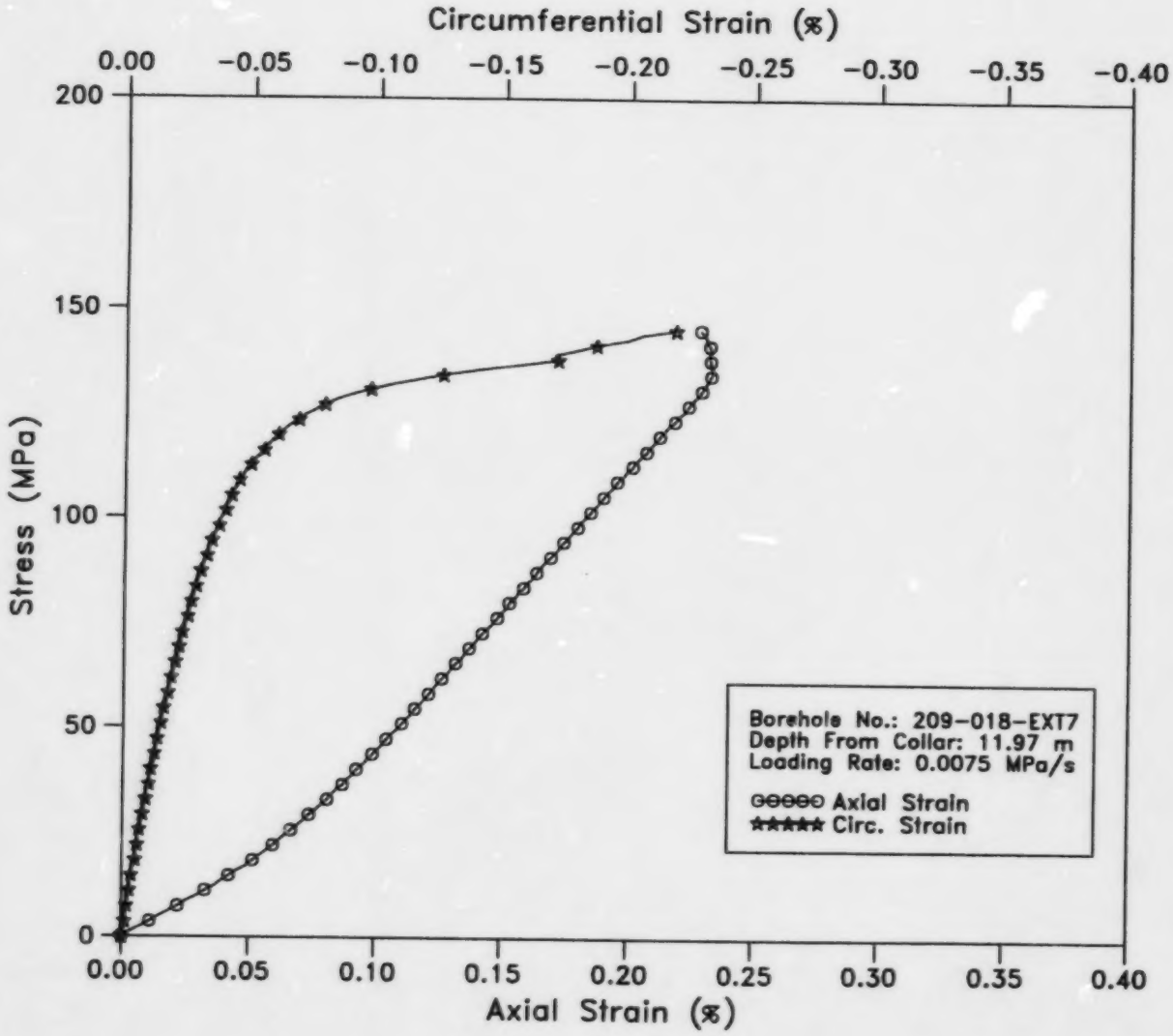

Figure A19: Stress/strain curves for Lac du Bonnet loading rate specimens

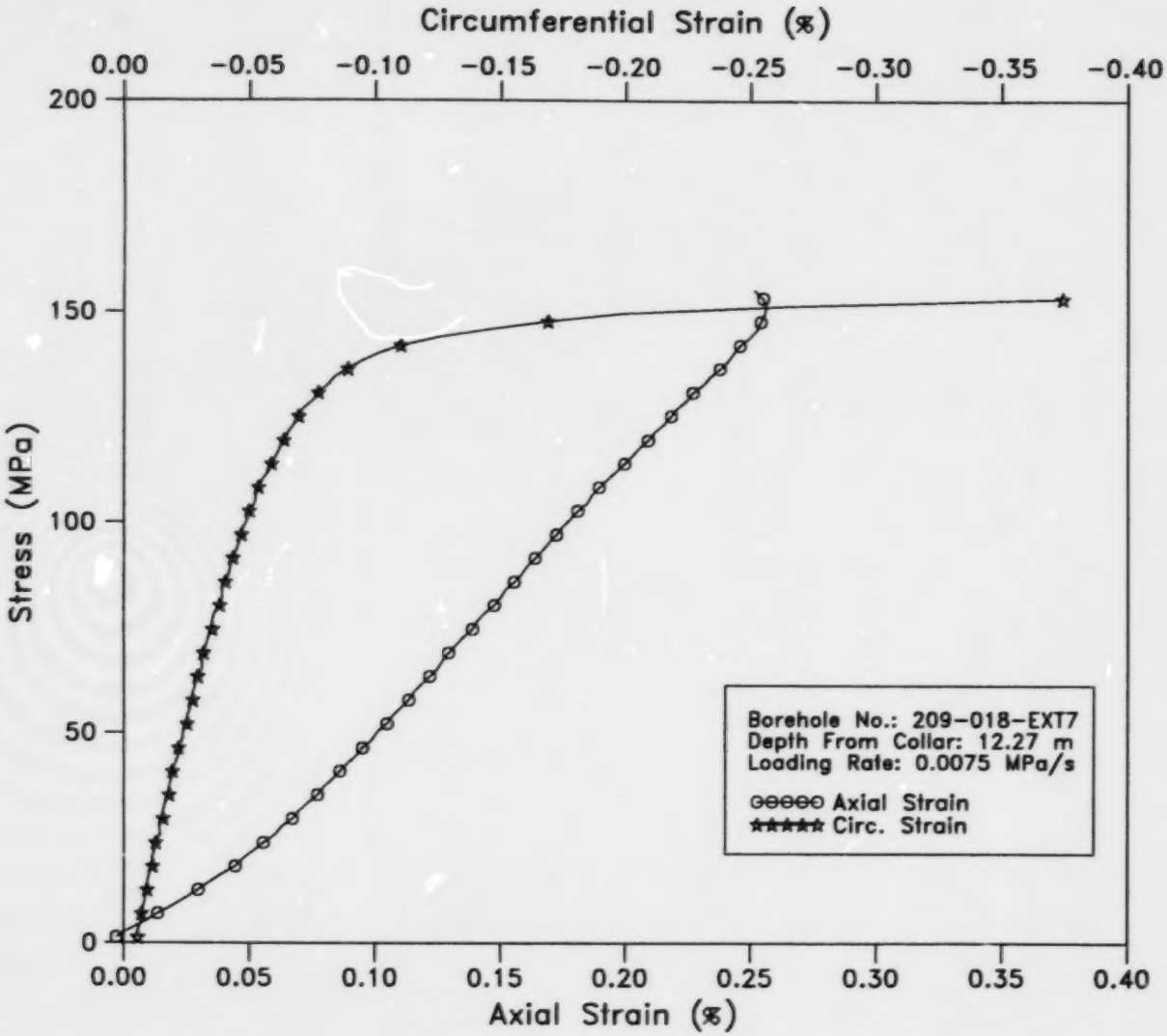

Figure A20: Stress/strain curves for Lac du Bonnet loading rate specimens

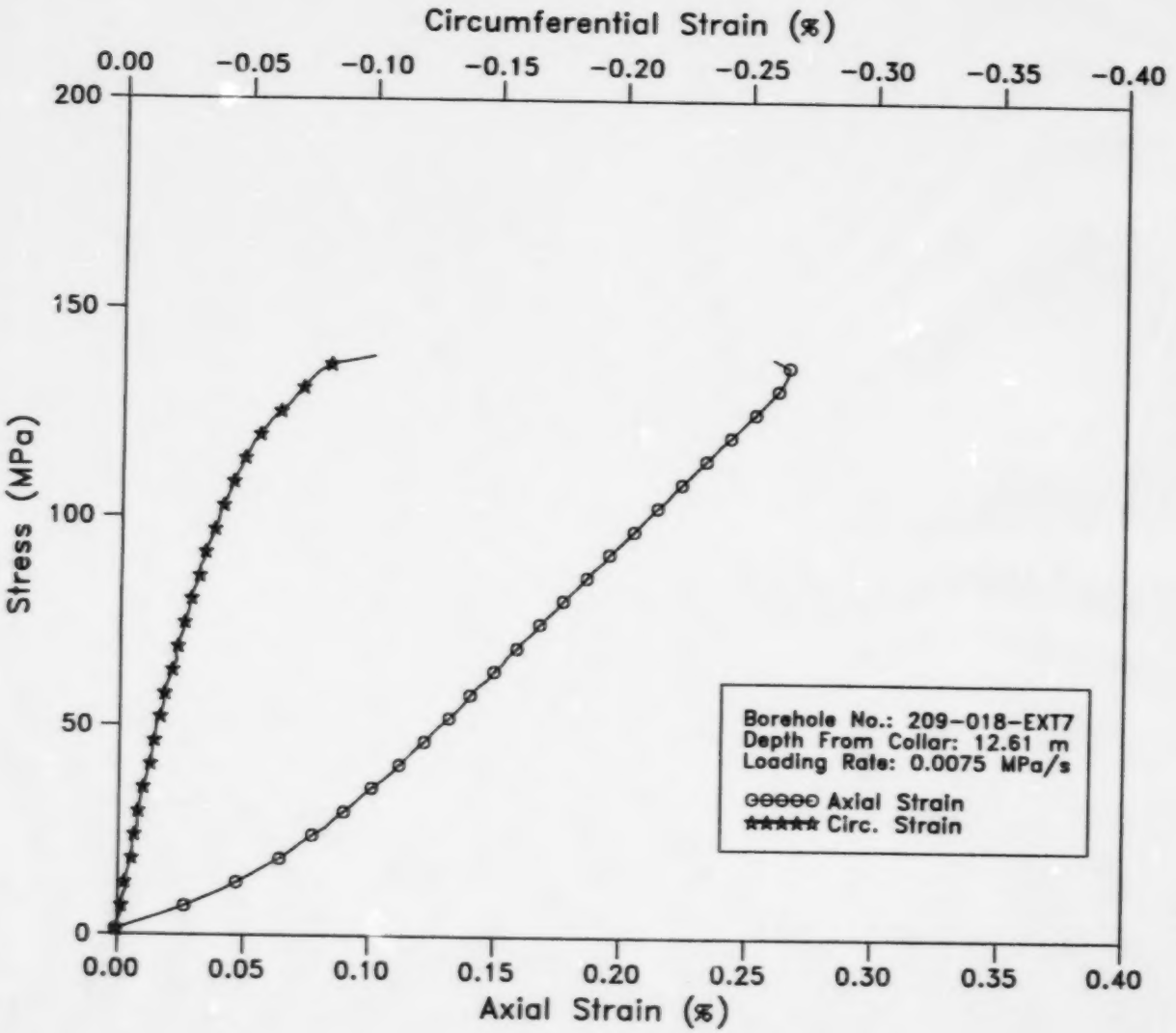

Figure A21: Stress/strain curves for Lac du Bonnet loading rate specimens

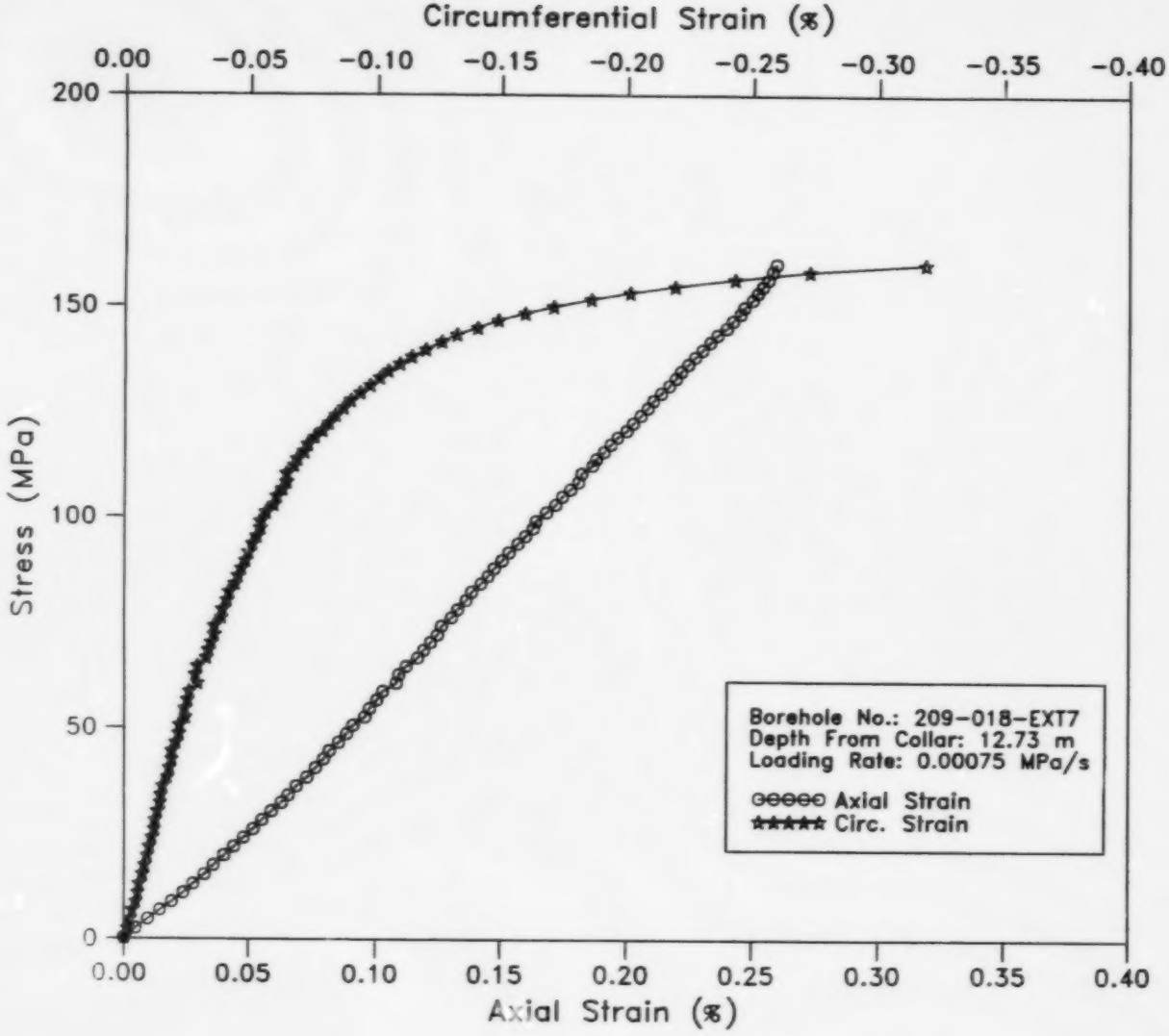

Figure A22: Stress/strain curves for Lac du Bonnet loading rate specimens

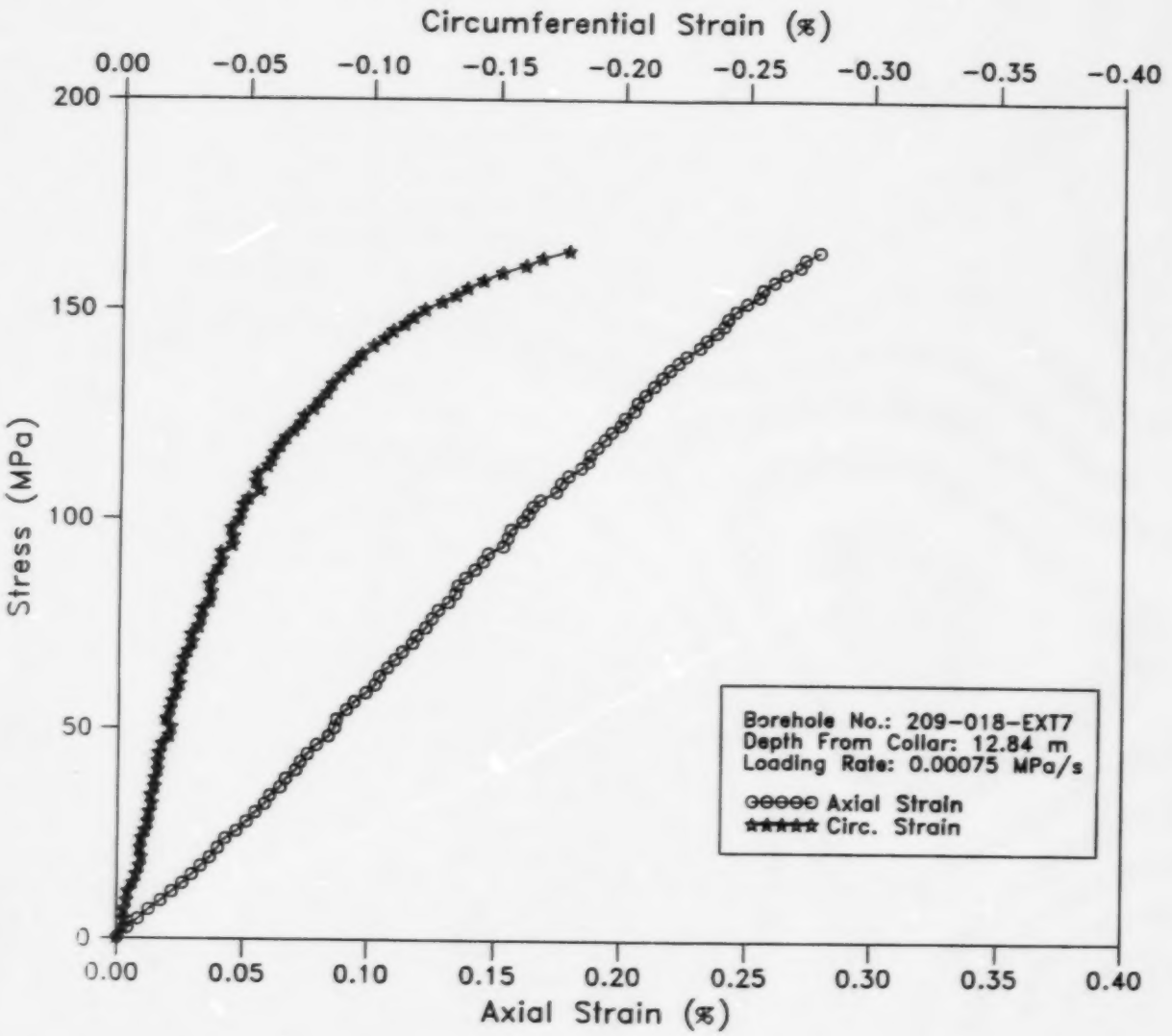

Figure A23: Stress/strain curves for Lac du Bonnet loading rate specimens

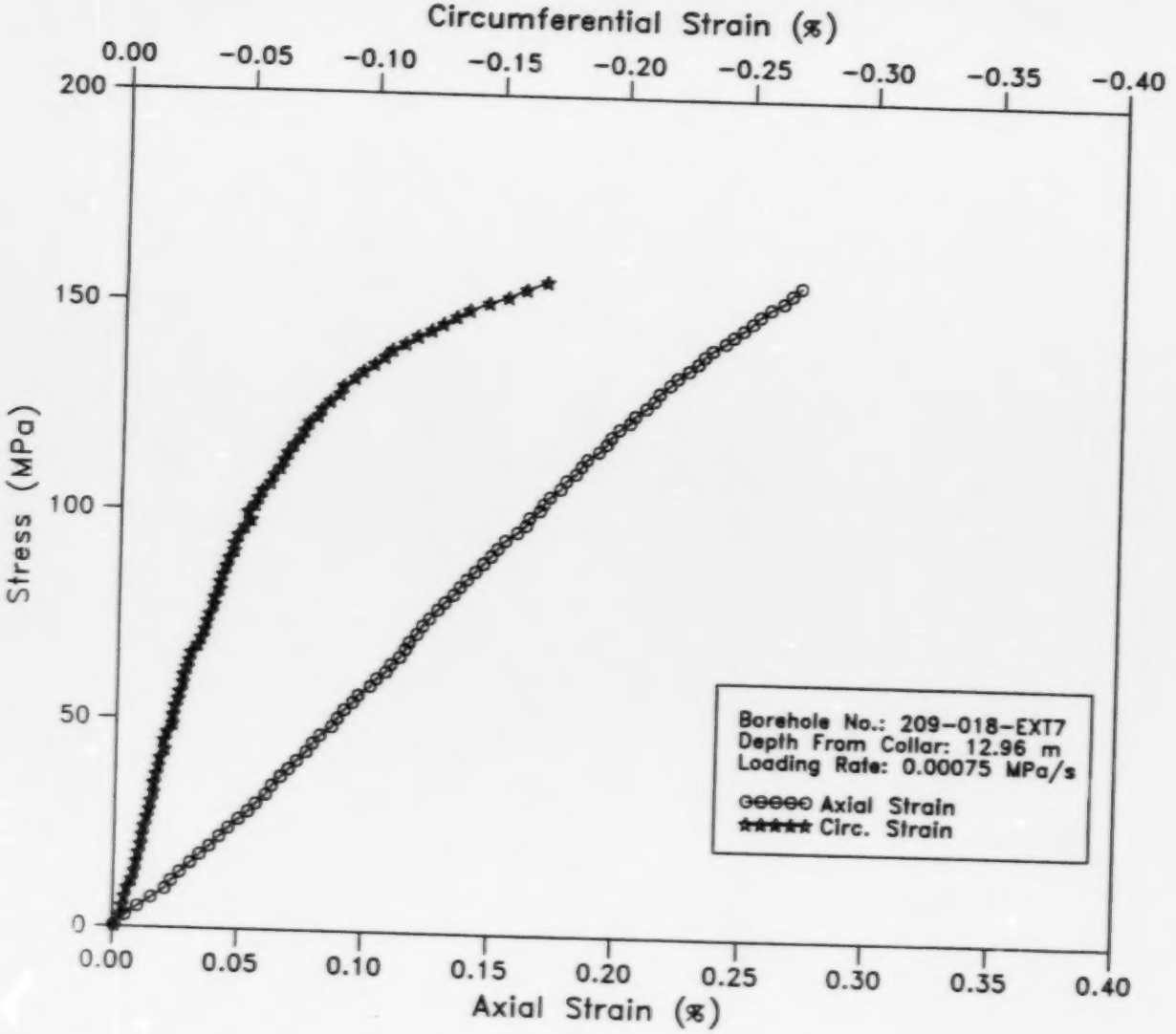

Figure A24: Stress/strain curves for Lac du Bonnet loading rate specimens

Appendix B

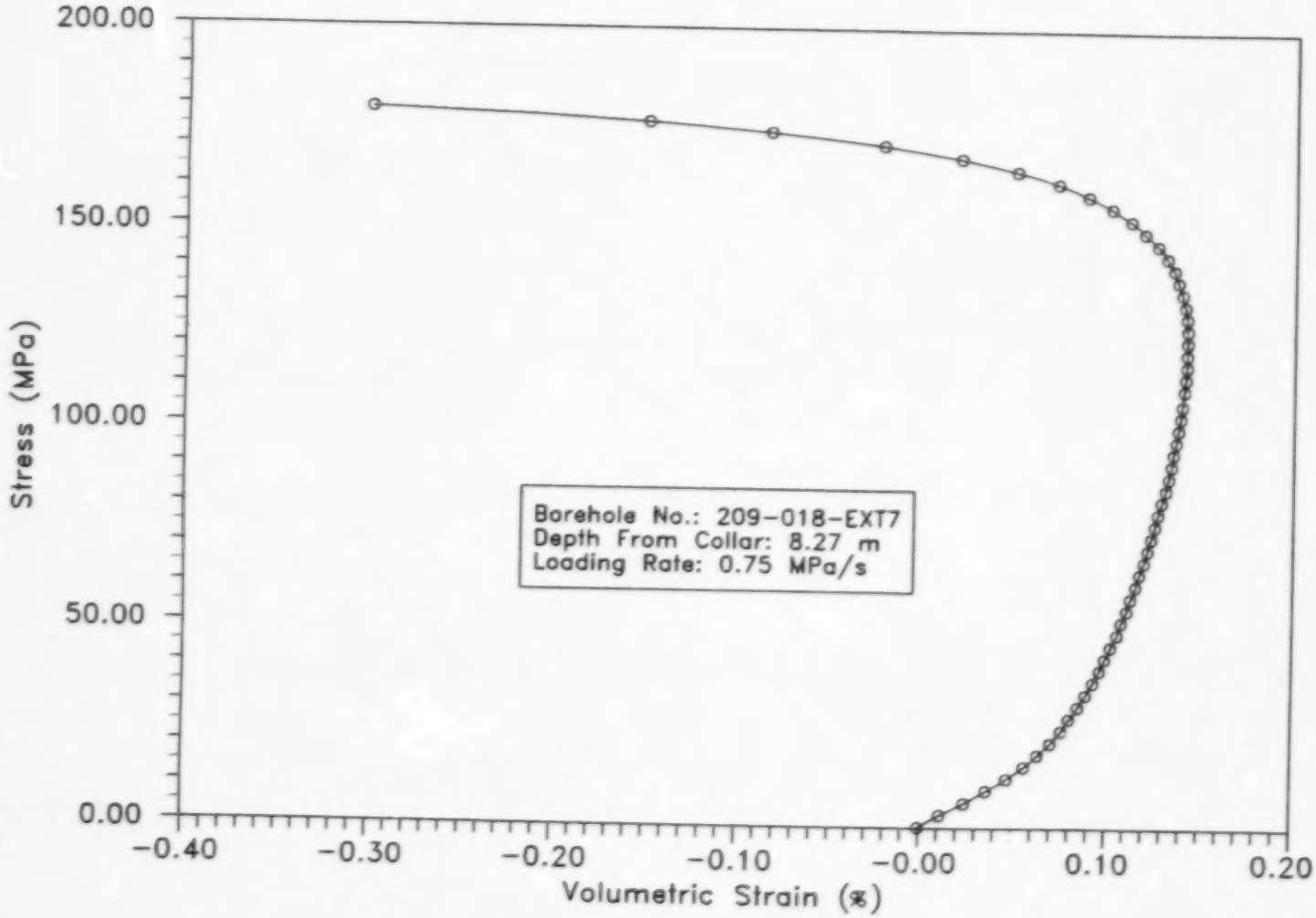

Figure B1: Volumetric Strain vs. Stress, Lac du Bonnet Loading Rate Specimens

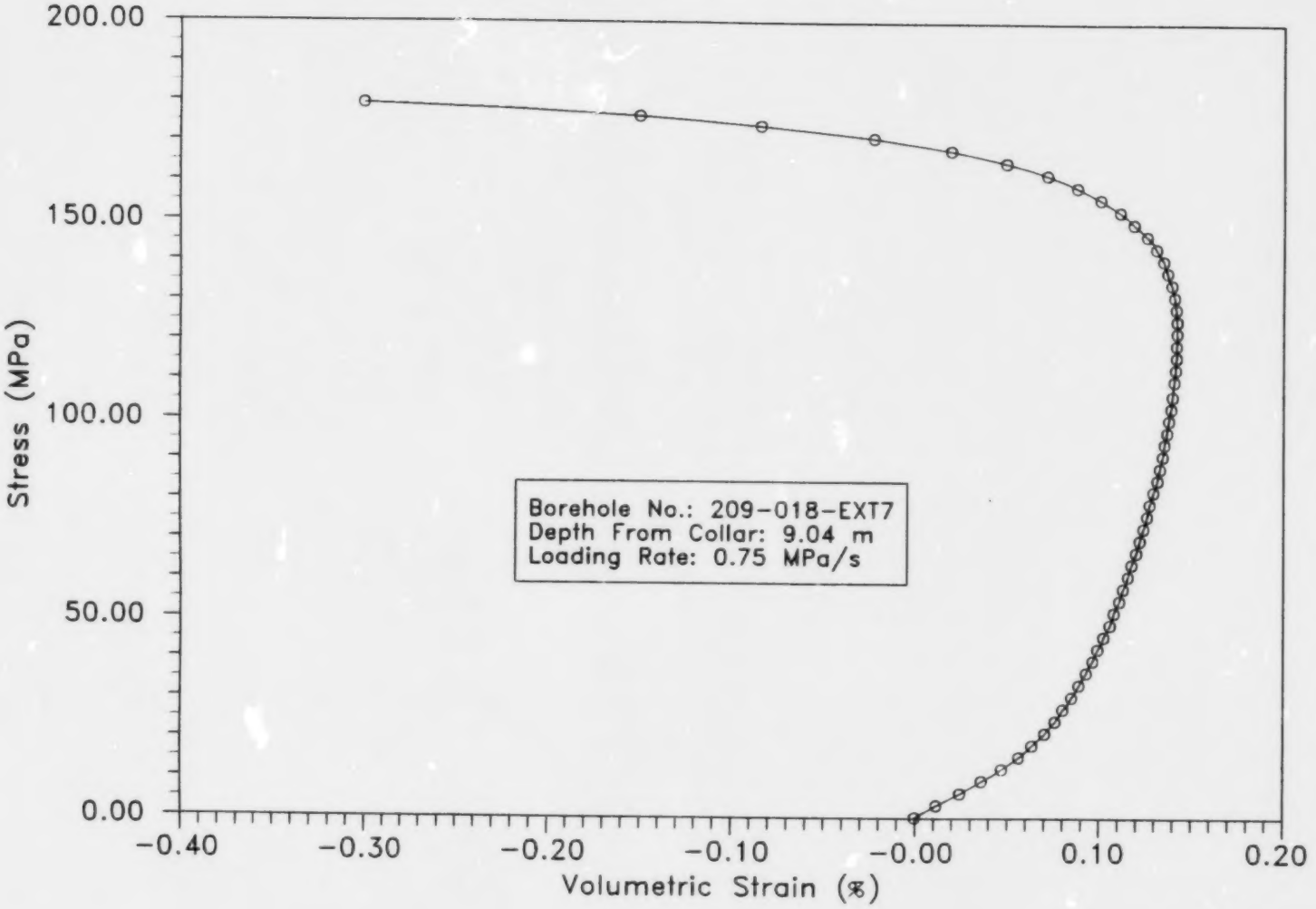

Figure B2: Volumetric Strain vs. Stress, Lac du Bonnet Loading Rate Specimens

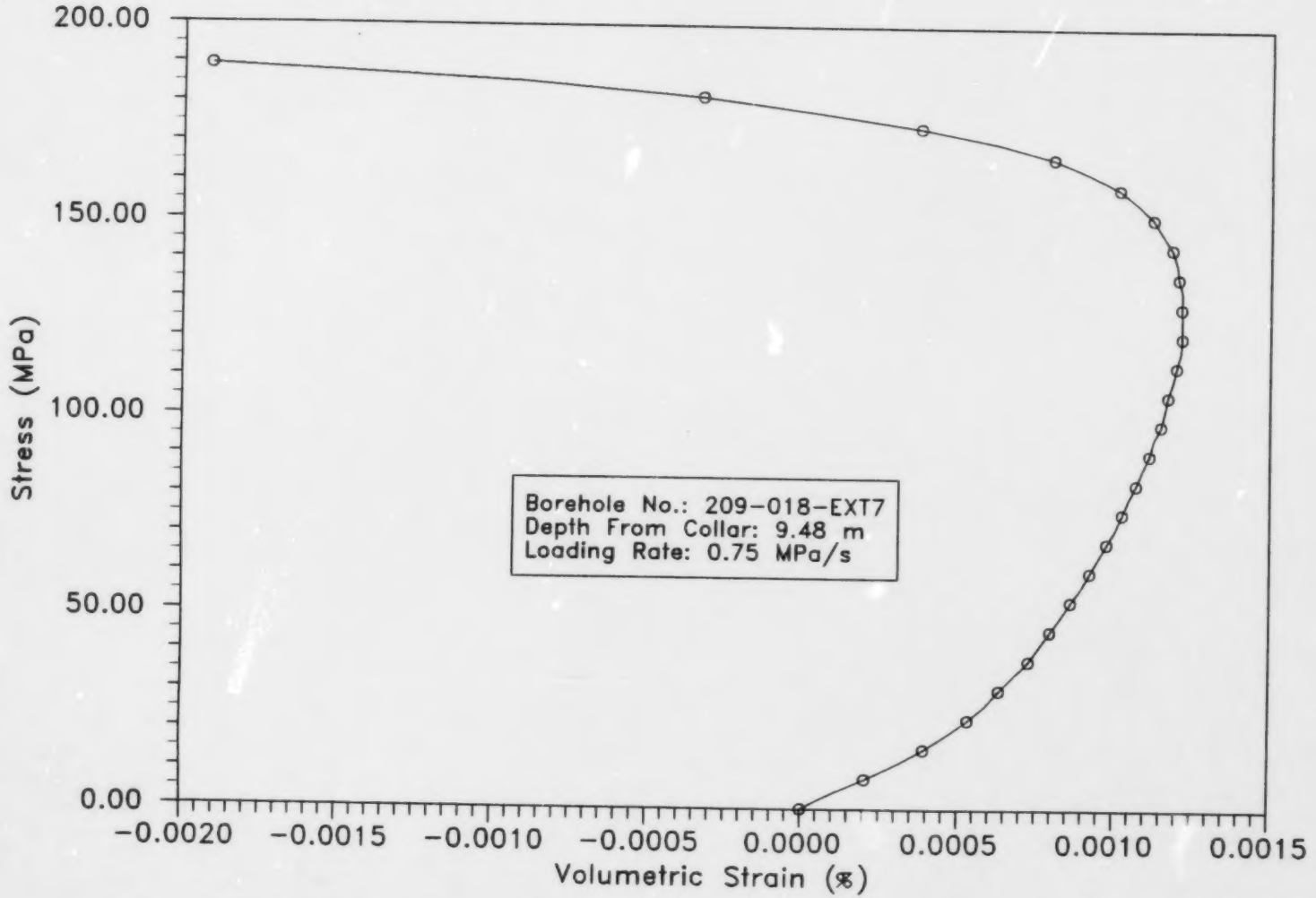

Figure B3: Volumetric Strain vs. Stress, Lac du Bonnet Loading Rate Specimens

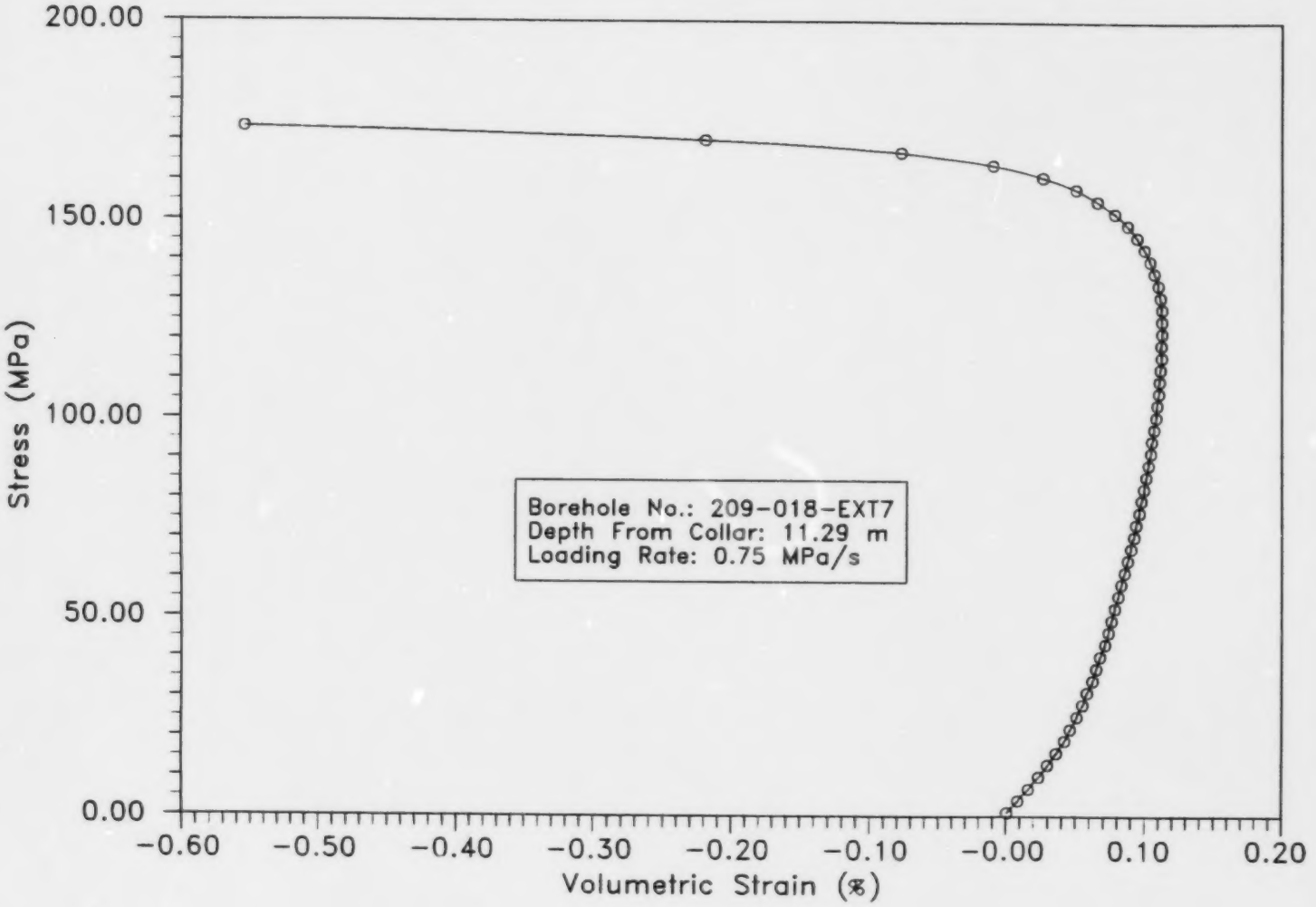

Figure B4: Volumetric Strain vs. Stress, Lac du Bonnet Loading Rate Specimens

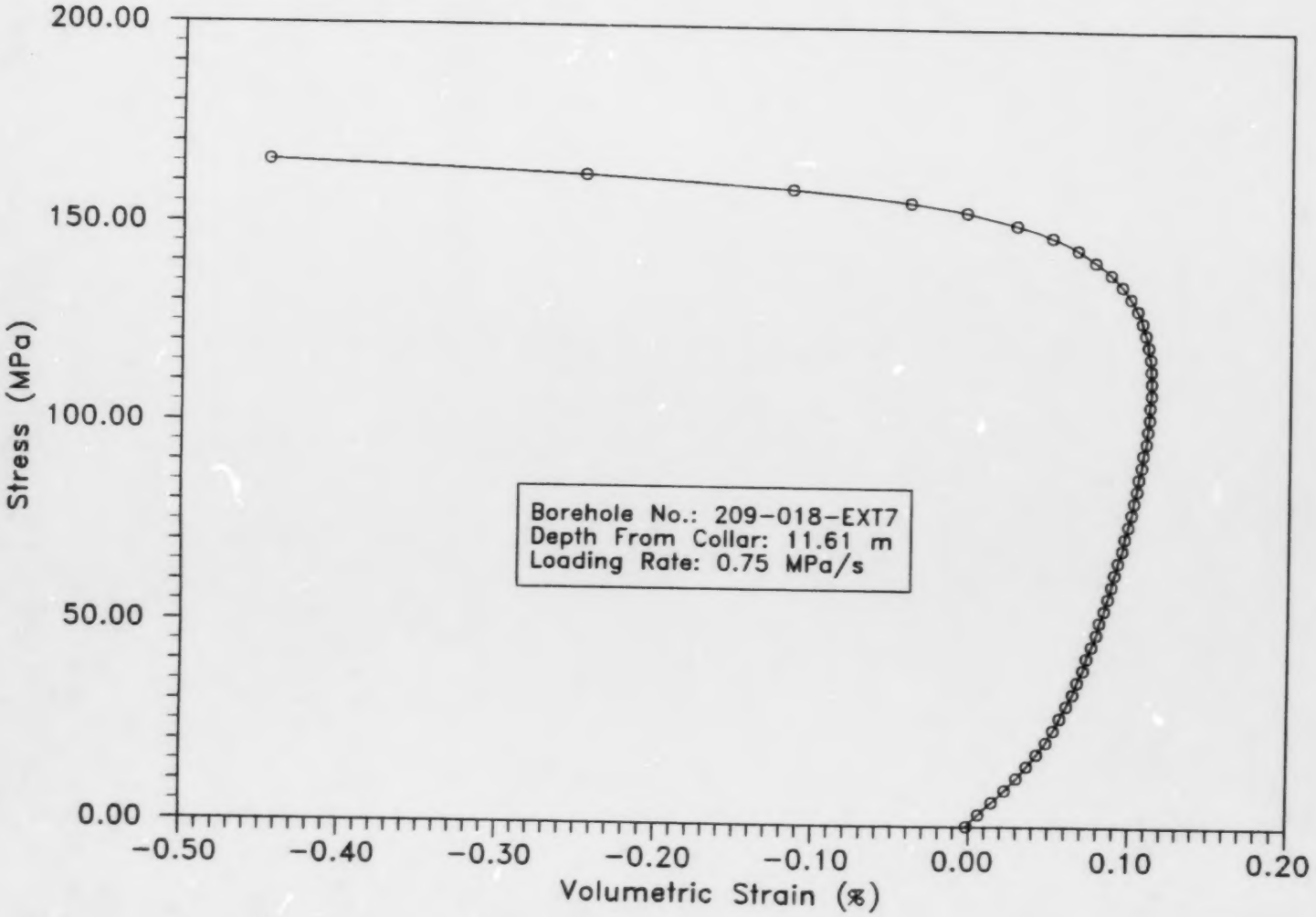

Figure B5: Volumetric Strain vs. Stress, Lac du Bonnet Loading Rate Specimens

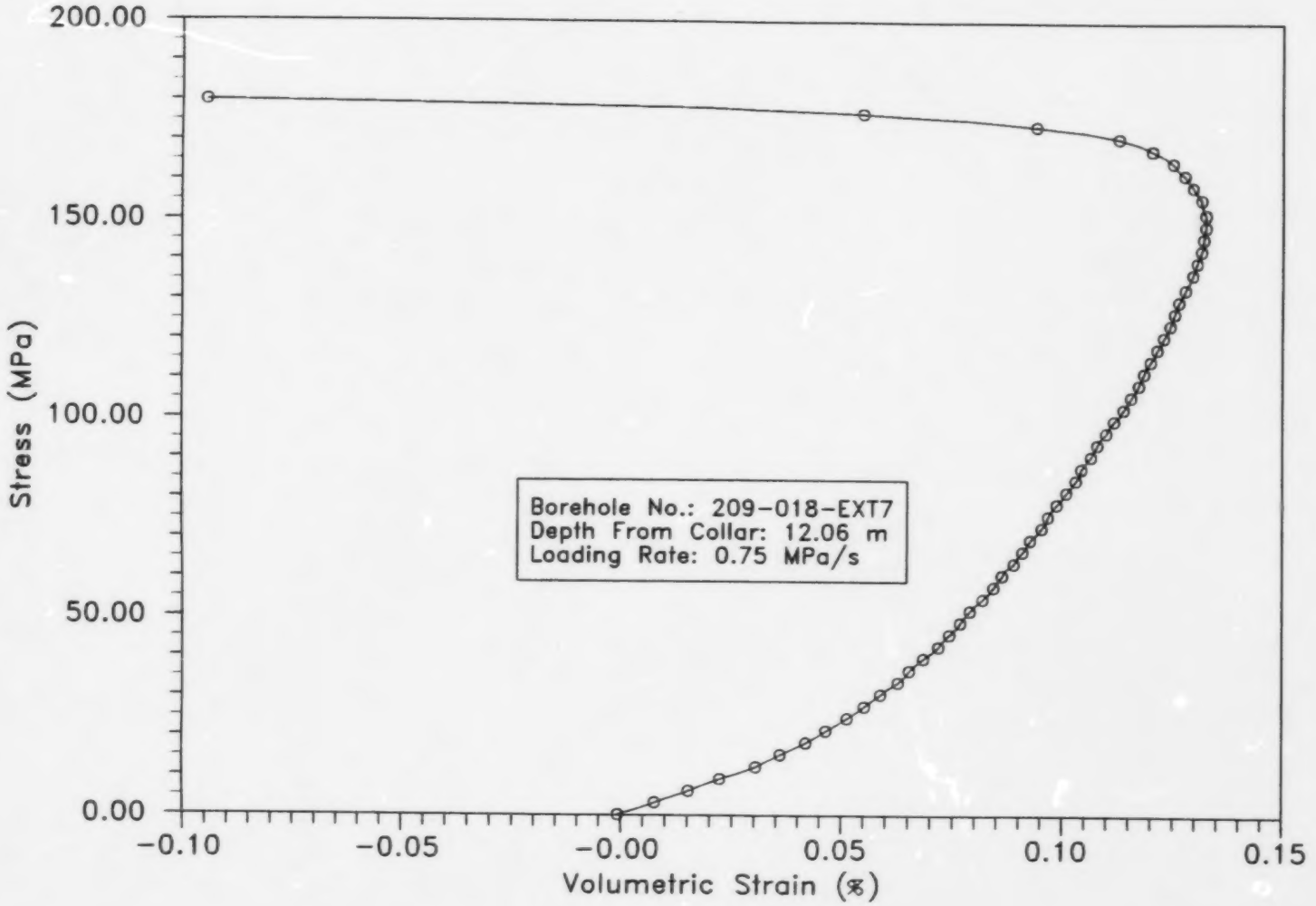

Figure B6: Volumetric Strain vs. Stress, Lac du Bonnet Loading Rate Specimens

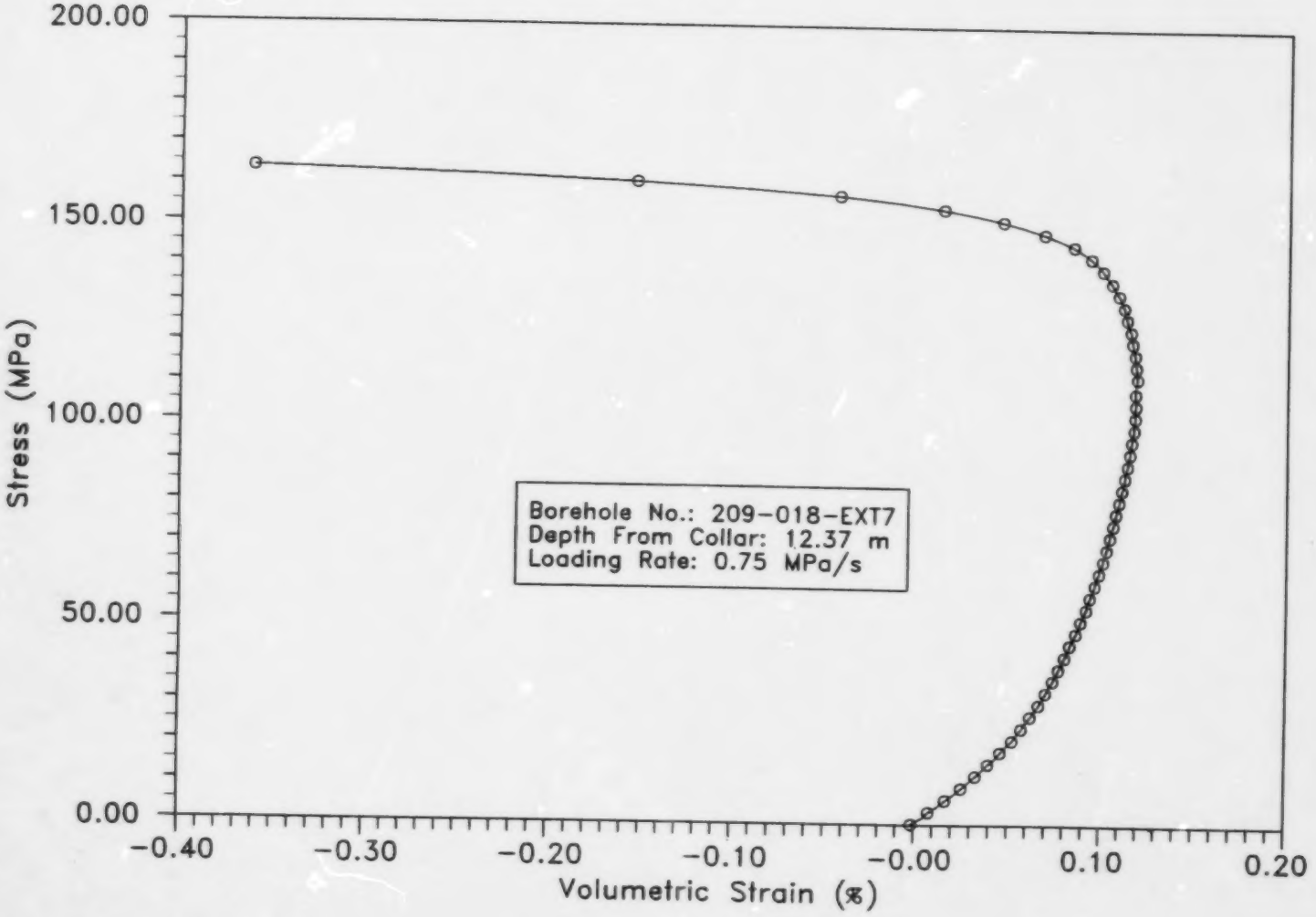

Figure B7: Volumetric Strain vs. Stress, Lac du Bonnet Loading Rate Specimens

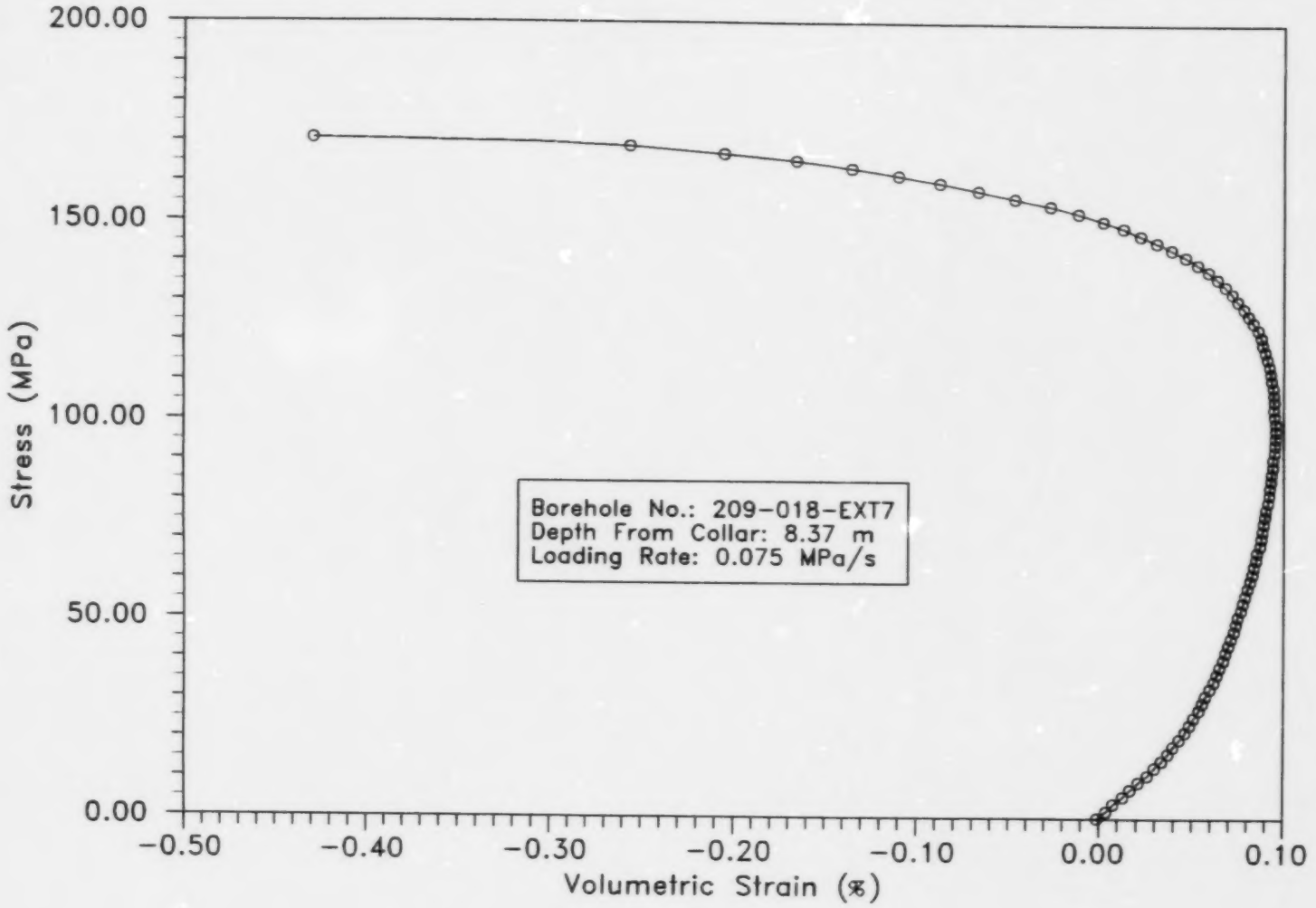

Figure B8: Volumetric Strain vs. Stress, Lac du Bonnet Loading Rate Specimens

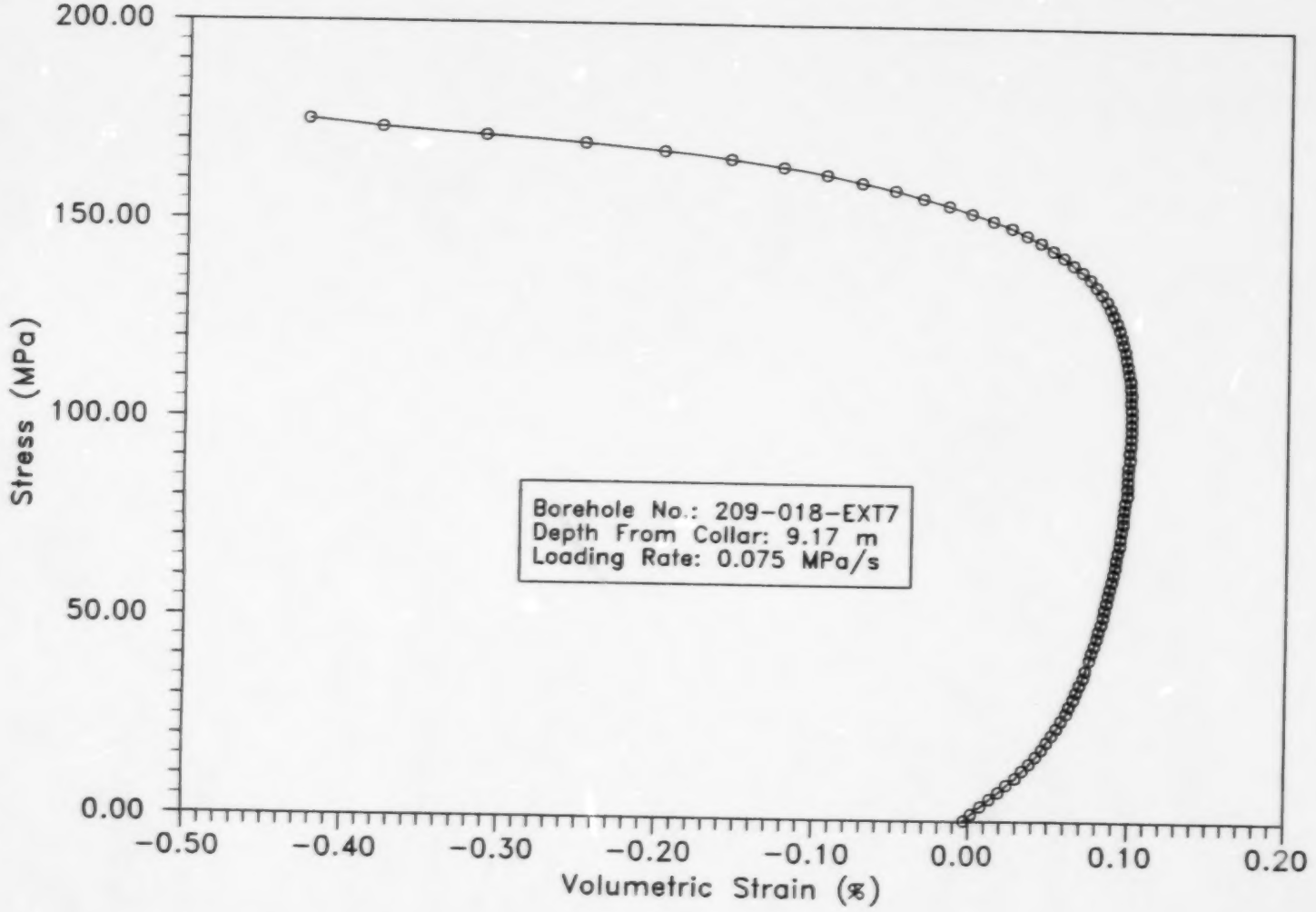

Figure B9: Volumetric Strain vs. Stress, Lac du Bonnet Loading Rate Specimens

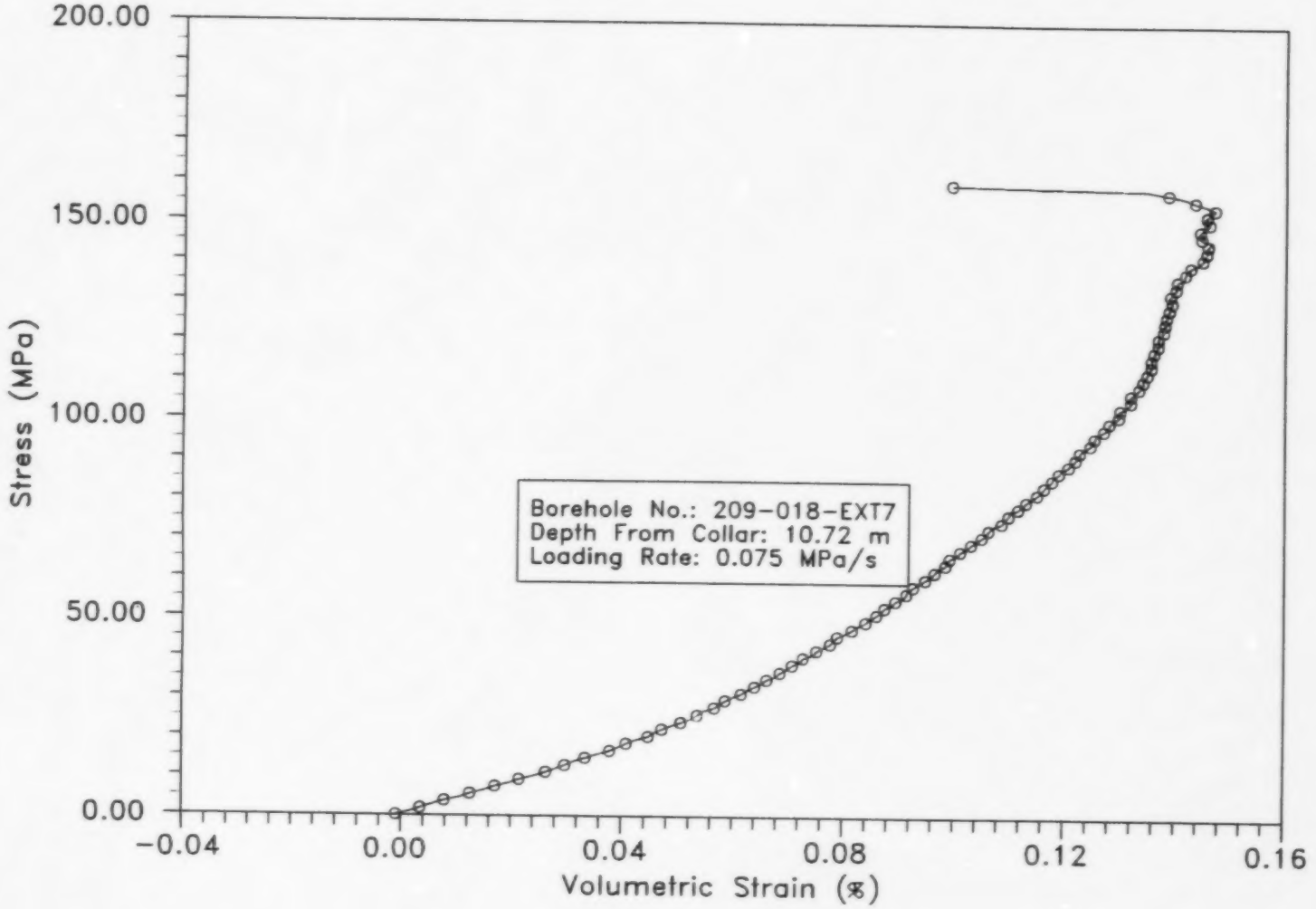

Figure B10: Volumetric Strain vs. Stress, Lac du Bonnet Loading Rate Specimens

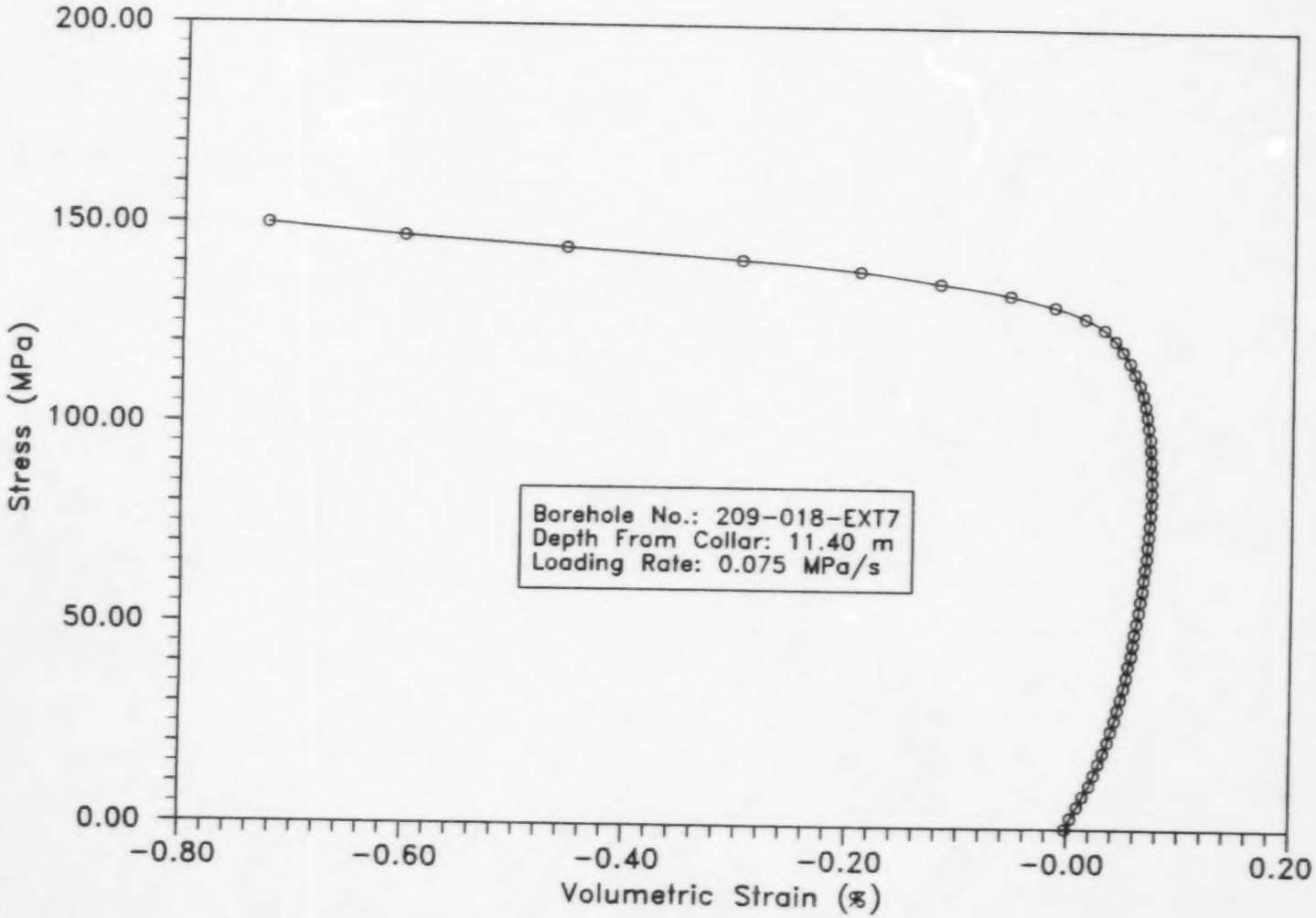

Figure B11: Volumetric Strain vs. Stress, Lac du Bonnet Loading Rate Specimens

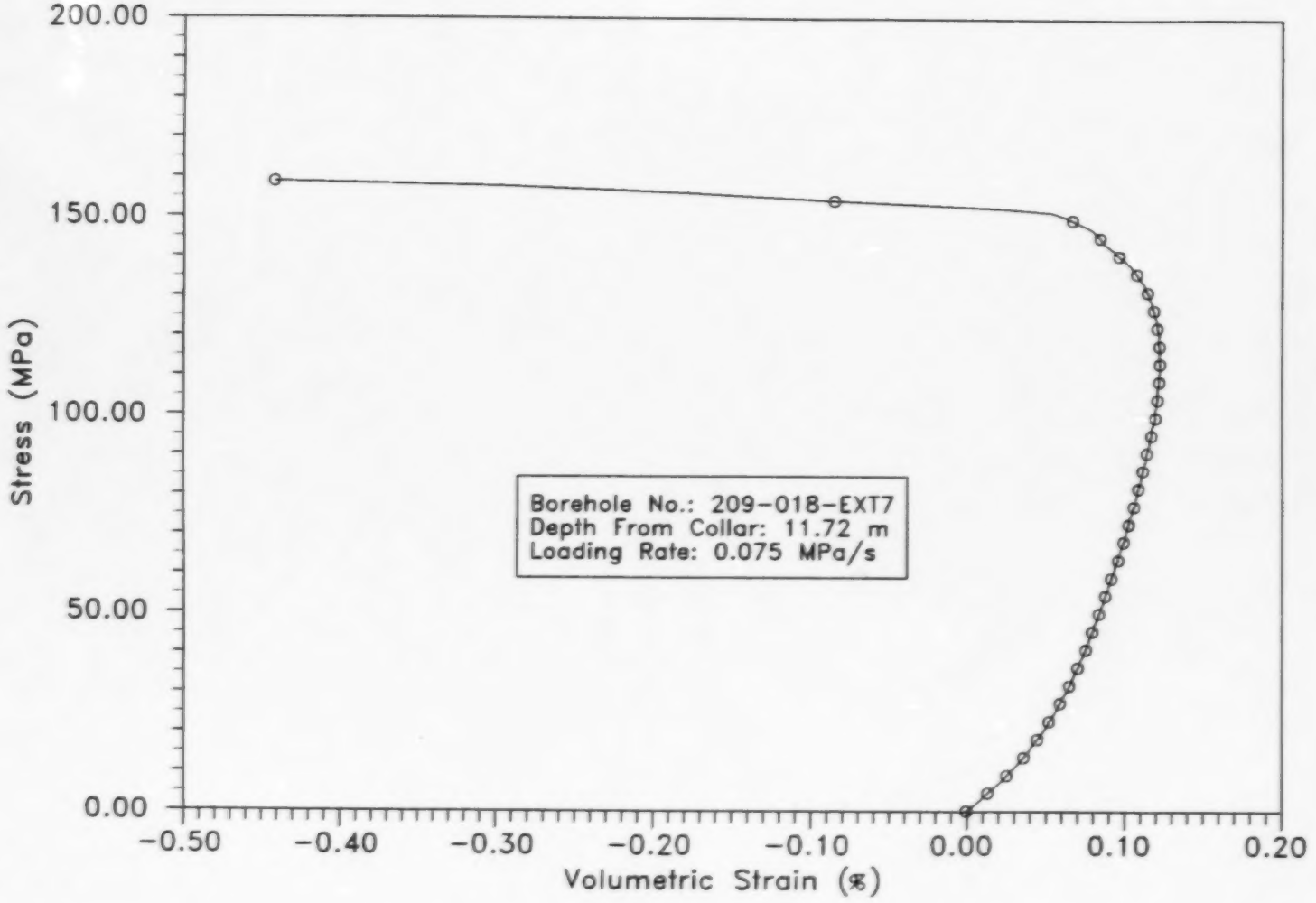

Figure B12: Volumetric Strain vs. Stress, Lac du Bonnet Loading Rate Specimens

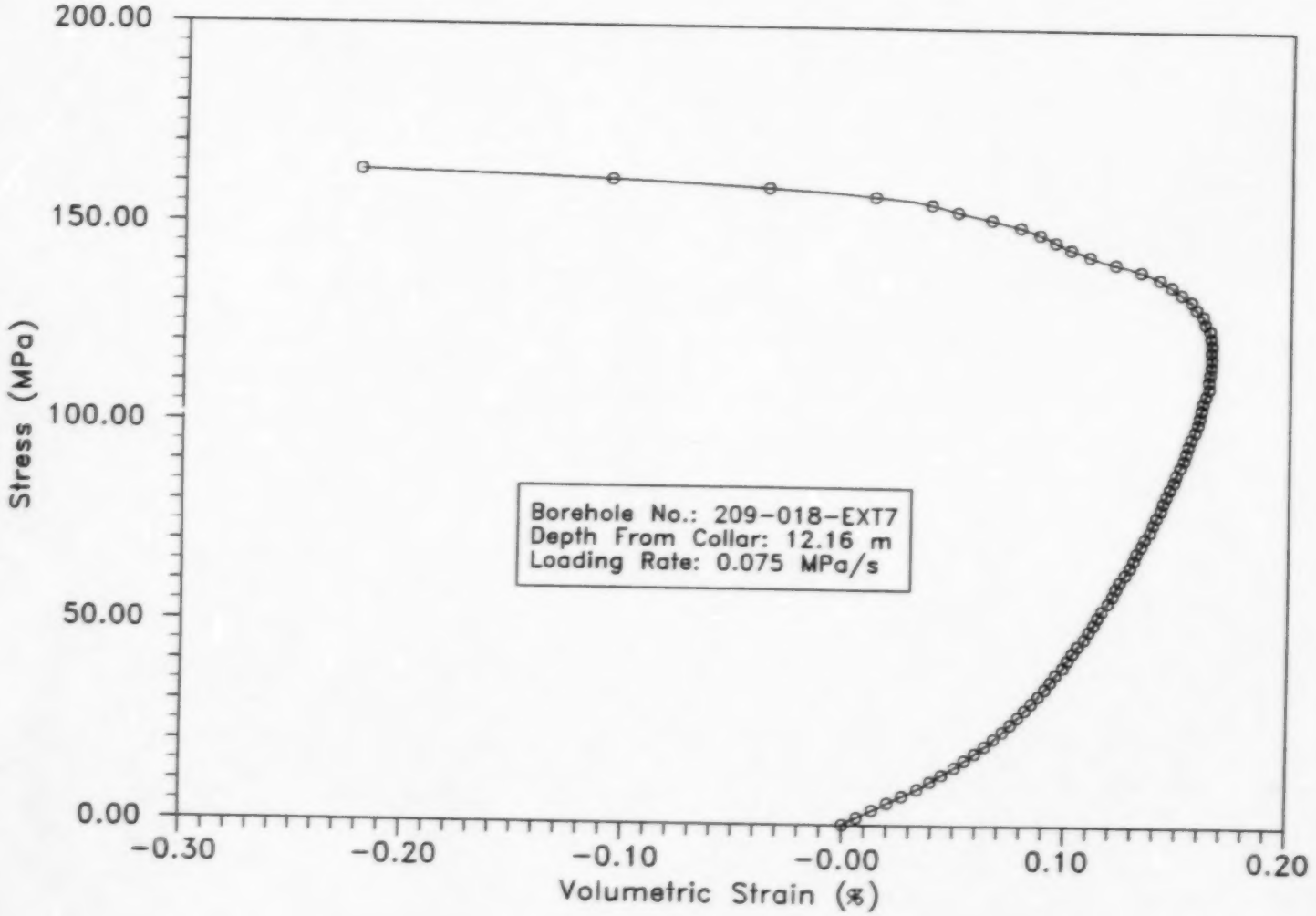

Figure B13: Volumetric Strain vs. Stress, Lac du Bonnet Loading Rate Specimens

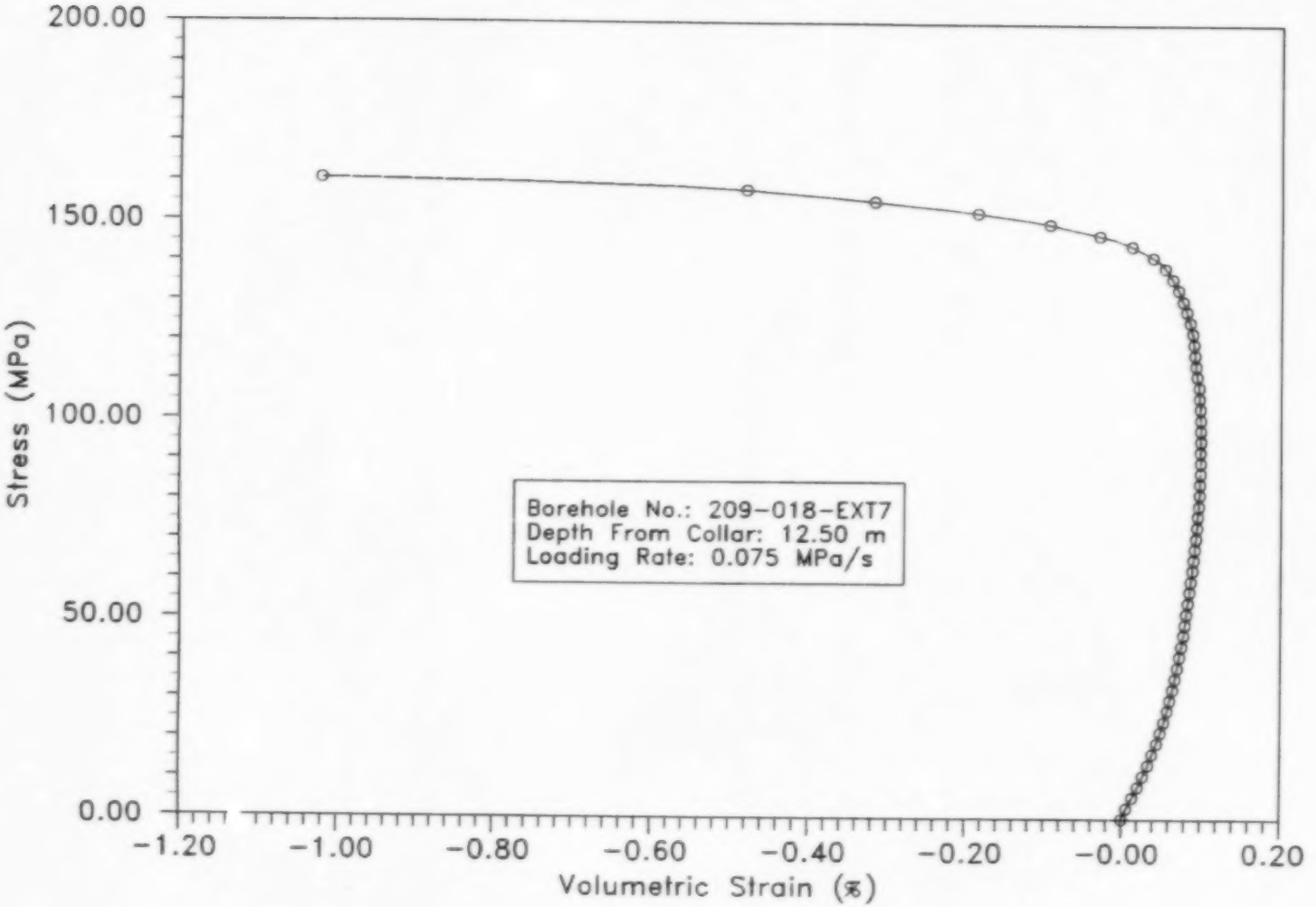

Figure B14: Volumetric Strain vs. Stress, Lac du Bonnet Loading Rate Specimens

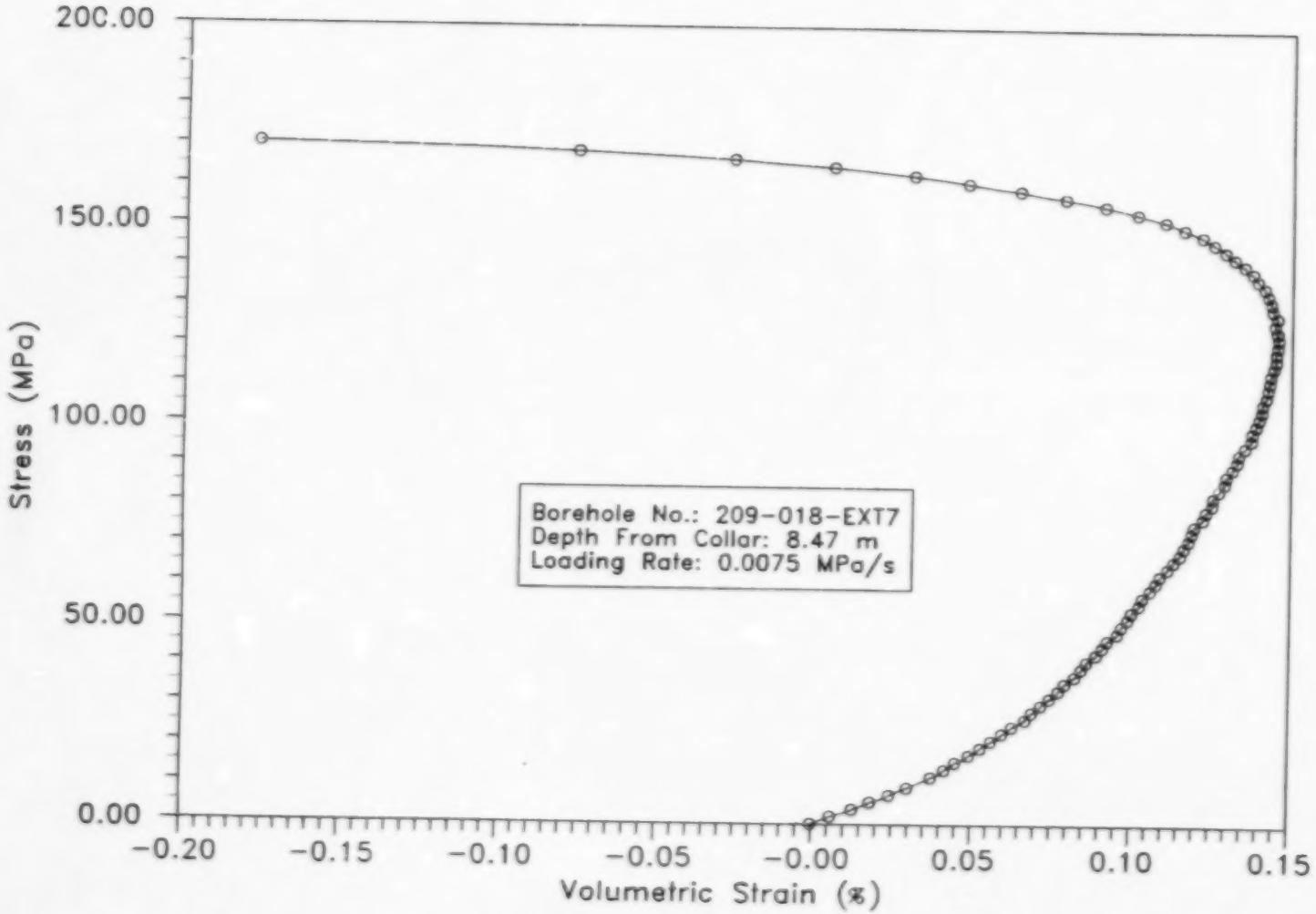

Figure B15: Volumetric Strain vs. Stress, Lac du Bonnet Loading Rate Specimens

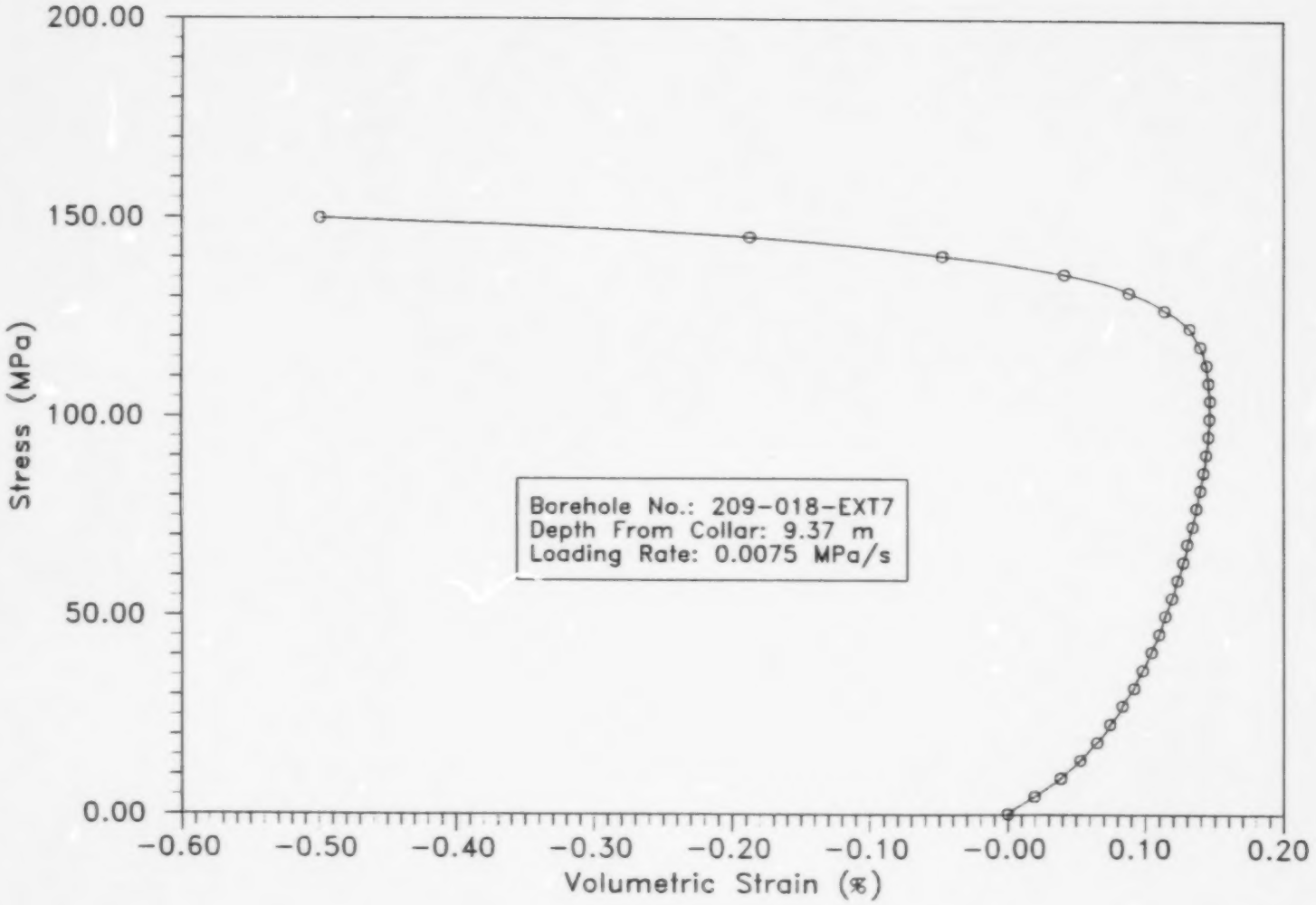

Figure B16: Volumetric Strain vs. Stress, Lac du Bonnet Loading Rate Specimens

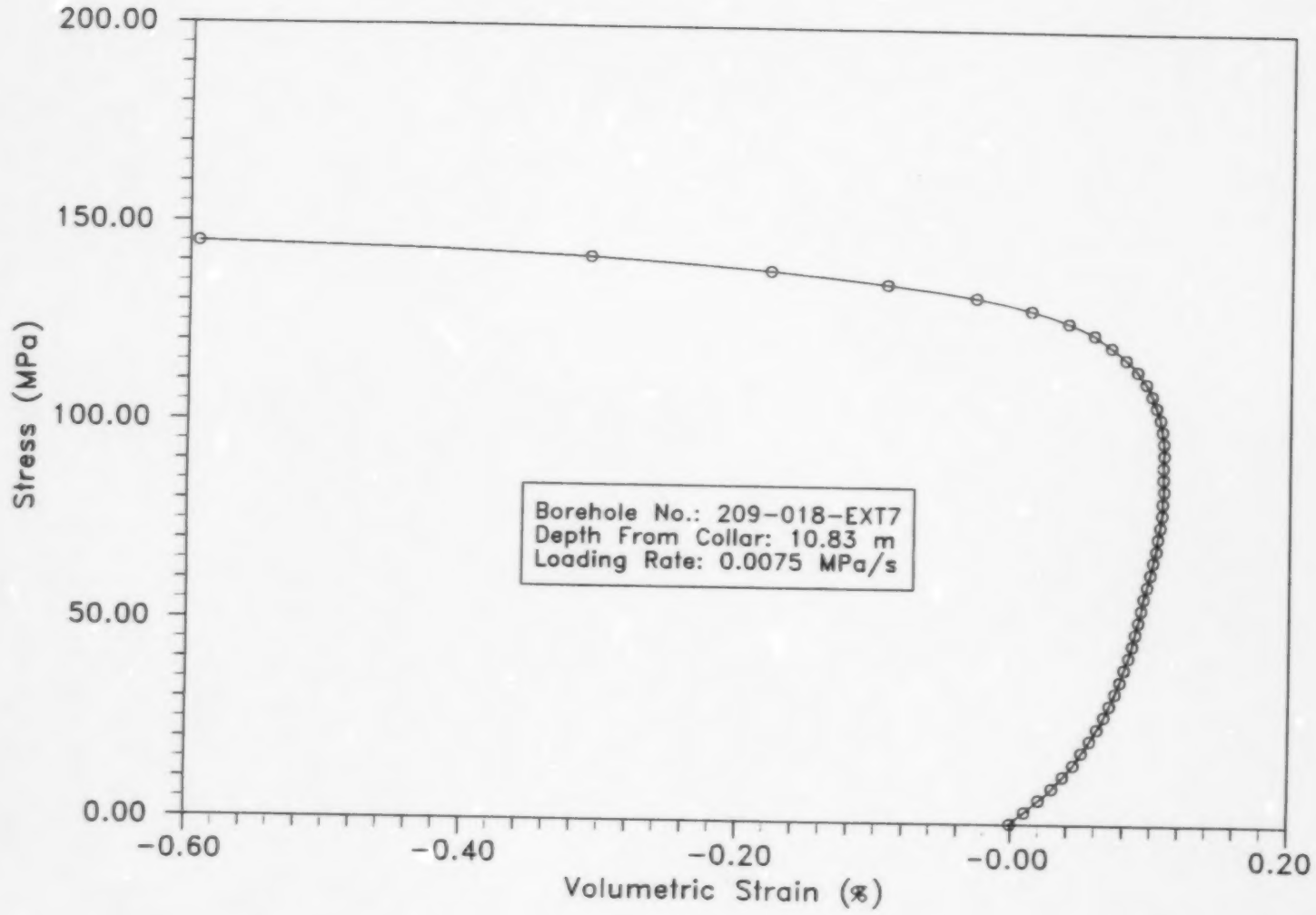

Figure B17: Volumetric Strain vs. Stress, Lac du Bonnet Loading Rate Specimens

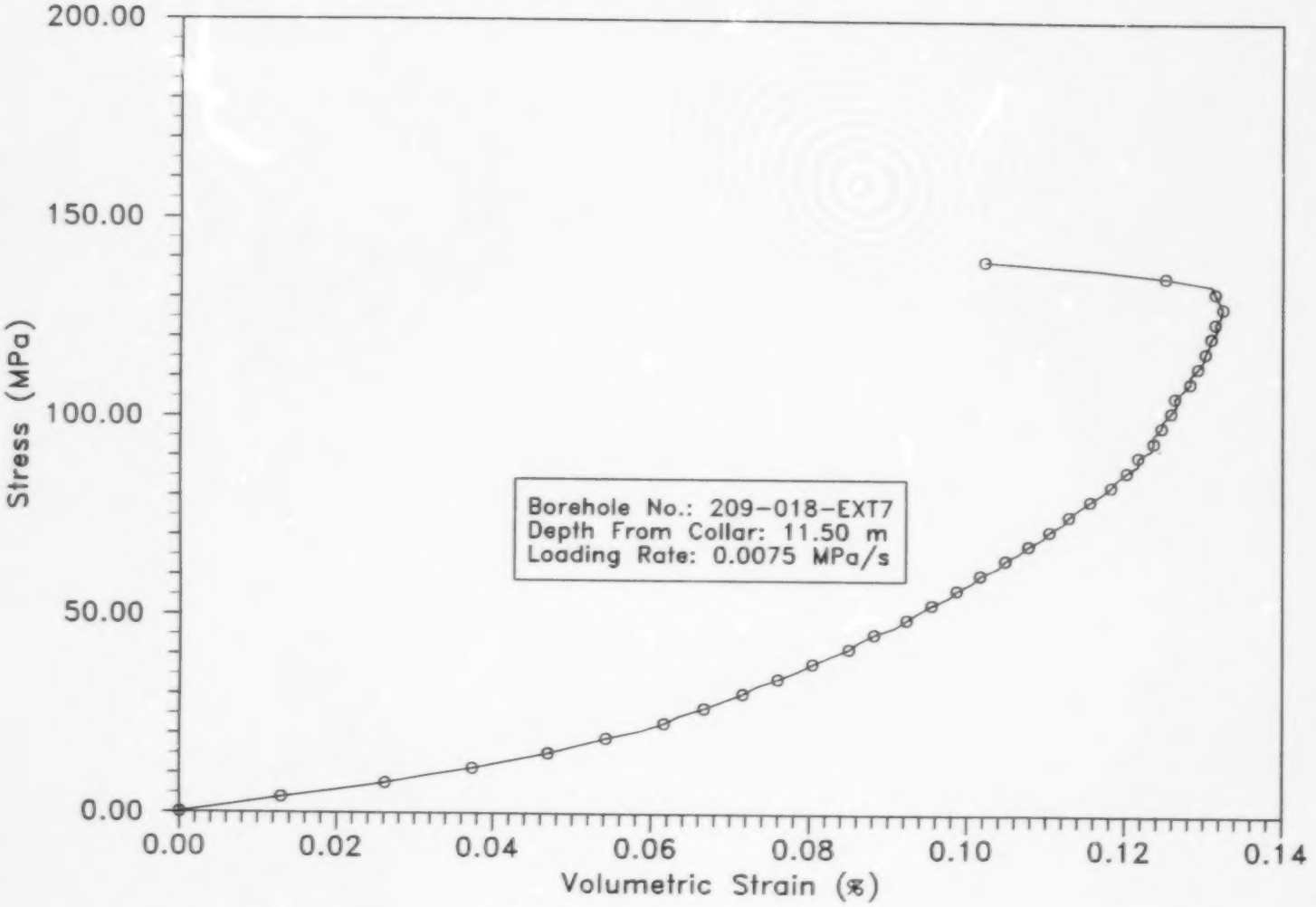

Figure B18: Volumetric Strain vs. Stress, Lac du Bonnet Loading Rate Specimens

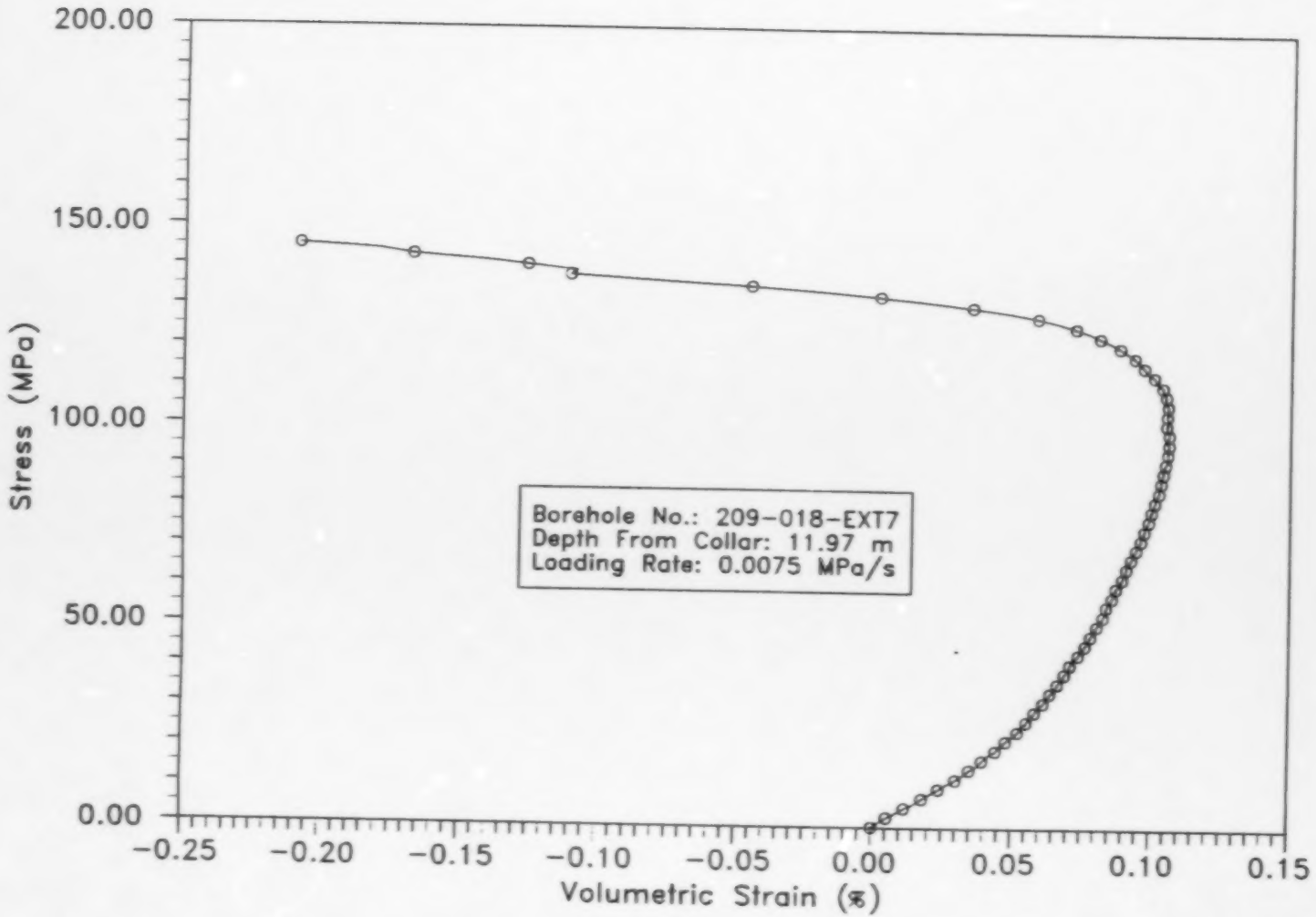

Figure B19: Volumetric Strain vs. Stress, Lac du Bonnet Loading Rate Specimens

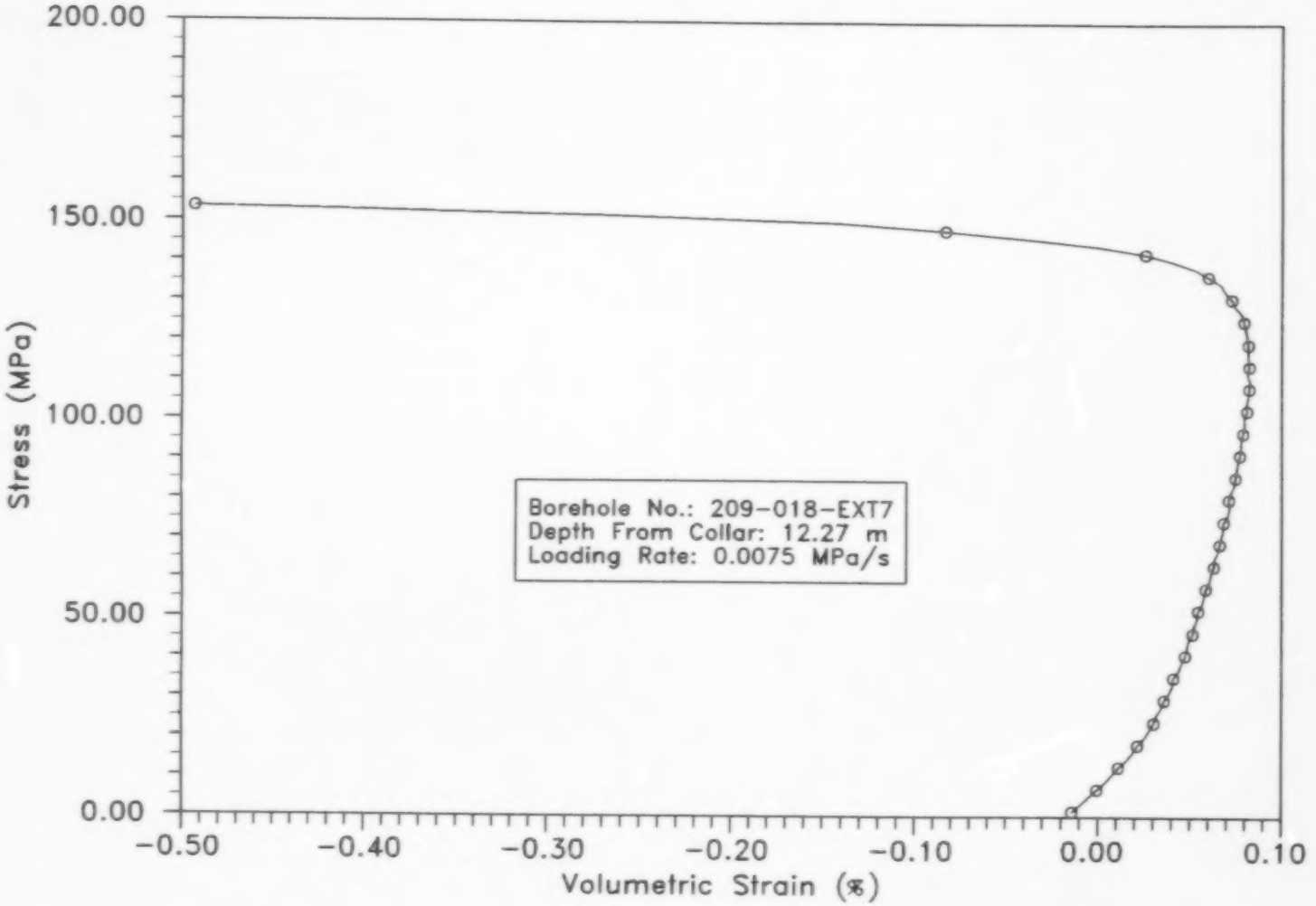

Figure B20: Volumetric Strain vs. Stress, Lac du Bonnet Loading Rate Specimens

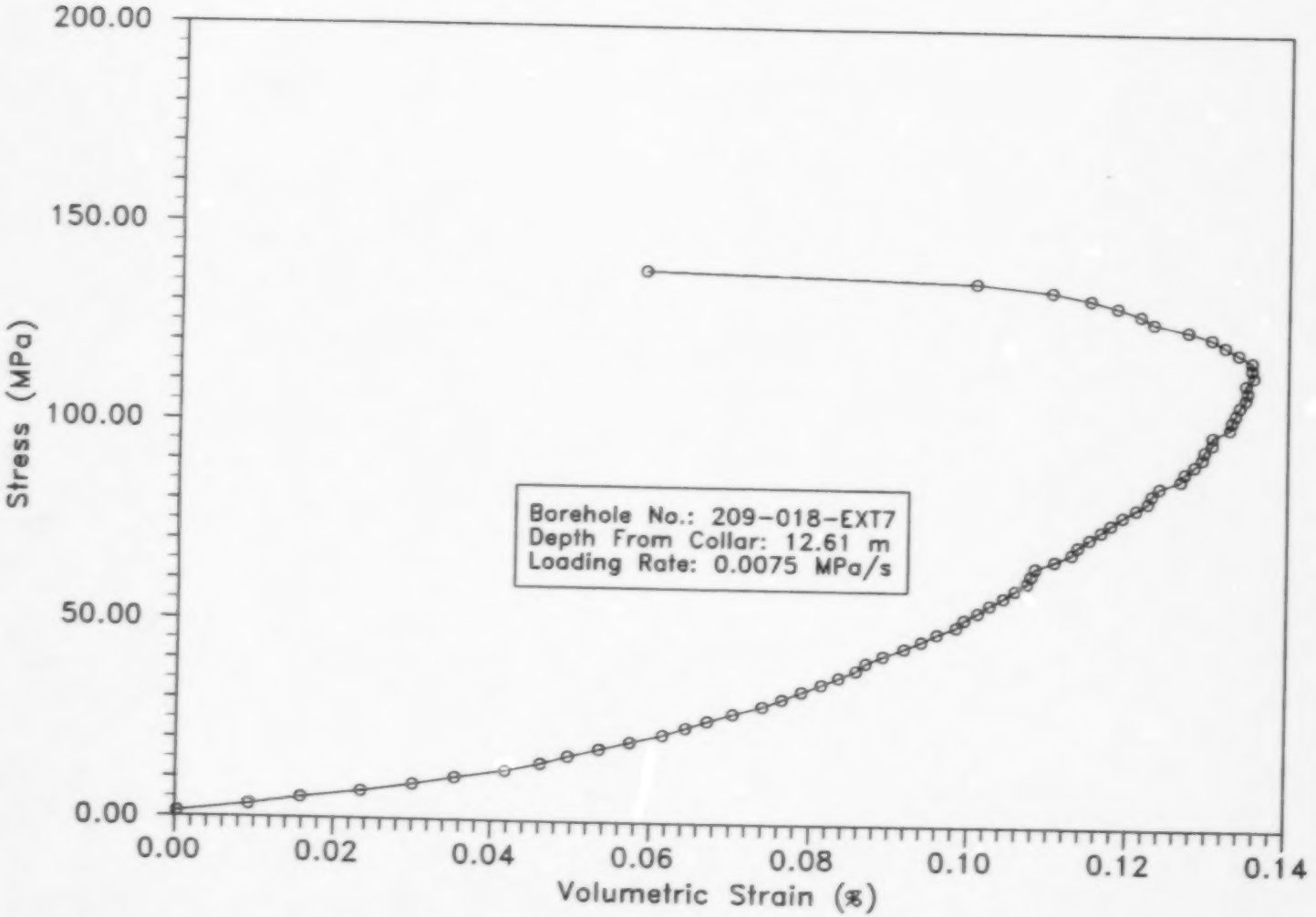

Figure B21: Volumetric Strain vs. Stress, Lac du Bonnet Loading Rate Specimens

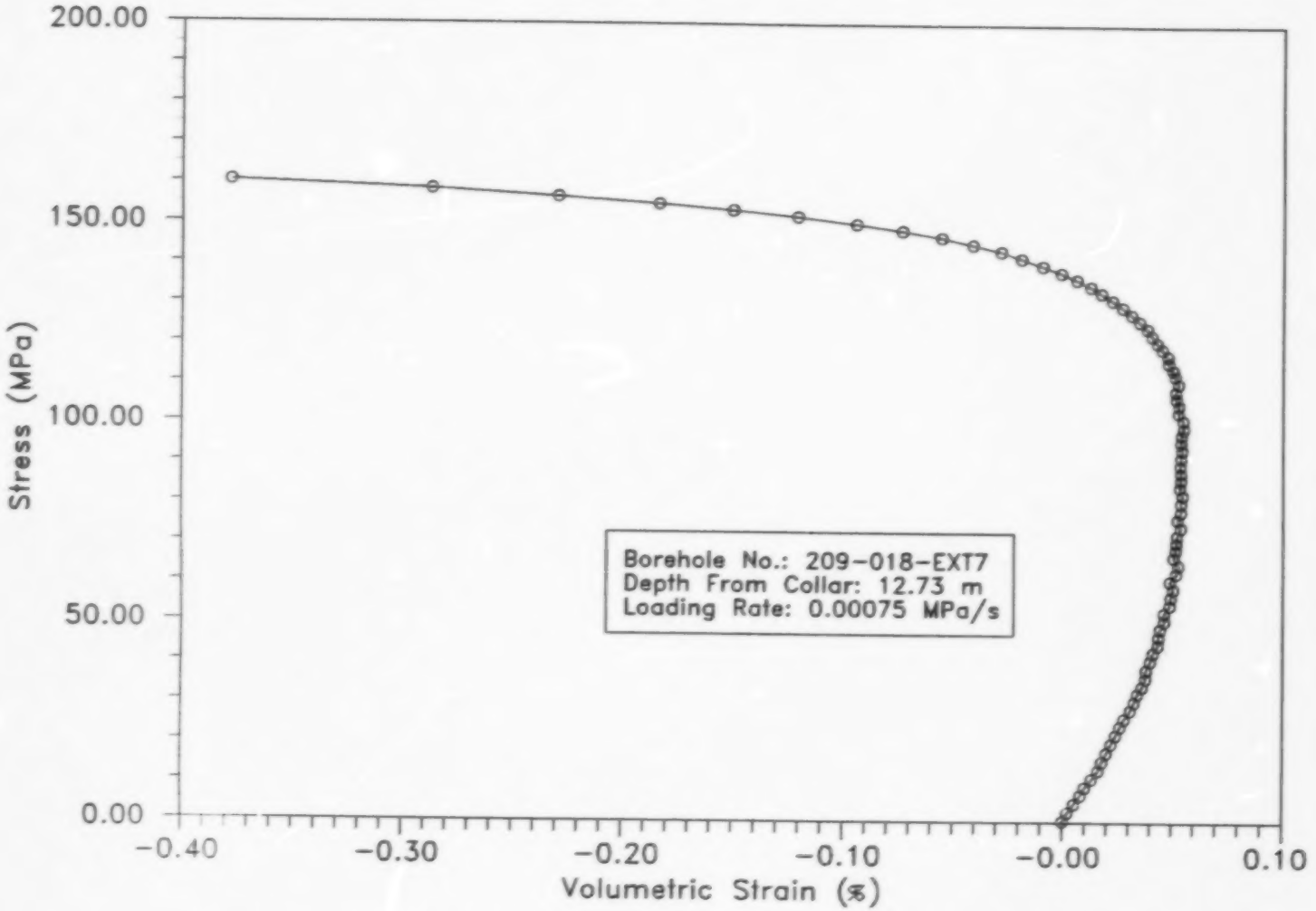

Figure B22: Volumetric Strain vs. Stress, Lac du Bonnet Loading Rate Specimens

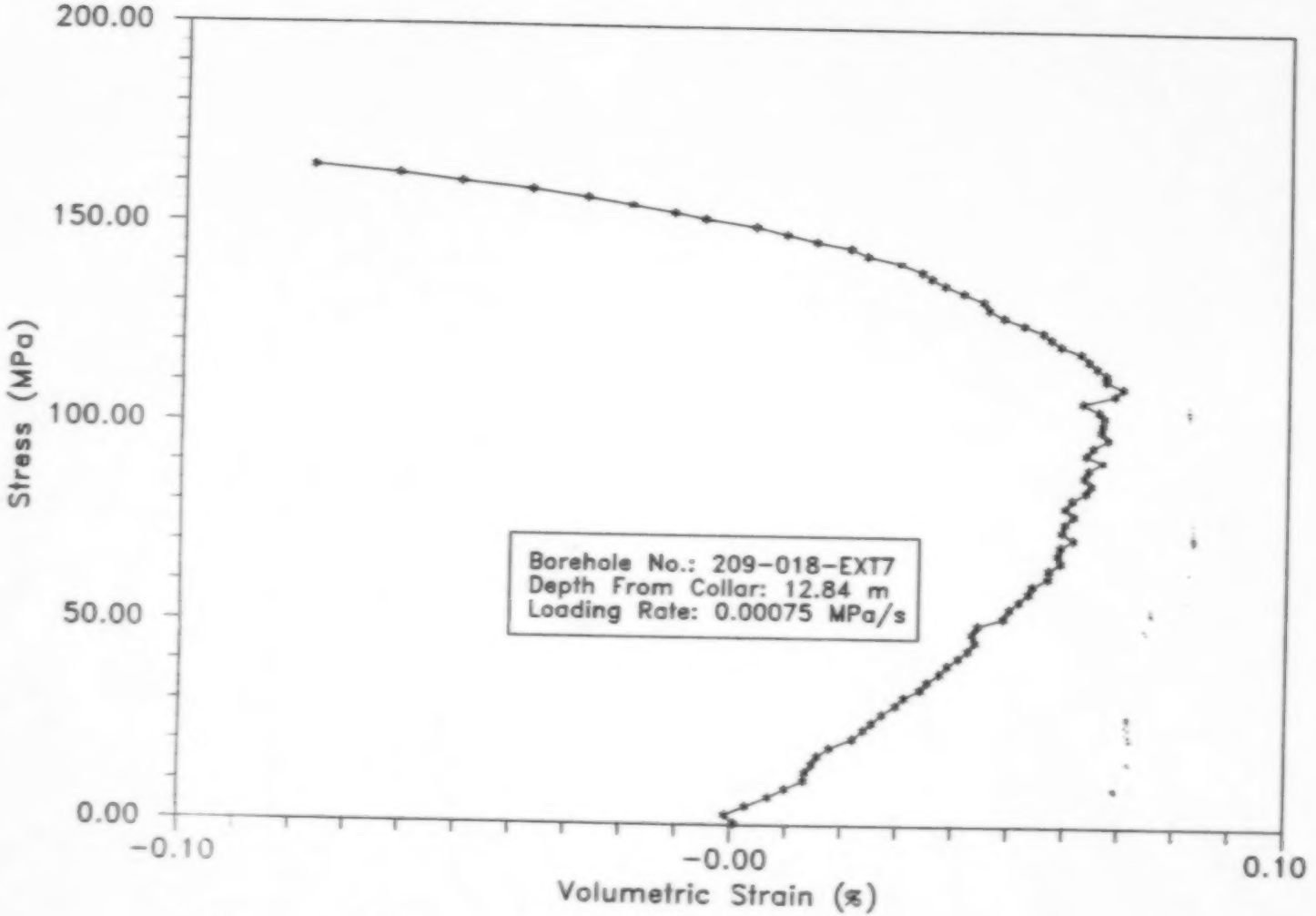

Figure B23: Volumetric Strain vs. Stress, Lac du Bonnet Loading Rate Specimens

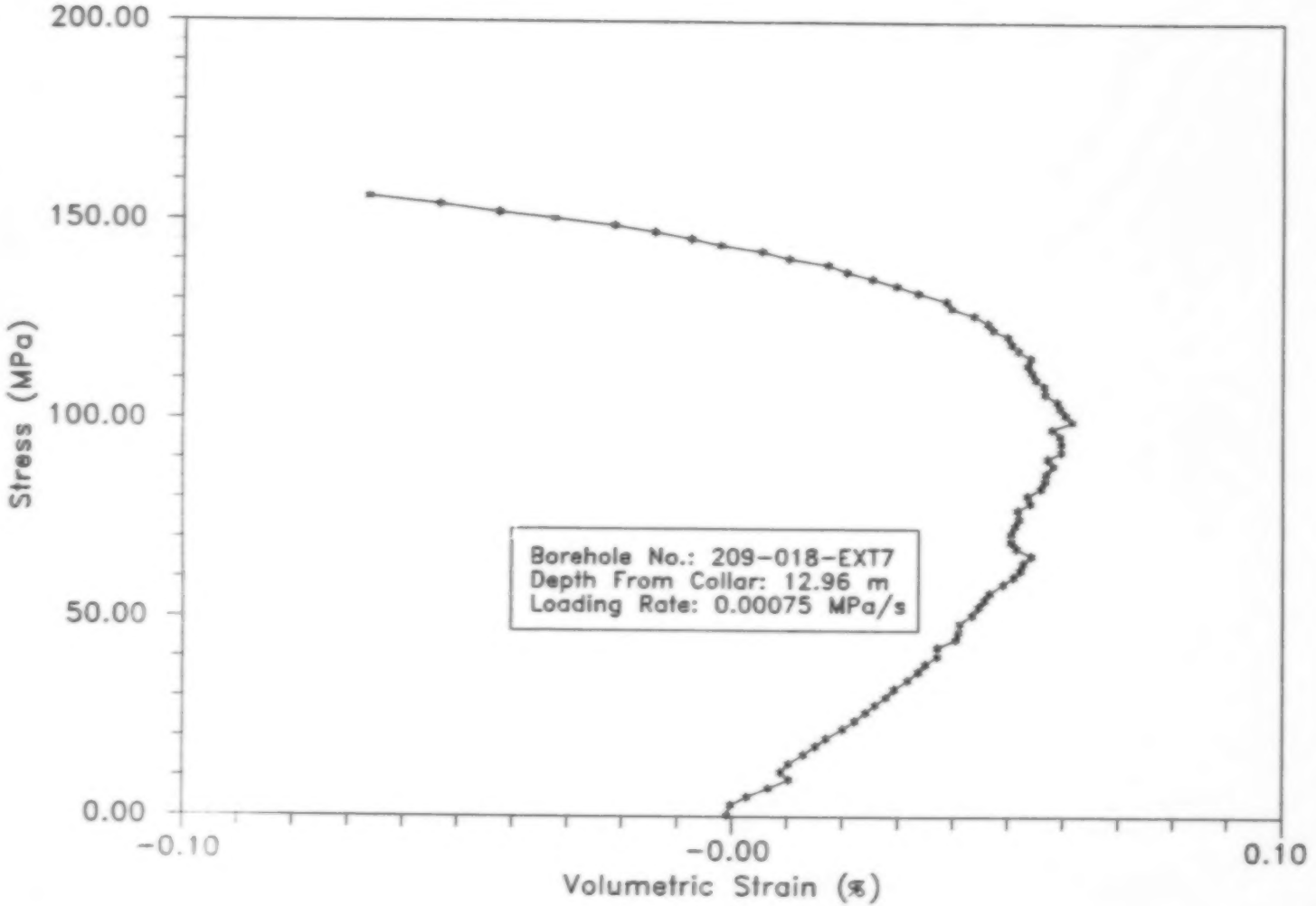

Figure B24: Volumetric Strain vs. Stress, Lac du Bonnet Loading Rate Specimens